A COMPUTATIONAL ANALYSIS OF AIR ENTRAINMENT WITH A NIP ROLLER

BY

JAE-YONG LEE

Bachelor of Science

Kon-Kuk University

Seoul, Korea

1997

Submitted to the Faculty of the
Graduate College of the
Oklahoma State University
in partial fulfillment of
the requirements for
the Degree of
MASTER OF SCIENCE
December 1999

A COMPUTATIONAL ANALYSIS OF AIR ENTRAINMENT

WITH A NIP ROLLER

Thesis Approved:

Young Bae Chang
Thesis Adviser

John J. Shelton

Wayne B. Powell
Dean of the graduate college

ACKNOWLEDGEMENT

I wish to express my sincere appreciation to my advisor, Dr. Young Bae Chang for his intelligent supervision, excellent guidance, and inspiration. My sincere appreciation extends to my other committee members Dr. John J. Shelton and Dr. Ronald D. Delahoussaye, whose guidance, assistance, and encouragement are also invaluable. I would also like to thank Dr. Keith Ducotey for providing me with a lot of valuable information and guidance.

This work was supported by the Web Handling Research Center (WHRC) at Oklahoma State University.

TABLE OF CONTENTS

Chapter Page

I. INTRODUCTION 1

1.1 Problem Statement 1

1.2 Objectives of the Study 1

1.3 Scope and Limitations 2

1.4 Literature Review 2

II. GOVERNING EQUATIONS 4

2.1 Reynolds Equation 6

2.2 Web Deflection Equation 8

III. NUMERICAL SOLUTION OF THE GOVERNING EQUATIONS 11

3.1 Dimensionless Forms 11

3.2 Finite Difference Forms 13

3.3 Computational Algorithm 18

IV. RESULTS AND DISCUSSIONS 24

4.1 Simple Foil Bearing Solution (Zero Nip Force) 25

4.1.1 Perfectly flexible web ($EI = 0$) 26

4.1.2 Stiff web ($E = 10^5$ *psi*, $t = 0 \sim 20$ *mils*) 33

4.2 Ballooning for Perfectly Flexible Web ($EI = 0$) 38

4.2.1 Air gap and pressure profiles ($EI = 0$) 38

4.2.2 Effects of wrap angle on ballooning ($EI = 0$) 48

4.3 Ballooning for a Web with Bending Stiffness ($EI > 0$) 49

4.3.1 Effects of bending stiffness on ballooning ($EI > 0$) 49

4.3.2 Effects of web speed on ballooning ($EI > 0$) 49

4.3.3 Effects of web tension on ballooning ($EI > 0$) 50

4.4 Air Entrainment 52

4.4.1 Air entrainment for perfectly flexible web ($EI = 0$) 52

4.4.2 Effects of nip force on air entrainment 58

4.4.3 Effects of web speed on air entrainment 63

4.4.4 Effects of web tension on air entrainment 64

V. SUMMARY AND CONCLUSIONS 66

VI. RECOMMENDATIONS FOR FUTURE STUDY 68

REFERENCES 69

APPENDIX A: DERIVATION OF THE NON-DIMENSIONAL FORMS OF THE MODIFIED REYNOLDS EQATION AND WEB DEFLECTION EQUATION 71

APPENDIX B: DERIVATION OF THE FINITE-DIFFERENCE EQUATIONS OF EQ. (23) AND EQ. (26) 74

APPENDIX C: DERIVATION OF THE FINITE-DIFFERENCE EQUATION OF EQ. (54) FOR THE TWO DIFFERENT SETS OF BOUNDARY CONDITIONS 81

APPENDIX D: COMPUTER PROGRAM 83

APPENDIX E: COMPUTER PROGRAM TO CALCULATE NIP FORCE AND THE AMOUNT OF THE AIR ENTRAINMENT 92

LIST OF FIGURES

Figure — Page

Figure 1. Schematic of model 5

Figure 2. Flow chart of the computational program 19

Figure 3. Two typical types of winding systems 24

Figure 4. Nominal clearance vs. compressibility (Gross, 1980b) 26

Figure 5. Simple foil bearing solution for perfectly flexible web 27

Figure 6. Effects of boundary conditions on the nominal clearance 28

Figure 7. Effects of boundary conditions on convergence 30

Figure 8. Trace of solution (pressure and gap) during iteration (BCs #1) 31

Figure 9. Trace of solution (pressure and gap) during iteration (BCs #2) 32

Figure 10. Simple foil bearing solution for stiff web ($E = 10^5$ *psi*, $t = 1 \sim 20$ *mils*) 33

Figure 11. Nominal clearance vs. stiffness parameter (Eshel, 1967) 34

Figure 12. Nominal clearance vs. stiffness parameter 34

Figure 13. Effects of span length, L_{in} and L_{out} (t = 20 mils) 36

Figure 14. Detailed description of Figure 13 36

Figure 15. Effects of span length, L_{in} and L_{out} (t = 40 mils) 37

Figure 16. Detailed description of Figure 15 37

Figure 17. Schematic of model 39

Figure 18. Gap profile h_1 for $\theta_{in} = 8^\circ$ and $EI = 0$ 40

Figure 19. Gap profile h_1 for $\theta_{in} = 13^\circ$ and $EI = 0$ 40

Figure 20. Gap profile h_1 for $\theta_{in} = 20^\circ$ and $EI = 0$ 41

Figure 21. Gap profile h_1 for $\theta_{in} = 30^\circ$ and $EI = 0$ 41

Figure 22. Gap profile h_1 for $\theta_{in} = 50^\circ$ and $EI = 0$ 42

Figure 23. Gap profile h_1 for $\theta_{in} = 8$, 13, 20, 30, and 50° and $EI = 0$ 42

Figure 24. Pressure profile p_1 for $\theta_{in} = 8^\circ$ and $EI = 0$ 43

Figure 25. Pressure difference $p_1 - p_2$ for $\theta_{in} = 8^\circ$ and $EI = 0$ 43

Figure 26. Pressure profile p_1 for $\theta_{in} = 13^\circ$ and $EI = 0$ 44

Figure 27. Pressure difference $p_1 - p_2$ for $\theta_{in} = 13^\circ$ and $EI = 0$ 44

Figure 28. Pressure profile p_1 for $\theta_{in} = 20^\circ$ and $EI = 0$ 45

Figure 29. Pressure difference $p_1 - p_2$ for $\theta_{in} = 20^\circ$ and $EI = 0$ 45

Figure 30. Pressure profile p_1 for $\theta_{in} = 30^\circ$ and $EI = 0$ 46

Figure 31. Pressure difference $p_1 - p_2$ for $\theta_{in} = 30^\circ$ and $EI = 0$ 46

Figure 32. Pressure profile p_1 for $\theta_{in} = 50^\circ$ and $EI = 0$ 47

Figure 33. Pressure difference $p_1 - p_2$ for $\theta_{in} = 50^\circ$ and $EI = 0$ 47

Figure 34. Maximum balloon height vs. incoming wrap angle ($EI = 0$) 48

Figure 35. Effect of web thickness on ballooning ($EI > 0$) 49

Figure 36. Effects of web speed on ballooning 50

Figure 37. Effects of web tension on ballooning 51

Figure 38. Detailed description of Figure 37 51

Figure 39. Air entrainment for $\theta_{in} = 8^{\circ}$ and $EI = 0$ 54

Figure 40. Air entrainment for $\theta_{in} = 13^{\circ}$ and $EI = 0$ 55

Figure 41. Air entrainment for $\theta_{in} = 20^{\circ}$ and $EI = 0$ 55

Figure 42. Air entrainment for $\theta_{in} = 30^{\circ}$ and $EI = 0$ 56

Figure 43. Air entrainment for $\theta_{in} = 50^{\circ}$ and $EI = 0$ 56

Figure 44. Air entrainment for $\theta_{in} = 8$, 13, 20, 30, and 50° and $EI = 0$ 57

Figure 45. Air entrainment for $\theta_{in} = 8$, 13, 20, 30, and 50° and $EI = 0$ 57

Figure 46. Web profiles 58

Figure 47. Comparison of two computational models 59

Figure 48. Effects of nip force on air entrainment 61

Figure 49. Effects of nip force on air entrainment 61

Figure 50. Effects of nip force on air entrainment 62

Figure 51. Effects of nip force on air entrainment 62

Figure 52. Effects of nip force on air entrainment 63

Figure 53. Effects of web speed on air entrainment 64

Figure 54. Effects of web tension on air entrainment 65

LIST OF TABLES

Table Page

Table 1. Effects of boundary conditions on convergence 29

Table 2. Conditions of calculation for perfectly flexible web 38

Table 3. Test conditions ($EI > 0$) 59

NOMENCLATURE

B	$\frac{R_1 P_a}{T}$
D	Dimensionless stiffness parameter, $\frac{Et^3}{12(1-\nu^2)TR^2}\varepsilon^{-2/3}$
E	Modulus of elasticity of web (psi)
E_R	Modulus of elasticity of roll (psi)
F	Nip force (lbf/in)
H_1	$\frac{h_1}{R_1}\varepsilon^{-2/3}$
H_2	$\frac{h_2}{R_1}\varepsilon^{-2/3}$
H_o	$\frac{h_o}{R_1}\varepsilon^{-2/3}$
H_s	$\frac{h_s}{R_1}\varepsilon^{-2/3}$
H^*	Non-dimensional nominal clearance constant, $\frac{h^*}{R}\varepsilon^{-2/3}$
h_1	Gap between web and winding roll (inch)
h_2	Gap between web and nip roller (inch)
h_c	Amount of air entrainment, equivalent to the air film thickness after the air expands to the ambient pressure (inch)
h_o	Gap between winding roll and nip roller at the center of nip (inch)

h_s	Gap between winding roll and nip roller approximated to a parabolic curve, $\frac{x^2}{2R_e} + h_o$ (inch)
h^*	Nominal clearance; a constant air film thickness over wrapped zone for zero nip force case (inch)
L_{in}	Length of incoming web span (inch)
L_{out}	Length of outgoing web span (inch)
P_1	$\frac{p_1}{p_a}$
P_2	$\frac{p_2}{p_a}$
p_1	Pressure between web and winding roll (psi)
p_2	Pressure between web and nip roller (psi)
p_a	Ambient pressure, 14.7 psi
R_1	Radius of winding roll (inch)
R_2	Radius of nip roller (inch)
R_e	Equivalent radius, $R_e = \frac{R_1 R_2}{R_1 + R_2}$ (inch)
S	Non-dimensional coordinate, $\frac{s}{R_1}\varepsilon^{-1/3}$
s	Coordinate (inch)
T	Web tension (lbf/in)
u	Web speed (inch/s)
W	$\frac{w}{R_1}\varepsilon^{-2/3}$
w	Web displacement (inch)

ε	Foil bearing number, $\frac{12\mu u}{T}$
Λ_a	$\frac{6\lambda_a}{R_1}\varepsilon^{-2/3}$
λ_a	Mean-free-path of the air molecules, 2.65E-6 inches
μ	Dynamic viscosity, 2.6396E-9 psi·s
ν	Poisson's ratio
θ_{in}	Incoming wrap angle of winding roll (degrees)
θ_{out}	Outgoing wrap angle of winding roll (degrees)

CHAPTER I

INTRODUCTION

1.1 Problem Statement

An excessive amount of air entrained in the winding roll can cause defects such as telescoping or dishing by making the web float and slide in the transverse direction. On the other hand too little air in a winding roll can cause different types of winding defects such as buckling. Proper contact between adjacent layers of web should be achieved to prevent winding defects.

Nip rollers are used for achieving intimate contact between the web and a process roller in many applications including drive rollers, heating and cooling drums, and surface-treatment rollers. One annoying problem with nip rollers is the ballooning phenomenon. When the balloon height is too large, wrinkling problems can occur. Knowledge of ballooning and air entrainment is necessary for proper design and operation of such systems that use nip rollers.

1.2 Objectives of the Study

The main objective of this study is to develop an understanding of the effects of a nip roller on the air entrainment and ballooning. The parameters considered in this study

include the radius of winding roll, radius of nip roller, wrap angle, web tension, web speed, nip force, and web stiffness.

1.3 Scope and Limitations

The present study is divided into two main areas: the air entrainment on the two sides of the web and the ballooning phenomenon. This study does not include the effects of the elastic deformation of the roller. The surfaces of the web and the rolls are assumed smooth, and the effects of asperity contact are not considered.

1.4 Literature Review

Knox and Sweeney (1971) applied the foil bearing theory to the air entrainment in a winding roll, but it can not be applied to the winding configuration assisted by a nip roller. According to the foil bearing theory, the air gap (h^*) is a function of web speed (u), web tension (T), viscosity of the air (μ), and the radius of roll (R) as

$$\frac{h^*}{R} = 0.643\left(\frac{12\mu u}{T}\right)^{2/3} \tag{1}$$

Baumann (1975) and Eshel (1974) discussed the use of opposing pressure pad and external air pressure for reducing the air entrainment. Eshel (1984b) analyzed the effects of a nip roller ignoring the air compressibility and the elastic deformation of the roll. Chang, Chambers, and Shelton (1994) developed prediction equations for air entrainment considering the elastic deformation of rolls, air compressibility, and the slip flow condition. Forrest (1995) investigated the air entrainment in a winding roll including the effects of asperity contact between the roll and the nip roller. However, none of the

papers to date included the existence of a web that may strongly influence the amount of air entrainment.

Numerous papers on the foil bearing problems had been published before Knox and Sweeney applied the foil bearing theory to web handling. In the 1960's and 1970's magnetic tape and head interface became an important subject of study, and further developments of the foil bearing theory have been made. Those studies include the effects of the slip flow condition, permeability of the web, side leakage of the air and the asperity contact. Burgdorfer (1959) modified the Reynolds equation to consider the slip flow condition. Eshel (1965) developed the foil bearing theory for an infinitely wide and perfectly flexible foil (or web), and solved the Reynolds equation and the force balance equation simultaneously. It was found that the gap over the wrapped zone is constant (the "nominal clearance") and the web undulates in the exit region where the minimum clearance is 71.6 percent of the nominal clearance. Barlow (1967) derived governing equations for a foil bearing, which include the bending stiffness of the foil and the compressibility of the lubricant. The effects of bending stiffness and compressibility and inertia of the lubricant were studied by Eshel (1967, 1968, 1984a, 1984b). It was found that the nominal clearance decreases with the increase of the compressibility parameter and the stiffness parameter, and the undulation disappears when the compressibility parameter is large. Similarly, Hashimoto (1997) solved the foil bearing problem where an external pressure is applied through a hollow porous shaft. Muftu (1996) performed a two-dimensional analysis that includes side leakage and asperity contact. Muftu (1995) studied the one-dimensional foil bearing problem including the permeability effects of the web.

CHAPTER II

GOVERNING EQUATIONS

The governing equations are the modified Reynolds equation and a web deflection equation. The modified Reynolds equation used by Chang, Chambers, Shelton (1996) is used to include the effects of fluid compressibility and the effects of slip boundary which is important when the gap is not much larger than the mean-free-path of the air molecules. The web deflection equation can be derived from a plate equation and a cylindrical shell equation. When the web is assumed to be perfectly flexible, the web deflection equation becomes a membrane equation.

Before describing the two governing equations more specifically, a schematic view of the winding system with a nip roller should be introduced here. The air gap between the web and the winding roll in the wrapped zone and that in the inlet and outlet zones are defined differently as shown in Figure 1.

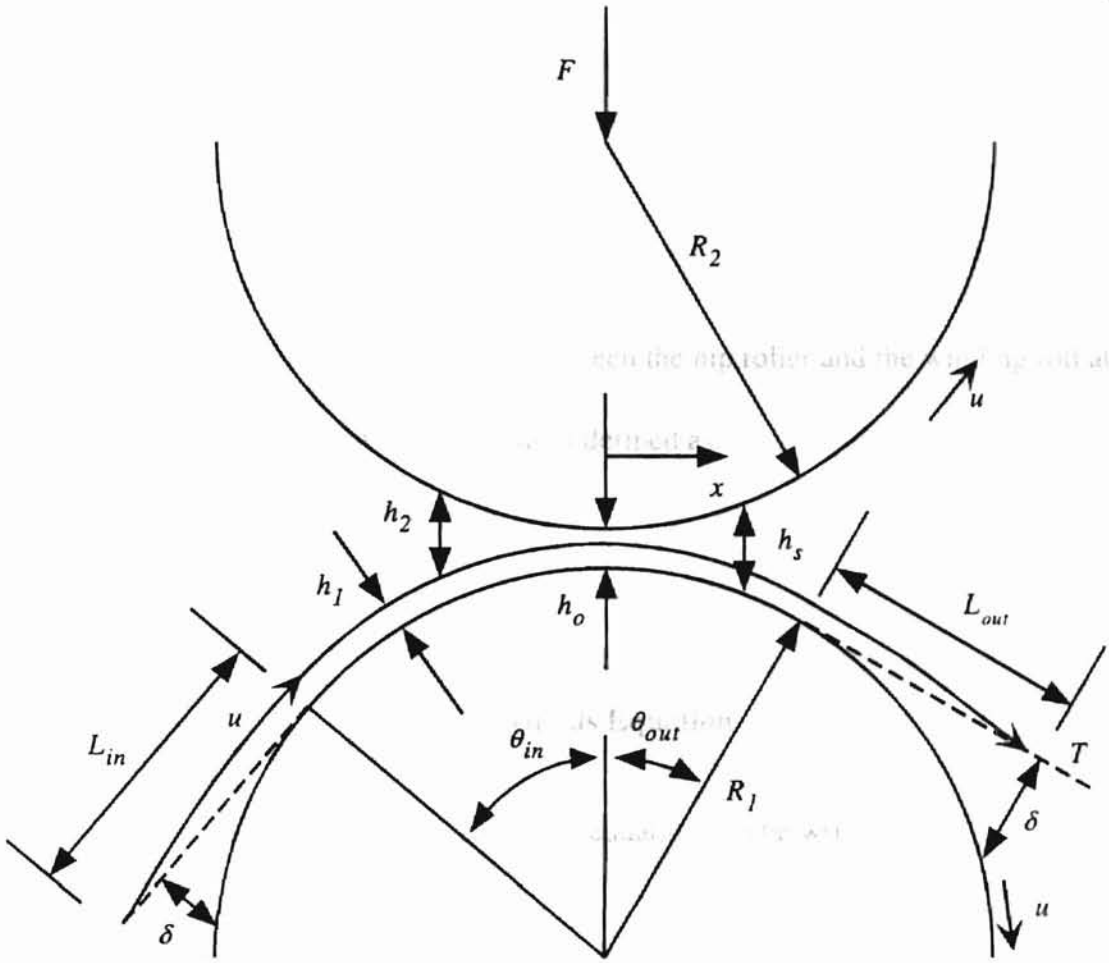

Figure 1. Schematic of model

The study model, schematically shown above, consists of a rigid winding roll, a rigid nip roller, and a non-permeable web. All moving surfaces have the same speed (u), and h_1 is defined as the air gap between the web and the winding roll. In the wrapped region, h_1 is measured in the radial direction so that a cylindrical coordinate system is used. In the inlet and outlet regions, h_1 is measured along the direction perpendicular to the tangents so that a rectangular coordinate system is used. However, the air gap between the web and the nip roller h_2 is approximated as

$$h_2 \approx h_s - h_1 \tag{2}$$

where

$$h_s \approx \frac{x^2}{2R_e} + h_o \tag{3}$$

which is a parabolic, and h_o is the air gap between the nip roller and the winding roll at the center of the nip. The equivalent radius is defined as

$$R_e = \frac{R_1 R_2}{R_1 + R_2} \tag{4}$$

2.1 Reynolds Equation

One-dimensional, steady-state Reynolds equation can be written as

$$\frac{d}{ds}\left(ph^3 \frac{dp}{ds} \right) = 12\mu u \frac{d}{ds}(ph) \tag{5}$$

The above Reynolds equation was derived from a combination of the Navier-Stokes equation and a continuity equation with the following assumptions (Cameron, 1966):

- Body forces are negligible.
- The lubrication process is isothermal.
- The lubricant is compressible.
- The curvatures of the bearing surfaces are much larger than the film thickness.
- No-slip flow occurs.
- The lubricant is a Newtonian fluid.

- The flow is laminar.
- The fluid inertia can be neglected.
- Fluid viscosity is constant.
- The web is infinitely wide.

Air film thickness near the center of the nip is very small, so that the no-slip boundary condition is invalid there. In other words, the fluid flow cannot be treated as a continuum near that region because the gap is not much larger than the mean-free path of air molecules. Therefore the modified Reynolds equation which includes the slip boundary condition is used in this study. The slip boundary condition is important when the Knuden number, defined as λ_a / h, is in the range from 0.01 to 15 (Gross, 1980a). Air compressibility is also important near the nip because the local pressure can be very high. The modified Reynolds equation to be used is

$$\frac{d}{ds}\left(ph^3 \frac{dp}{ds} + 6\lambda_a p_a h^2 \frac{dp}{ds} \right) = 12\mu u \frac{d}{ds}(ph) \tag{6}$$

where the term $6\lambda_a p_a h^2 dp/ds$ is for the slip boundary effect, λ_a is the mean-free-path of the air molecules (2.65×10^{-6} *inches*), μ is the dynamic viscosity of the air (2.6396×10^{-9} *psi·s* at 70 degrees F), u is the speed of the web and the two rollers, and p_a is the ambient pressure (14.7 *psia*). Note that the pressure in Eq. (6) is absolute pressure.

The pressure boundary conditions at the start and end points of the web are

$$p\big|_{s=0} = 14.7\ psia \quad \text{and} \quad p\big|_{s=L} = 14.7\ psia \tag{7}$$

These pressures are the same as the ambient pressure because the locations are far from the wrapped zone.

The pressure between the web and the winding roll, p_1, is obtained by solving the Reynolds equation with given h_1, and the other pressure, p_2, is calculated in the same way with given h_2. For the simple foil bearing problem (zero nip force case), p_2 is replaced by the ambient pressure.

2.2 Web Deflection Equation

A force balance equation of the web can be written in a one-dimensional form including the bending stiffness of the web and the contact pressure (Muftu, 1995). The web can be modeled as a cylindrical shell subjected to the air pressures, wrap pressure, and contact pressure.

$$\bar{d}\frac{d^4w}{ds^4} - T\frac{d^2w}{ds^2} = p_1 - p_2 - \bar{p}_w + p_c \tag{8}$$

where w is web displacement, T is web tension, p_1 is the pressure between the web and winding roll, p_2 is the pressure between web and nip roller, $\bar{p}_w$ is the wrap pressure, p_c is the contact pressure, and $\bar{d}$ is the bending stiffness of the web defined as

$$\bar{d} = \frac{Et^3}{12\left(1-\nu^2\right)} \tag{9}$$

The tension causes a pull down pressure over the wrapped region, $\bar{p}_w$, which is defined as

$$\bar{p}_w = \begin{cases} 0 & \text{inlet region} \\ T/R_1 & \text{wrapped region} \\ 0 & \text{outlet region} \end{cases} \tag{10}$$

The contact pressure, p_c in Eq. (8), should be considered when the air film thickness is smaller than the surface roughness. Usually when the web is permeable, the gap can be very small so that the contact pressure should be considered. When the roller is grooved, the web can contact the roller locally so that the contact pressure becomes important. In this study, we assume that the surfaces of the web and the rollers are perfectly smooth and the contact pressure term is neglected. The force balance equation can be rewritten as

$$\bar{d}\frac{d^4w}{ds^4} - T\frac{d^2w}{ds^2} = p_1 - p_2 - \bar{p}_w \tag{11}$$

The air gaps in the regions of the inlet and outlet are defined as the web displacement plus the inlet and outlet geometry that can be approximated as a parabolic curve.

$$h = w + \delta \tag{12}$$

where h is the air gap and δ is the inlet and outlet geometry (Figure 1).

The above equation requires four boundary conditions. The following boundary conditions are used in this study:

$$w\big|_{s=0} = 0, \quad \left.\frac{d^2w}{ds^2}\right|_{s=0} = 0, \quad w\big|_{s=L} = 0, \text{ and } \left.\frac{d^2w}{ds^2}\right|_{s=L} = 0 \tag{13}$$

Another possible boundary conditions are

$$\left.\frac{dw}{ds}\right|_{s=0} = 0\,, \quad \left.\frac{d^2w}{ds^2}\right|_{s=0} = 0\,, \quad w|_{s=L} = 0\,, \text{ and } \left.\frac{d^2w}{ds^2}\right|_{s=L} = 0 \tag{14}$$

The reason that Eq (13) is chosen in this study is described in Section 4.1.

CHAPTER III

NUMERICAL SOLUTION OF THE GOVERNING EQUATIONS

A closed-form solution that satisfies the two governing equations, Eq. (6) and Eq. (11), could not be obtained analytically because one of the equations has a stiff non-linear term $p\frac{dp}{ds}$. Therefore, a numerical method (finite-difference method) was chosen to solve them. In this chapter, non-dimensional forms of the two equations will be introduced, then finite-difference equations of them will be shown after linearizing the non-linear term, $p\frac{dp}{ds}$. At the final step, the computational algorithm will be presented.

3.1 Dimensionless Forms

Reynolds equations

One of the most common methods of non-dimensionalizing the Reynolds equation for foil bearing problems is to introduce the following non-dimensional parameters:

$$\varepsilon = \frac{12\mu u}{T}, \quad S = \frac{s}{R_1}\varepsilon^{-1/3}, \quad H = \frac{h}{R_1}\varepsilon^{-2/3}, \quad \text{and} \quad P = \frac{p}{p_a} \tag{15}$$

where the foil bearing number $\varepsilon = \frac{12\mu u}{T}$ is used for scaling because the film thickness h is very small in the wrapped zone, especially near the nip. Too small numbers may cause round-off errors. The non-dimensional form of the equation is

$$\frac{d}{dS}\left(PH^3 \frac{dP}{dS} + \Lambda_a H^2 \frac{dP}{dS} \right) = \frac{1}{B}\frac{d}{dS}(PH) \tag{16}$$

where $\Lambda_a = \frac{6\lambda_a}{R_1}\varepsilon^{-2/3}$ and $B = \frac{R_1 P_a}{T}$. For more detailed derivation of Eq. (16), see Appendix A.

Web deflection equation

The web deflection equation, Eq. (11), can be non-dimensionalized as

$$D\frac{d^4W}{dS^4} - \frac{d^2W}{dS^2} = B(P_1 - P_2) - P_w \tag{17}$$

where the following non-dimensional parameters are used

$$\varepsilon = \frac{12\mu u}{T}, \quad S = \frac{s}{R_1}\varepsilon^{-1/3}, \quad W = \frac{w}{R_1}\varepsilon^{-1/3}, \quad P_1 = \frac{p_1}{P_a}, \text{ and } P_2 = \frac{p_2}{P_a} \tag{18}$$

and the non-dimensional bending stiffness and wrap pressure are

$$D = \frac{Et^3}{12(1-\nu^2)TR_1^2}\varepsilon^{-2/3} \tag{19}$$

$$P_w = \begin{cases} 0 & \text{inlet zone} \\ 1 & \text{wrapped zone} \\ 0 & \text{outlet zone} \end{cases} \tag{20}$$

For the derivation of these equations, see appendix A.

3.2 Finite Difference Forms

Reynolds equations

The non-linear term $p\frac{dp}{ds}$ cab be linearized as shown below.

$$\begin{aligned} P\frac{dP}{dS} &= \left[\overline{P} + \left(P - \overline{P}\right)\right]\left[\frac{d\overline{P}}{dS} + \left(\frac{dP}{dS} - \frac{d\overline{P}}{dS}\right)\right] \\ &= \overline{P}\frac{d\overline{P}}{dS} + \left(P - \overline{P}\right)\frac{d\overline{P}}{dS} + \overline{P}\left(\frac{dP}{dS} - \frac{d\overline{P}}{dS}\right) + \left(P - \overline{P}\right)\frac{d(P - \overline{P})}{dS} \\ &\cong P\frac{d\overline{P}}{dS} - \overline{P}\frac{d\overline{P}}{dS} + \overline{P}\frac{dP}{dS} \end{aligned} \tag{21}$$

where the upper bar designates the value calculated one step before. The last term in the second line of Eq. (21) can be neglected by the assumption that a very small change occurs in the calculated pressure at each iteration (Chang, Chambers, and Shelton, 1994), $\left(P - \overline{P}\right)\frac{d(P - \overline{P})}{dS} \approx 0$. The resulting Reynolds equation is

$$\frac{d}{dS}\left[H^3\left(P\frac{d\overline{P}}{dS} - \overline{P}\frac{d\overline{P}}{dS} + \overline{P}\frac{dP}{dS}\right) + \Lambda_a H^2\frac{dP}{dS}\right] = \frac{1}{B}\frac{d}{dS}(PH) \tag{22}$$

By taking central-difference approximations, the finite-difference form of Eq. (22) can be written as

$$A_i P_{i-1} + B_i P_i + C_i P_{i+1} = D_i \tag{23}$$

where

$$A_i = H_{i+1}^3 \overline{P}_{i+1} + H_{i-1}^3 \left(\overline{P}_{i+1} - 4\overline{P}_i + 6\overline{P}_{i-1}\right) + \Lambda_a \left(H_{i+1}^2 + 3H_{i-1}^2\right) + 2\Delta S H_{i-1} / B$$

$$B_i = -4\left(H_{i+1}^3 \overline{P}_{i+1} + H_{i-1}^3 \overline{P}_{i-1}\right) - 4\Lambda_a \left(H_{i+1}^2 + H_{i-1}^2\right)$$

$$C_i = H_{i+1}^3 \left(6\overline{P}_{i+1} - 4\overline{P}_i + \overline{P}_{i-1}\right) + H_{i-1}^3 \overline{P}_{i-1} + \Lambda_a \left(3H_{i+1}^2 + H_{i-1}^2\right) - 2\Delta S H_{i+1} / B$$

$$D_i = H_{i+1}^3 \overline{P}_{i+1} \left(3\overline{P}_{i+1} - 4\overline{P}_i + \overline{P}_{i-1}\right) + H_{i-1}^3 \overline{P}_{i-1} \left(\overline{P}_{i+1} - 4\overline{P}_i + 3\overline{P}_{i-1}\right)$$

Appendix B shows more details of the derivation. The two boundary conditions (Eq. (7)) become

$$P_0 = 1 \text{ and } P_{n+1} = 1 \tag{24}$$

The matrix form of Eq. (23) is

$$\begin{bmatrix} B_1 & C_1 & 0 & & & & \\ A_2 & B_2 & C_2 & 0 & & & \\ 0 & . & . & . & 0 & & \\ & 0 & A_i & B_i & C_i & 0 & \\ & & 0 & . & . & . & 0 \\ & & & 0 & A_{n-1} & B_{n-1} & C_{n-1} \\ & & & & 0 & A_n & B_n \end{bmatrix} \begin{Bmatrix} P_1 \\ P_2 \\ . \\ P_i \\ . \\ P_{n-1} \\ P_n \end{Bmatrix} = \begin{Bmatrix} D_1 - A_1 P_0 \\ D_2 \\ . \\ D_i \\ . \\ D_{n-1} \\ D_n - C_n P_{n+1} \end{Bmatrix} \tag{25}$$

By solving this matrix equation, a new pressure profile can be obtained for a given gap profile with a guessed initial pressure profile, which is just a part of the entire calculation discussed in the next section, 3.3. In order to obtain an accurate solution for a given gap profile, Eq. (25) needs to be solved iteratively replacing $\overline{P}_i$ s with P_i s at each iteration. With a well-guessed initial pressure profile, the iteration number can be one or two, but with a roughly guessed one, it can be four or more. The algorithm of the entire calculation will be discussed in Section, 3.3.

Web deflection equation

The finite-difference form of the web deflection equation (Eq. (17)) can be written by taking central-difference approximations.

$$E_1 W_{i-2} + E_2 W_{i-1} + E_3 W_i + E_4 W_{i+1} + E_5 W_{i+2} = F_i \qquad i = 1,2,\ldots \text{n} \tag{26}$$

where

$$E_1 = E_5 = \frac{D}{\Delta S^4} + \frac{1}{12\Delta S^2}$$

$$E_2 = E_4 = -\left(\frac{4D}{\Delta S^4} + \frac{4}{3\Delta S^2}\right)$$

$$E_3 = \frac{6D}{\Delta S^4} + \frac{5}{2\Delta S^2} \tag{27}$$

$$F_i = B(P_{1i} - P_{2i}) - P_{bw}$$

The matrix form of Eq. (26) can be written as below by applying the boundary conditions (Eq. (13)).

$$\begin{bmatrix} E_{1,1} & E_{1,2} & E_{1,3} & 0 & & & & & \\ E_2 & E_3 & E_4 & E_5 & 0 & & & & \\ E_1 & E_2 & E_3 & E_4 & E_5 & 0 & & & \\ 0 & . & . & . & . & . & 0 & & \\ & 0 & . & . & . & . & . & 0 & \\ & & 0 & E_1 & E_2 & E_3 & E_4 & E_5 & \\ & & & 0 & E_1 & E_2 & E_3 & E_4 & \\ & & & & 0 & E_{n,n-2} & E_{n,n-1} & E_{n,n} & \end{bmatrix} \begin{bmatrix} W_1 \\ W_2 \\ W_3 \\ . \\ . \\ W_{n-2} \\ W_{n-1} \\ W_n \end{bmatrix} = \begin{bmatrix} F_1 \\ F_2 \\ F_3 \\ . \\ . \\ F_{n-2} \\ F_{n-1} \\ F_n \end{bmatrix} \tag{28}$$

where $E_{1,1}, E_{1,2}, E_{1,3}, E_{n,n-2}, E_{n,n-1}, E_{n,n}$ are changed by applying the boundary conditions.

The non-dimensional expression of the boundary conditions are

$$W\big|_{S=0} = 0, \quad \left.\frac{d^2W}{dS^2}\right|_{S=0} = 0, \quad W\big|_{S=L} = 0, \text{ and } \left.\frac{d^2W}{dS^2}\right|_{S=L} = 0 \tag{29}$$

The finite-difference forms of Eq. (29) are

$$W_0 = 0 \tag{30}$$

$$\left.\frac{d^2W}{dS^2}\right|_{i=1} = \frac{-W_3 + 16W_2 - 30W_1 + 16W_0 - W_{-1}}{12\Delta S^2} = 0 \tag{31}$$

$$W_{n+1} = 0 \tag{32}$$

$$\left.\frac{d^2W}{dS^2}\right|_{i=n} = \frac{-W_{n+2} + 16W_{n+1} - 30W_n + 16W_{n-1} - W_{n-2}}{12\Delta S^2} = 0 \tag{33}$$

The fictitious points, W_{-1}, W_0, W_{n+1}, and W_{n+2} can be replaced by the combination of W_1, W_2, . . W_{n-1}, and W_n as shown below.

$$W_0 = 0 \tag{34}$$

$$W_{-1} = -30W_1 + 16W_2 - W_3 \tag{35}$$

$$W_{n+1} = 0 \tag{36}$$

$$W_{n+2} = -30W_n + 16W_{n-1} - W_{n-2} \tag{37}$$

The resulting modified elements of the matrix in Eq. (28) are

$$E_{1,1} = E_3 - 30E_1 = \left(\frac{6D}{\Delta S^4} + \frac{5}{2\Delta S^2}\right) - 30\left(\frac{D}{\Delta S^4} + \frac{1}{12\Delta S^2}\right) = -24\frac{D}{\Delta S^4}$$

$$E_{1,2} = 16E_1 + E_4 = 16\left(\frac{D}{\Delta S^4} + \frac{1}{12\Delta S^2}\right) - \left(\frac{4D}{\Delta S^4} + \frac{4}{3\Delta S^2}\right) = 12\frac{D}{\Delta S^4}$$

$$E_{1,3} = E_5 - E_1 = 0$$

$$E_{n,n-2} = E_1 - E_5 = E_5 - E_1 = E_{1,3} = 0$$

$$E_{n,n-1} = E_2 + 16E_5 = E_4 + 16E_1 = E_{1,2} = 12\frac{D}{\Delta S^4}$$

$$E_{n,n} = E_3 - 30E_5 = E_3 - 30E_1 = E_{1,1} = -24\frac{D}{\Delta S^4}$$

Appendix B shows a more detailed derivation. By solving this matrix equation (Eq. (28)) the gap profile between the web and winding roll (H_1) can be obtained for given pressure profiles (P_1 and P_2). Contrary to solving the Reynolds equation, it is not an iterative calculation but just a one-time calculation because the web deflection equation is linear.

The gap profile between the web and the nip roller (H_2) is obtained in a different way, which will be explained in the next section.

3.3 Computational Algorithm

The detailed structure of the computer program, written in C-language, is described in this section. Figure 2 shows the flow chart of this program. Guessed initial pressure profile and gap profile are inputted, then a new pressure profile between the web and the winding roll (P_1) is obtained by solving the Reynolds equation, and the other pressure profile between the web and the nip roller (P_2) is calculated by solving the same governing equation. Now, a new gap profile between the web and the winding roll (H_1) can be computed by solving the web deflection equation with the new pressure profiles. The other gap between the web and the nip roller (H_2) is calculated with a simple geometric relation (Eq. (2)). This is the completion of one iteration. The new profiles H_1, H_2, P_1, and P_2 are used as initial profiles for the next iteration, and the iteration continues until the solutions converge. Note that solving the Reynolds equation is also an iterative process. The flow chart (Figure 2) will be described step by step.

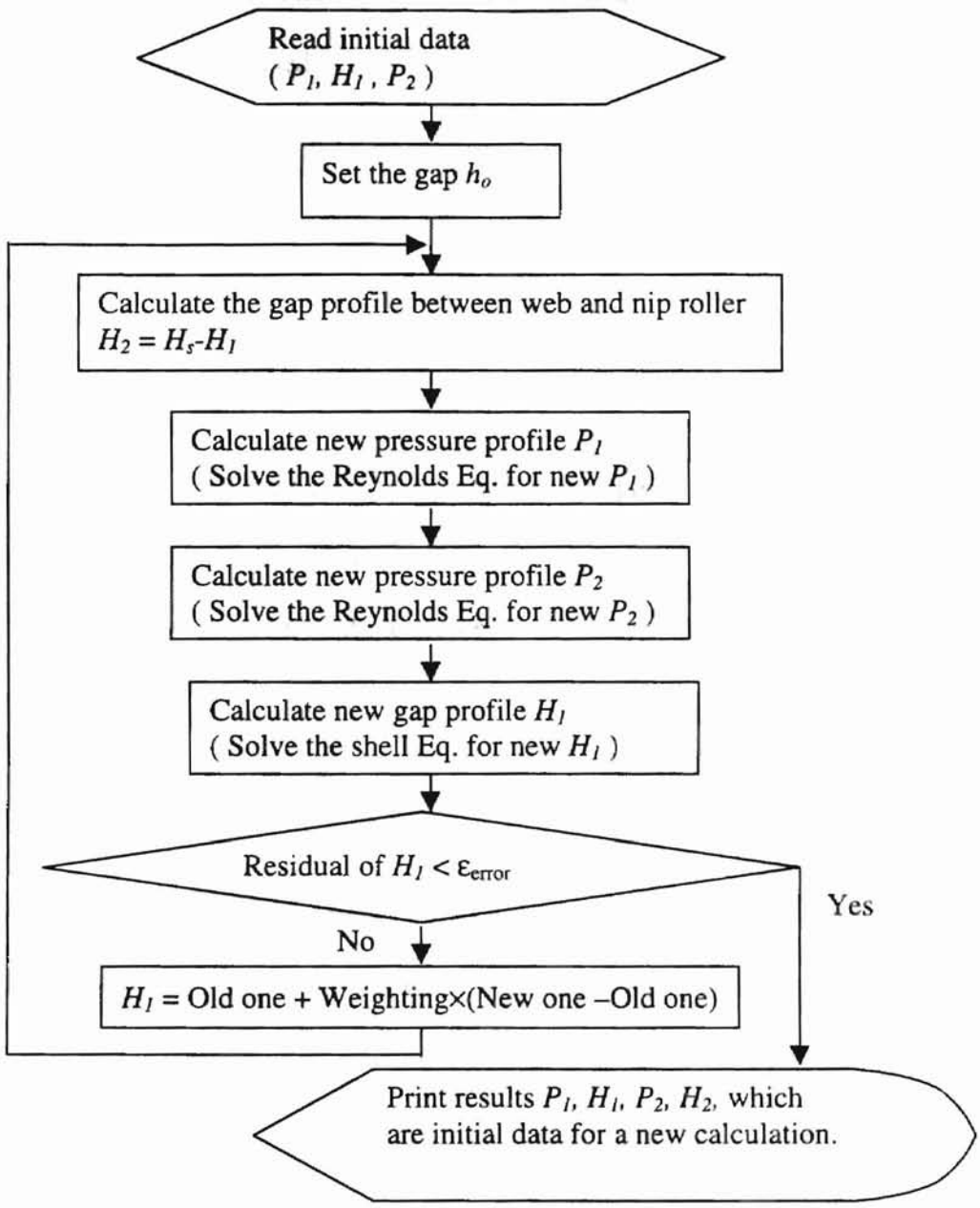

Figure 2. Flow chart of the computational program

Step 1: Read initial data, H_1, P_1, and P_2

To solve the foil-bearing problem by the finite-difference method, very good initial guessed profiles are needed. For the first iteration, curve-fitted initial profiles

based on known foil bearing solutions are used. For the wrapped zone the following solutions for foil bearings are used

$$\frac{h}{R}\left(\frac{12\mu u}{T}\right)^{-2/3} = 0.643 \tag{38}$$

$$\frac{p - p_a}{T/R} = 1 \tag{39}$$

After getting the solution for the case of zero nip force, the pressure and web deflection profiles are used as initial profiles for a case of small nip force. The new solution then provides the initial pressure and web deflection profiles for another case where the nip force is slightly larger.

Step 2: Set the gap at the center of nip, h_o

After setting the gap at the center of the nip (h_o), the gap profile between the nip roller and the winding roll (H_S) is determined by Eq. (3), which is non-dimensionlized as

$$H_S = H_o + \left(\frac{R_1 + R_2}{2R_2}\right)X^2 \tag{40}$$

where

$$X = \frac{x}{R_1}\varepsilon^{-1/3} \quad , \quad H_o = \frac{h_o}{R_1}\varepsilon^{-2/3} \quad , \quad H_S = \frac{h_s}{R_1}\varepsilon^{-2/3} \tag{41}$$

Step 3: Calculate the gap profile between web and nip roller, H_2

H_2 is defined as $H_2 = H_s - H_1$, which is a dimensionless form of Eq. (2)

Step 4: Solve the Reynolds equation for P_1 and P_2

The Reynolds equation is solved to determine the pressure profile for a given gap profile. As mentioned in Section 3.2, the Reynolds equation requires iteration process to be solved. However, the solution converges within a few iterations without any under-relaxation. The iteration of the entire calculation will be mentioned in Step 5. P_1 and P_2 are calculated for given h_1 and h_2, respectively.

Step 5: Determine web deflection and H_1

In Step 4, we obtained the new pressure profiles P_1 and P_2, but they are not the final solution because the given gap profiles used to obtain P_1 and P_2 are not the final solution. However, we can calculate a more accurate gap profile H_1 with the new pressure profiles by solving the web deflection equation (Eq. (17)). Unlike the Reynolds equation, the web deflection equation can be solved without iteration because it is a linear differential equation. If the new gap profile is used without under-relaxation on the next iteration, it may diverge very quickly. Therefore a weighted profile is used on the next iteration, which is defined as

$$\text{Weighted profile} = (\text{Old one}) + (\text{Weighting}) \times (\text{New one} - \text{Old one}) \qquad (42)$$

If the residual of H_1 is larger than the criterion, go back to the Step 3. Then iterate until the solution converges. The value of the weighting factor required for convergence depends on the values of test conditions such as nip force, initial data, and web stiffness.

Typically, the weighting factor needs to be smaller than 0.01. Sometimes, especially when the nip force is large, it should be less than 0.0001. When relatively large weighting factors are used, several thousand iterations are needed. When the weighting factor is under 0.0001, more than one hundred thousand iterations are necessary for convergence.

Step 6: Print results of P_1, P_2, H_1, H_2, h_{1c}, h_{2c}, and F

After the solution has converged, print out the pressure and gap profiles, as well as the nip force calculated by integrating P_2 using Simpson's 1/3 rule. The amount of entrained air is determined based on the air film thickness and the pressure at the location where the pressure gradient is zero. The lubricant process is assumed isothermal so that

$$\frac{p}{\rho} = C = \text{constant}$$

The flow velocity profile is

$$u(z) = \frac{1}{2\mu}\frac{dp}{dx}\left(z^2 - hz\right) + \left(u_2 - u_1\right)\frac{z}{h} + u_1 \tag{43}$$

When $dp/dx = 0$ and the speeds of the two surfaces are the same ($u_1 = u_2 = u$), the velocity profile is uniform.

$$u(z) = u \tag{44}$$

The mass flow rate can be written as

$$\rho_1 \cdot u \cdot h_1 = \rho_a \cdot u \cdot h_{1c} \tag{45}$$

where ρ_1 and h_1 are the air density and the air gap where the pressure is maximum, and ρ_a is the air density at the ambient pressure. From Eq. (45) we obtain

$$h_{1c} = h_1 \cdot \frac{p_1}{p_a} \tag{46}$$

Therefore, the amounts of air entrainment, h_{1c} and h_{2c}, can be obtained as

$$\begin{aligned} h_{1c} &= h_1 \times \frac{p_1}{p_a} \qquad \text{at} \quad \frac{dp_1}{dx} = 0 \\ h_{2c} &= h_2 \times \frac{p_2}{p_a} \qquad \text{at} \quad \frac{dp_2}{dx} = 0 \end{aligned} \tag{47}$$

The solution in Step 6 is just for one case, which can be a good initial data for a little different case. In order to study the effects of nip force, the value of h_o is changed, new solutions are obtained, and the value of nip force is obtained by integrating the pressure profile p_2. The computer program shown in Appendix E calculates the nip force and the amount of air entrainment.

CHAPTER IV

RESULTS AND DISCUSSIONS

Typical wrapping conditions for winding with a nip roller can be divided into two groups: The first is the case where the web wraps the winding roll prior to the nip (Type A), and the other is the case where the web first wraps the nip roller (Type B).

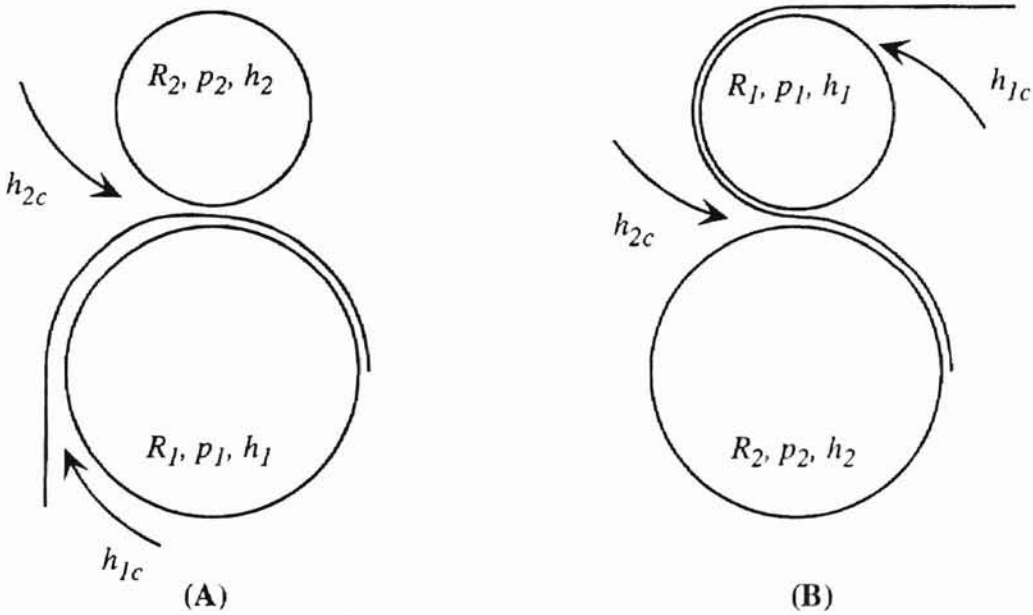

Figure 3. Two typical types of winding systems

Type A is chosen as the computational model in this study, but the results for Type A can be applied to Type B to some extent. It is believed that the wrapping condition after the nip has very little effects on the results.

One of the interesting phenomena related to winding with a nip roller is ballooning which sometimes causes a wrinkling problem. Section 4.2 and Section 4.3

discuss how the ballooning phenomenon is affected by the design and operation parameters such as nip force, incoming wrap angle, web stiffness, web speed, and web tension. Section 4.4 discusses the effects of the above parameters on the air entrainment. The computational model of this study is limited to rigid rolls, which is believed to be adequate for predicting the ballooning phenomena.

4.1 Simple Foil Bearing Solution (Zero Nip Force)

Before starting to analyze the effects of nip roller, we need to compare the simple foil bearing solutions of this study with the solutions obtained by others. The nominal clearance for an infinitely wide, perfectly flexible foil is (Eshel, 1965)

$$\frac{h^*}{R} = 0.643\left(\frac{12\mu u}{T}\right)^{2/3} \tag{48}$$

This equation can be used with negligibly small errors when (Gross, 1980b):

Stiffness: $$D \equiv \frac{Et^3}{12(1-\nu^2)TR^2}\varepsilon^{-2/3} < 0.8 \tag{49}$$

Compressibility: $$\frac{1}{B} \equiv \frac{T}{p_a R} < 0.12 \tag{50}$$

Inertia: $$I \equiv \frac{1}{2}\frac{\rho_a u^2}{T/R} < 0.05 \tag{51}$$

Wrap angle: $$S \equiv \frac{\theta}{\varepsilon^{1/3}} \geq 6 \tag{52}$$

Foil width (b): $$\sqrt{tR} \ll 2b \tag{53}$$

4.1.1 Perfectly flexible web ($EI = 0$)

Eshel examined the compressibility effects on the one-dimensional perfectly flexible foil bearing (Eshel, 1967). Figure 4 shows that the nominal clearance decreases with the compressibility parameter (T/p_aR). Figure 5 is a solution of the current study for an infinitely wide, perfectly flexible foil for the compressibility parameter ($1/B$) of 0.017; the nominal clearance constant is 0.6348 in this study. From Figure 4, the nominal clearance constant is about 0.64 for the compressibility parameter of 0.017. It can be said that the results of the current study for perfectly flexible web show a good agreement with the solutions obtained by Eshel.

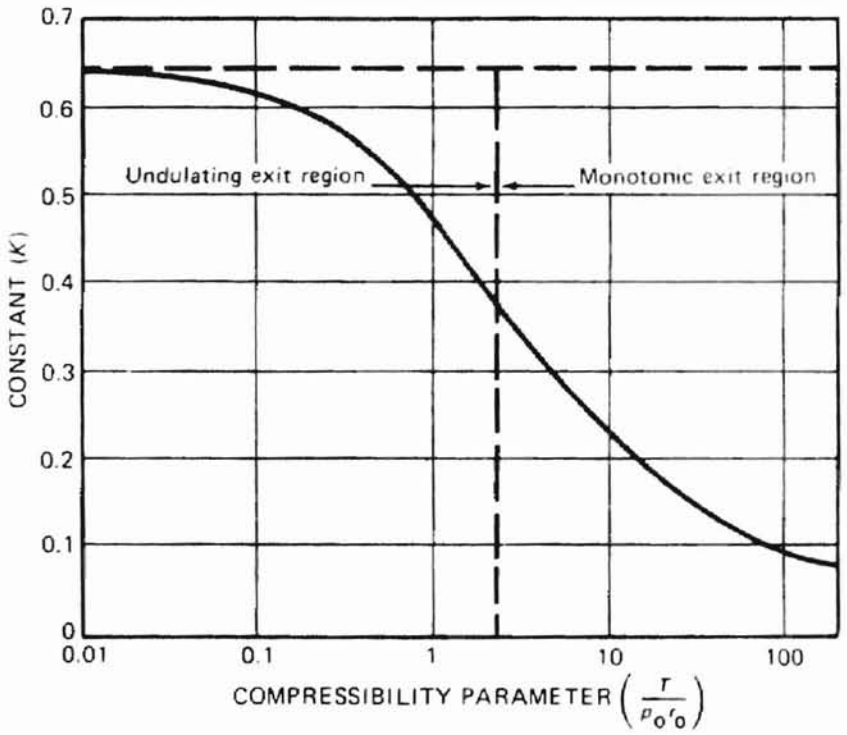

Figure 4. Nominal clearance vs. compressibility (Gross, 1980b)

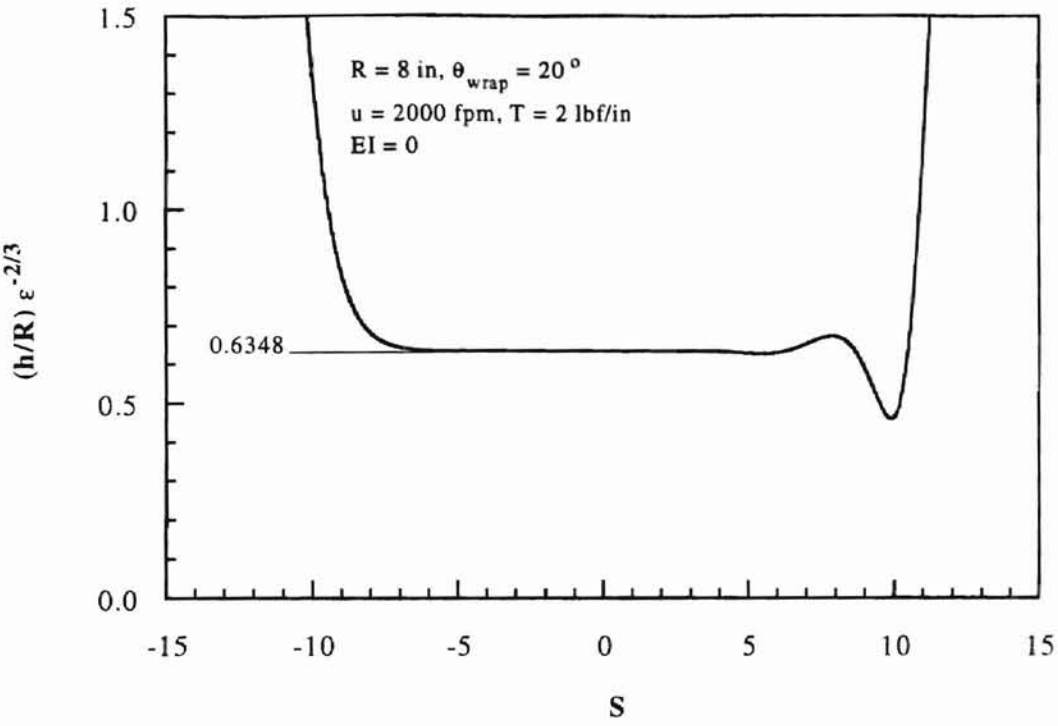

Figure 5. Simple foil bearing solution for perfectly flexible web

Ignoring the bending stiffness term, the web deflection equation (Eq. (11)) becomes a second-order linear differential equation, which is generally called membrane equation.

$$-T\frac{d^2w}{ds^2} = p_1 - p_2 - \bar{p}_w \tag{54}$$

There are two possible sets of boundary conditions for the above membrane equation:

$$w\big|_{s=0} = 0\,, \quad w\big|_{s=L} = 0 \qquad : \text{BCs \#1} \tag{55}$$

$$\left.\frac{dw}{ds}\right|_{s=0} = 0\,, \quad w\big|_{s=L} = 0 \qquad : \text{BCs \#2} \tag{56}$$

For the shell equation, the two possible sets of boundary conditions are given by Eq. (13) and Eq. (14). The two solutions for a membrane with the two different sets of boundary conditions are shown in Figure 6. The nominal clearance constants, H^*, for the two cases are almost the same. The BCs #1 is chosen in this study mainly because the solution converged much faster with BCs #1 especially when the nip force is large.

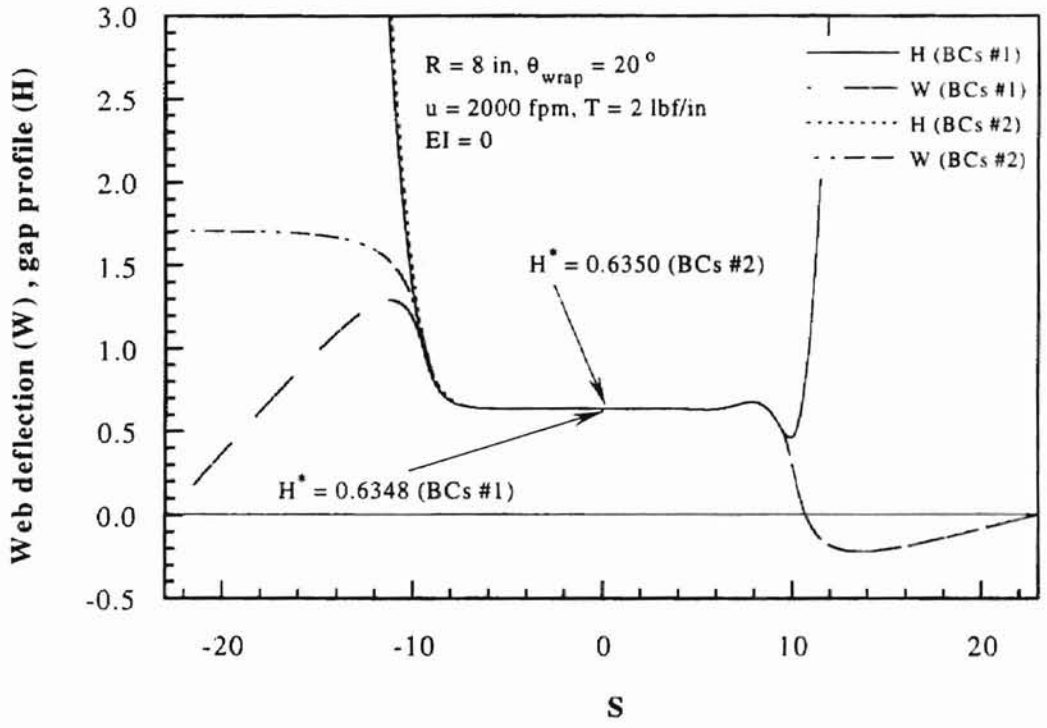

Figure 6. Effects of boundary conditions on the nominal clearance

A detailed discussion of the finite-difference equations of the membrane equation with the two different sets of boundary conditions is included in Appendix C.

The convergence behaviors for the two cases are further discussed here. Table 1 shows how the weighting factor was varied during an example calculation for each set of boundary condition (refer to Figure 2). In order to start the iteration with roughly guessed initial data, very small weighting factor was needed; and the weighting factor

could be gradually increased to accelerate the calculation. The allowable increment of the weighting factor depends mainly on the radii of the rolls, wrap angle, and the boundary conditions. For nipped cases, it is also highly dependent on the value of nip force. As shown in Table 1, the weighting factor could be increased up to 0.0045, and the number of iteration for convergence was 3800 when BCs #1 was chosen. However, when BCs #2 was chosen, the weighting factor could not be increased over 0.0005, and a large number of iteration (19600 in this example) was needed for convergence.

Table 1. Effects of boundary conditions on convergence

BCs #1		BCs #2	
Iteration	Weighting Factor	Iteration	Weighting Factor
1 ~ 100	0.0001	1 ~ 100	0.0001
101 ~ 300	0.0005	101 ~ 600	0.0003
301 ~ 800	0.0020	601 ~ 19600	0.0005
801 ~ 1800	0.0040		
1801 ~ 3800	0.0045		
Other conditions : R = 8 in, θ_{wrap} = 20°, u = 2000 ft/min, T = 2 lbf/in,			

Figure 7 shows how the value of pressure changes at $S = 0$ (center of the nip) during the iteration. The trace for BCs #2 shows why the weighting factor could not be over 0.0005. When the trace oscillates like a sinusoidal function, computations with slightly worse conditions such as larger radius or larger wrap angle would not converge. Therefore, it can be said that BCs #1 is much better than BCs #2 for convergence. The solutions for the two cases are almost identical (error in H^* between the two cases is smaller than 0.05 % as shown in Figure 6). Figure 8 and Figure 9 show different convergence behaviors for the two different sets of boundary conditions, which are very helpful to determine convergence. For some cases, the solutions diverge very slowly

while drawing a spiral as shown in Figure 9. If the spiral is getting bigger, the solutions will diverge after all. In some cases, reducing the value of the weighting factor helps convergence; in other cases, solutions diverge regardless of the value of the weighting factor.

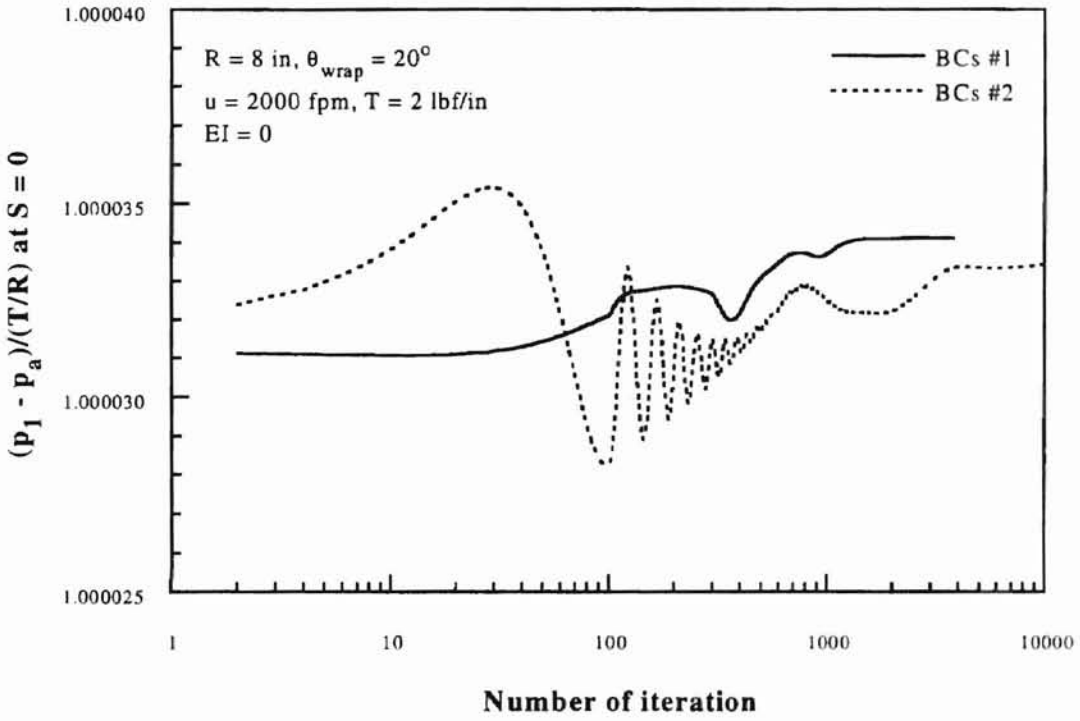

Figure 7. Effects of boundary conditions on convergence

In general, a solution is said to have converged when the difference between values of previous iteration and current iteration is smaller than a certain criterion. However, that simple concept cannot be used in this study because the criterion for convergence varies with operating conditions such as nip force or boundary condition. For the example case shown in Figure 9, the spiral was drawn within 500 iteration, then the values changed very slowly and very much, where the final converged point is very far from the end point of the spiral. For large nip force cases, convergence can be

obtained with relatively large residual that is defined as the summation of the value differences between iterations at each node. Most of the convergence behaviors of the computations in this study are very similar to the two typical cases like Figure 8 and Figure 9. The convergence in this study is determined manually based on the values of residual and solution trace graphs such as Figure 8 or Figure 9.

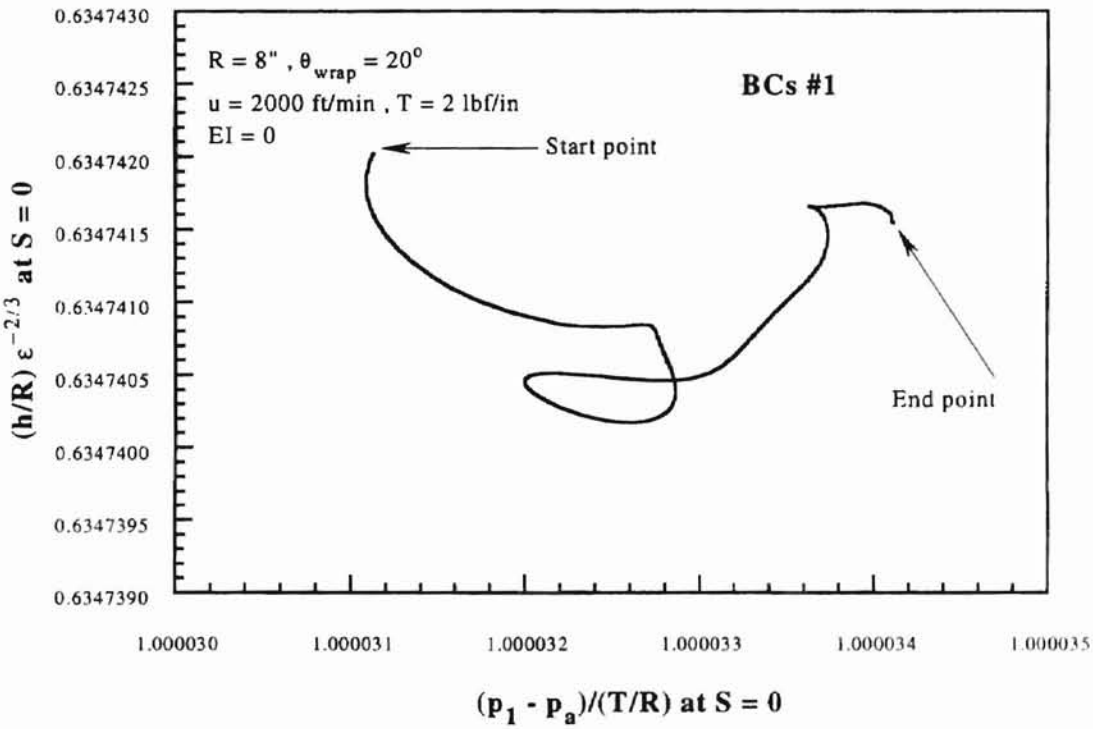

Figure 8. Trace of solution (pressure and gap) during iteration (BCs #1)

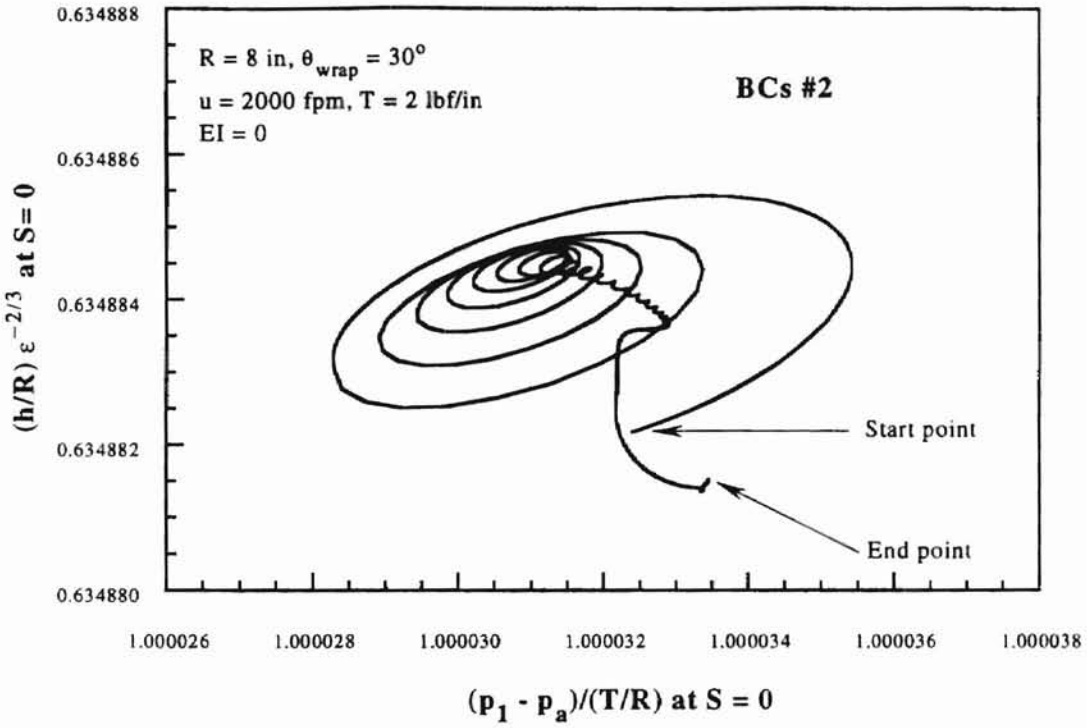

Figure 9. Trace of solution (pressure and gap) during iteration (BCs #2)

Even though Figure 8 and Figure 9 have different starting points, they can be used for examining convergence behavior because the convergence problem is highly dependent on the type of boundary conditions (BCs #1 or BCs#2).

4.1.2 Stiff web ($E = 10^5$ *psi*, $t = 0 \sim 20$ *mils*)

Figure 10 shows solutions with bending stiffness of the web taken into account as well as the compressibility of the air. The nominal clearance appears to increase with the bending stiffness of the web. Eshel examined the effects of foil stiffness for one-dimensional foil bearing (1967). Figure 11 shows that the nominal clearance decreases with the stiffness parameter (S in Figure 11 is the same as D in Figure 12). However, in Figure 12, the computational results of this study show the opposite trend. Note that Eshel's work (Figure 11) does not include the air compressibility effect, which is included in the current study (Figure 12).

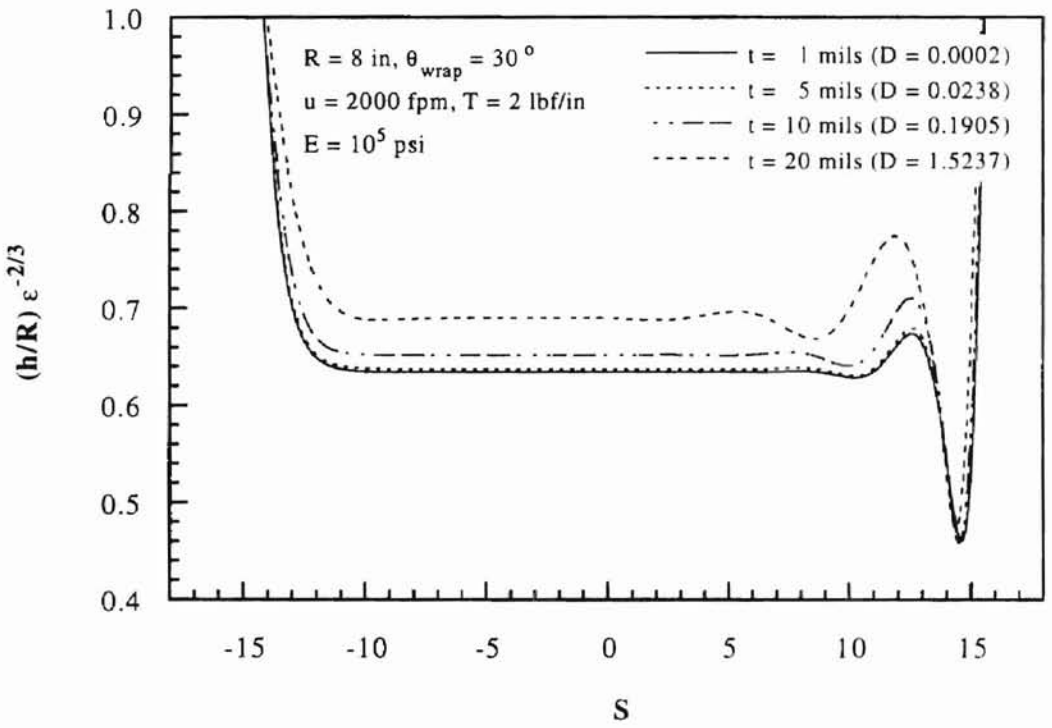

Figure 10. Simple foil bearing solution for stiff web ($E = 10^5$ *psi*, $t = 1 \sim 20$ *mils*)

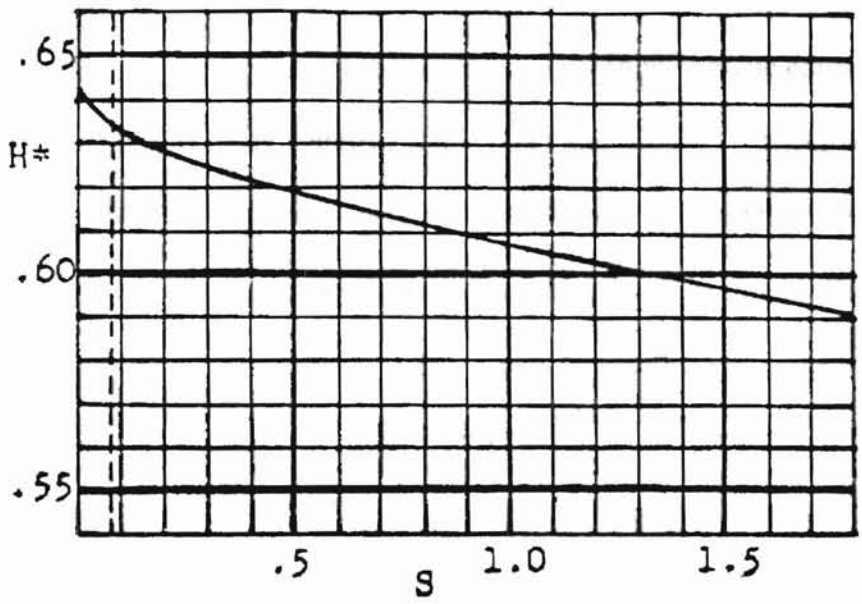

Figure 11. Nominal clearance vs. stiffness parameter (Eshel, 1967)

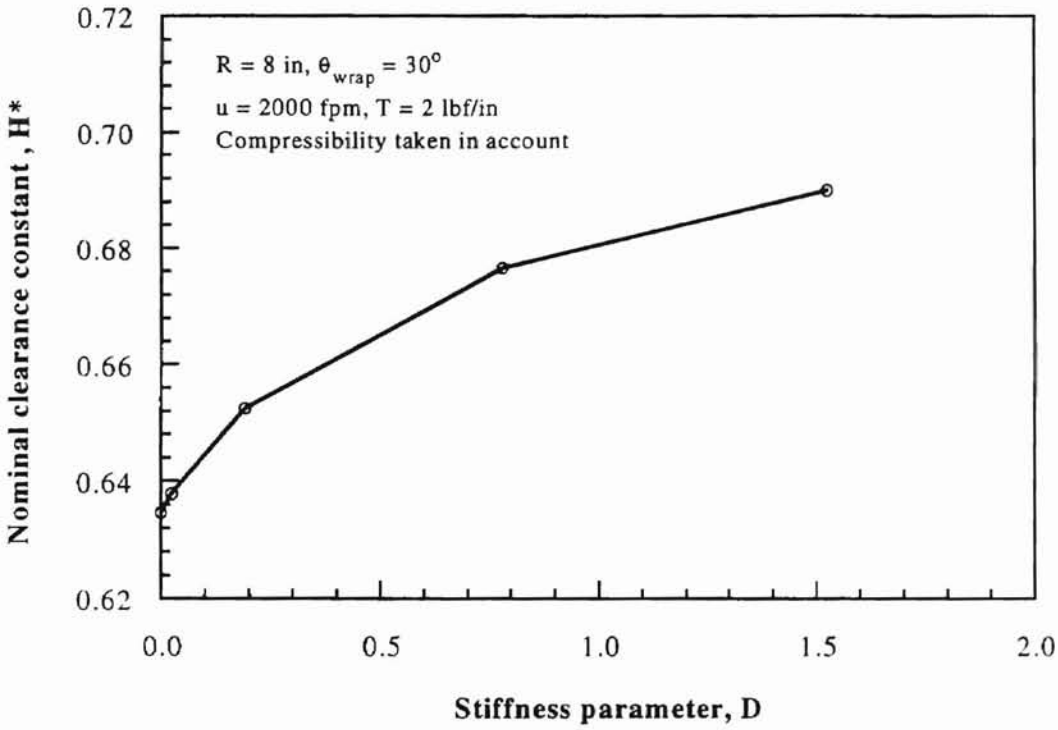

Figure 12. Nominal clearance vs. stiffness parameter

In Section 4.1.1, it is described that BCs #1 (Eq. (55)) is more preferable than BCs #2 (Eq. (56)) for convergence of the computation with membrane equation. In the same way, BCs #1 (Eq. (13)) is preferred to the other one (Eq (14)) for convergence of the computation with shell equation. When the web is very stiff and the web spans (L_{in} and L_{out}) are short, the calculation results are affected by the span length. For webs having $E = 10^5$ *psi* and $t = 20$ and 40 *mils*, the effects of span length on the nominal clearance constant is examined in Figure 13 through Figure 16. In Figure 13, the nominal clearance constants (H^*) for $L_{in} = L_{out} = 2$ *in* , 4 *in* , and 8 *in*, are 0.6851, 0.6896, and 0.6903, respectively. Figure 14 shows more detailed description of Figure 13. It is believed that the solution for the 8 *in* span case is most accurate. Compared to the nominal clearance (H^*) for $L_{in} = L_{out} = 8$ *in*, H^* for $L_{in} = L_{out} = 4$ *in* is 0.1 % lower, and H^* for $L_{in} = L_{out} = 2$ *in* is 0.7 % lower. For a stiffer web ($E = 10^5$, $t = 40$ *mils*), the nominal clearance constants for the three cases, 2 *in* span , 4 *in* span, and 8 *in* span, are 0.6865, 0.7104, and 0.7164, respectively (Figure 15 and Figure 16). The nominal clearance (H^*) for $L_{in} = L_{out} = 4$ *in* and 2 *in* are 0.8 % and 4.2 % lower than that for 8 *in*. Therefore, stiff webs (stiffness parameter, $D \geq 1.5$) require long inlet and outlet span length for accurate calculations. In order to save node numbers, most of the calculations were done with very short inlet and outlet span length, which is 2 *in*. However, stiffness parameter (D) was limited to 1.5 to avoid significant errors.

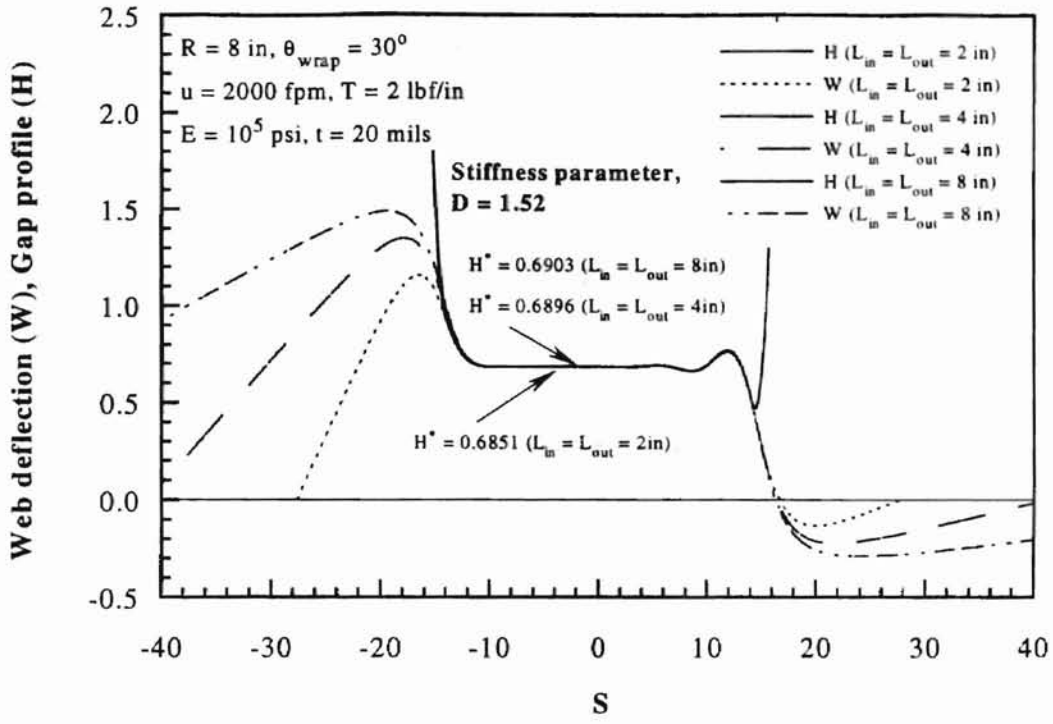

Figure 13. Effects of span length, L_{in} and L_{out} (t = 20 mils)

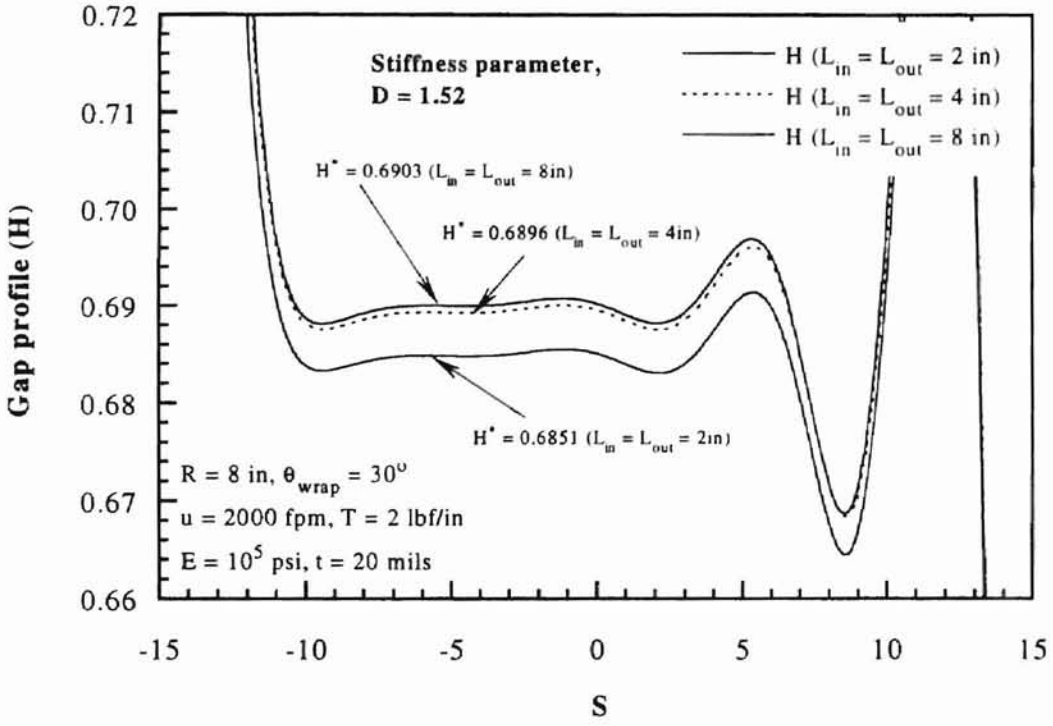

Figure 14. Detailed description of Figure 13

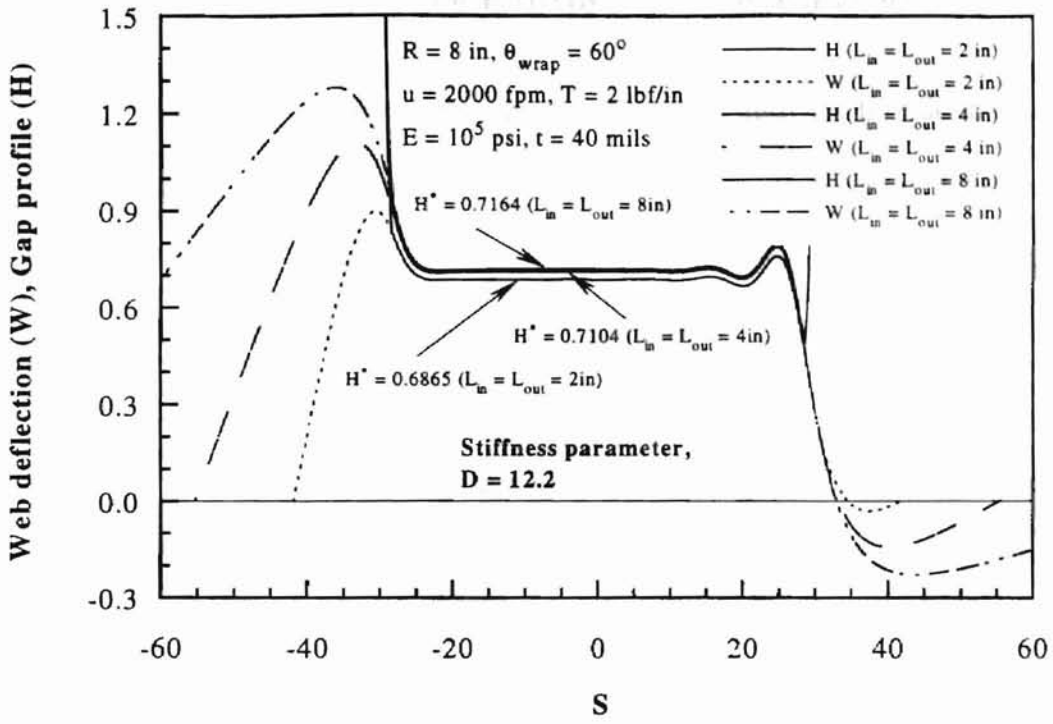

Figure 15. Effects of span length, L_{in} and L_{out} (t = 40 mils)

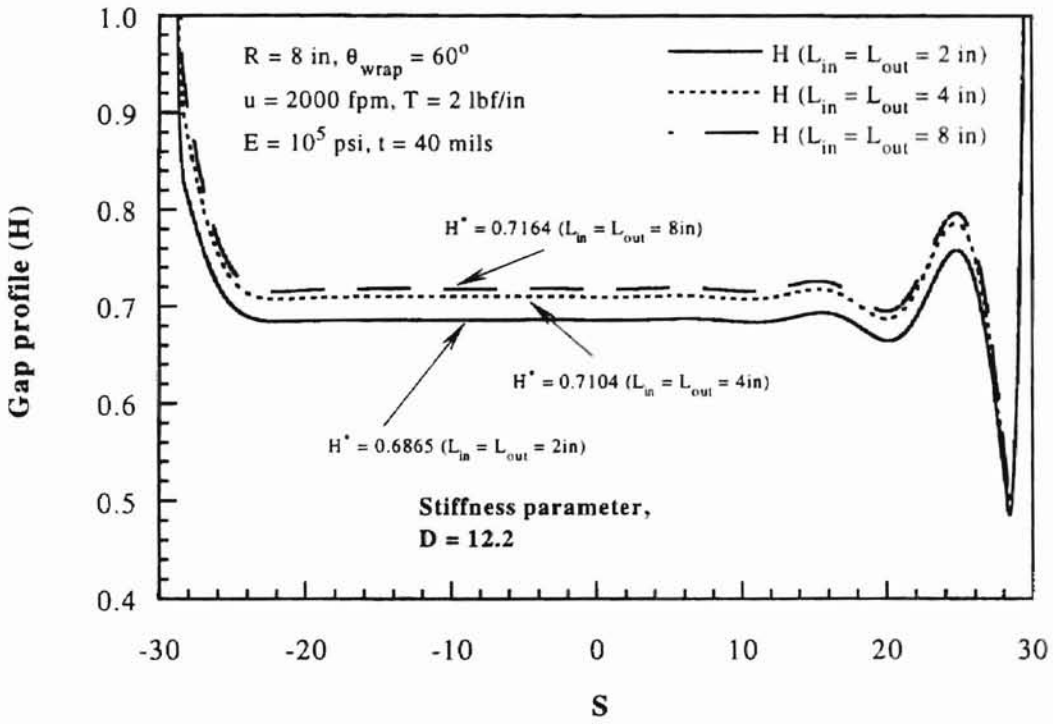

Figure 16. Detailed description of Figure 15

4.2 Ballooning for Perfectly Flexible Web ($EI = 0$)

At first, perfectly flexible webs were considered to study the formation of a balloon. It was found that there is a critical nip force above which ballooning occurs, and the incoming wrap angle affects the size of the balloon. In super-critical conditions, the balloon size does not change very much with the nip force. A large nip force causes a sharp peak pressure near the nip. Difficult convergence problems were experienced with perfectly flexible webs when the nip force and the wrap angle are large. To overcome this convergence problem, stiffness of the web was taken into account, then the effects of the web thickness and the incoming wrap angle on ballooning were examined. In addition, the effects of web speed and web tension on ballooning were examined for stiff webs, which will be discussed in Section 4.3.

4.2.1 Air gap and pressure profiles ($EI = 0$)

The values of important variables and constants are shown in Table 2. One of the most important parameters that affect the balloon shape is the incoming wrap angle of the web (θ_{in}) as shown in Figure 23. However, it is believed that the outgoing wrap angle does not influence the results, so that a very small angle was chosen (2 degrees) to reduce the number of nodes. Refer to Figure 17 for definition of variables.

Table 2. Conditions of calculation for perfectly flexible web

R_1 (inches)	R_2 (inches)	T (lb/in)	U (ft/min)	θ_{in} (degree)	θ_{out} (degree)
8	8	2	2000	8,13,20,30,50	2

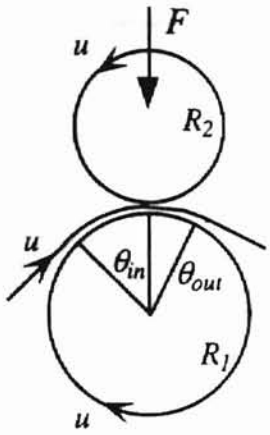

Figure 17. Schematic of model

Figure 18 and Figure 19 show that a balloon is not formed when the nip force is very small. Above a certain value of nip force, the gaps in front of the nip get larger dramatically, where there must be a back flow of air. The value of nip force above which ballooning occurs is called the critical nip force. The balloon shape and the maximum balloon height are not sensitive to the nip force, as shown in Figure 18 through Figure 22. The maximum balloon height increases with the incoming wrap angle, θ_{in}, as shown in Figure 23.

Pressure profiles and pressure difference profiles corresponding to Figure 18 through Figure 22 are shown in Figure 24 through Figure 32. The total number of nodes is 4000 for all these cases. This number is large enough to handle sharp pressure changes near the nip.

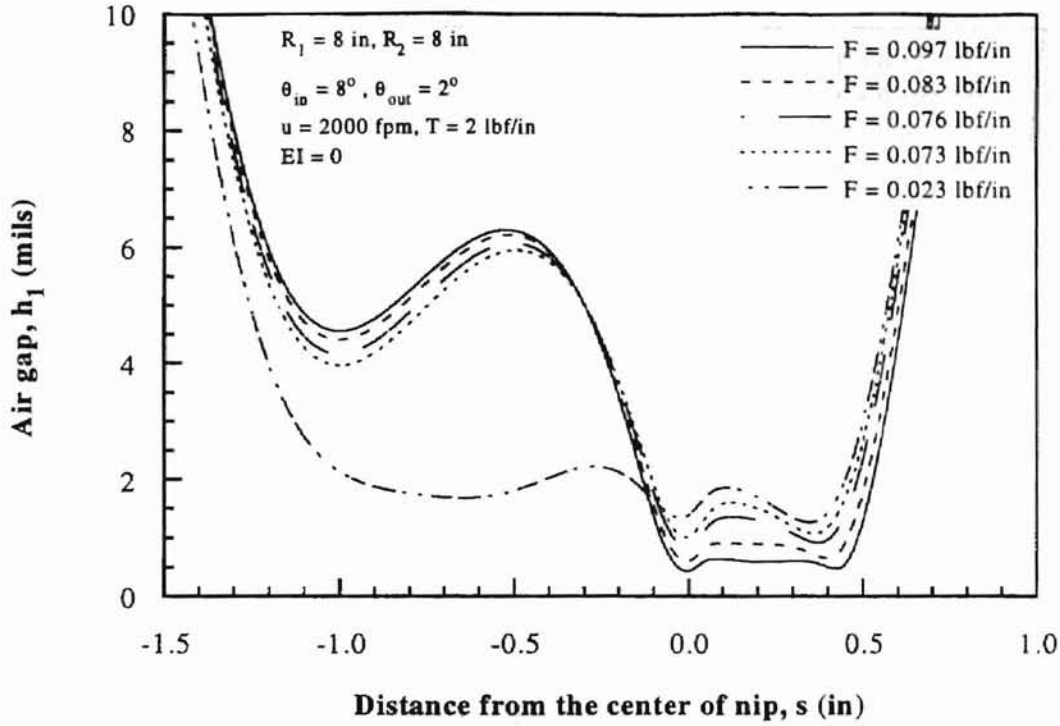

Figure 18. Gap profile h_1 for $\theta_{in} = 8^{\circ}$ and $EI = 0$

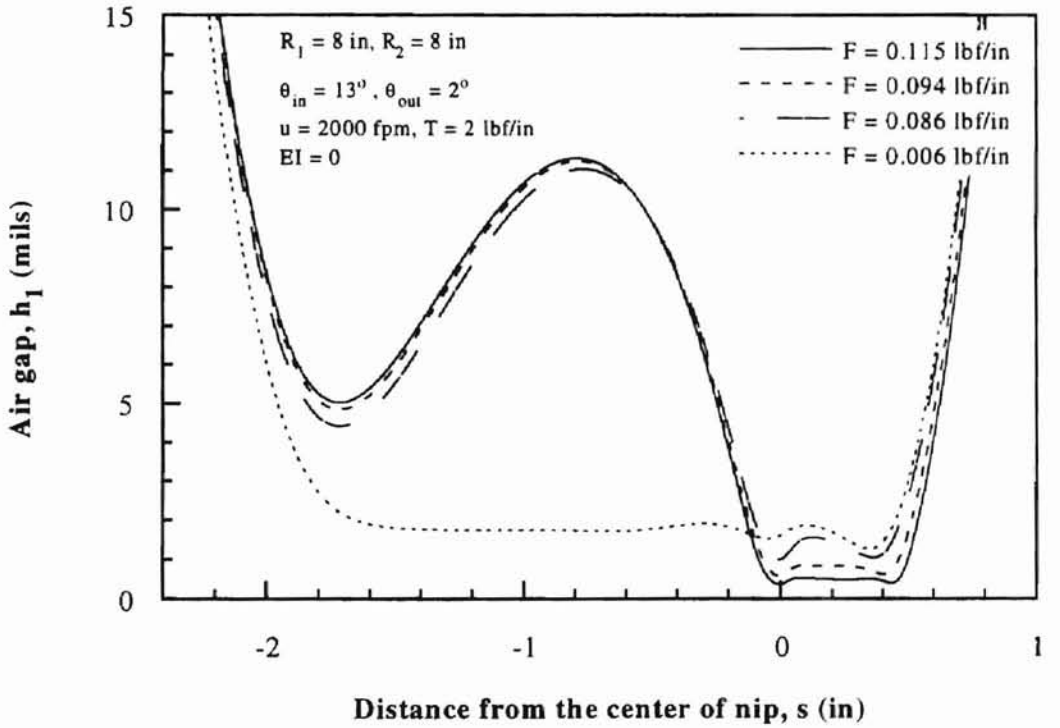

Figure 19. Gap profile h_1 for $\theta_{in} = 13^{\circ}$ and $EI = 0$

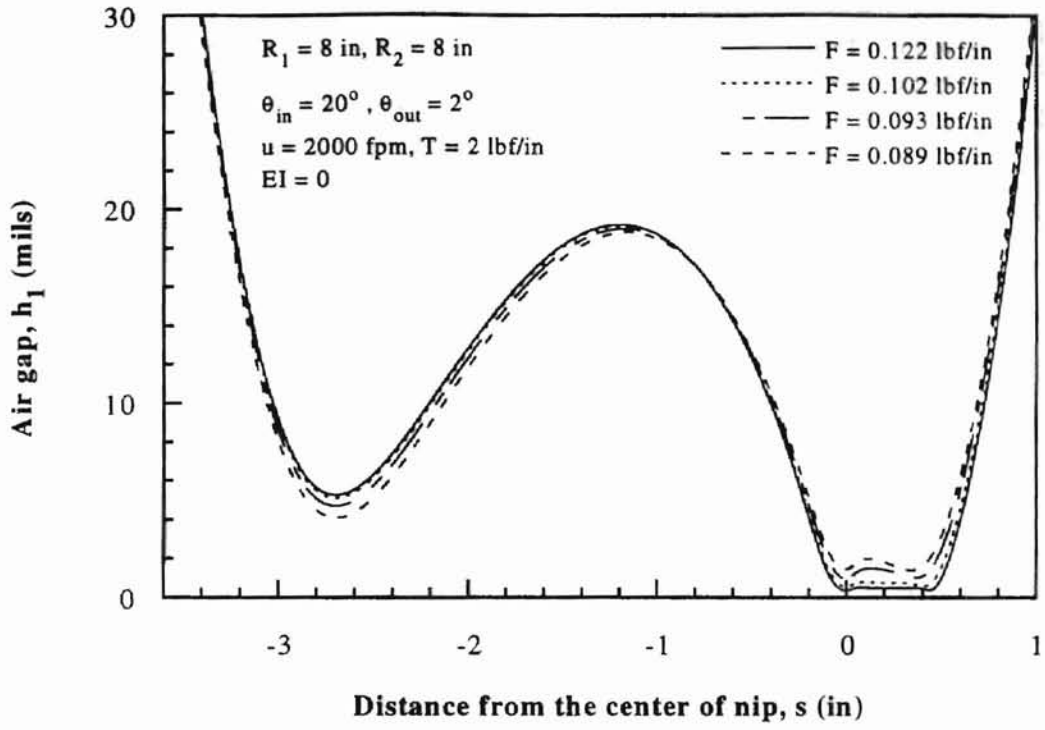

Figure 20. Gap profile h_1 for $\theta_{in} = 20^{\circ}$ and $EI = 0$

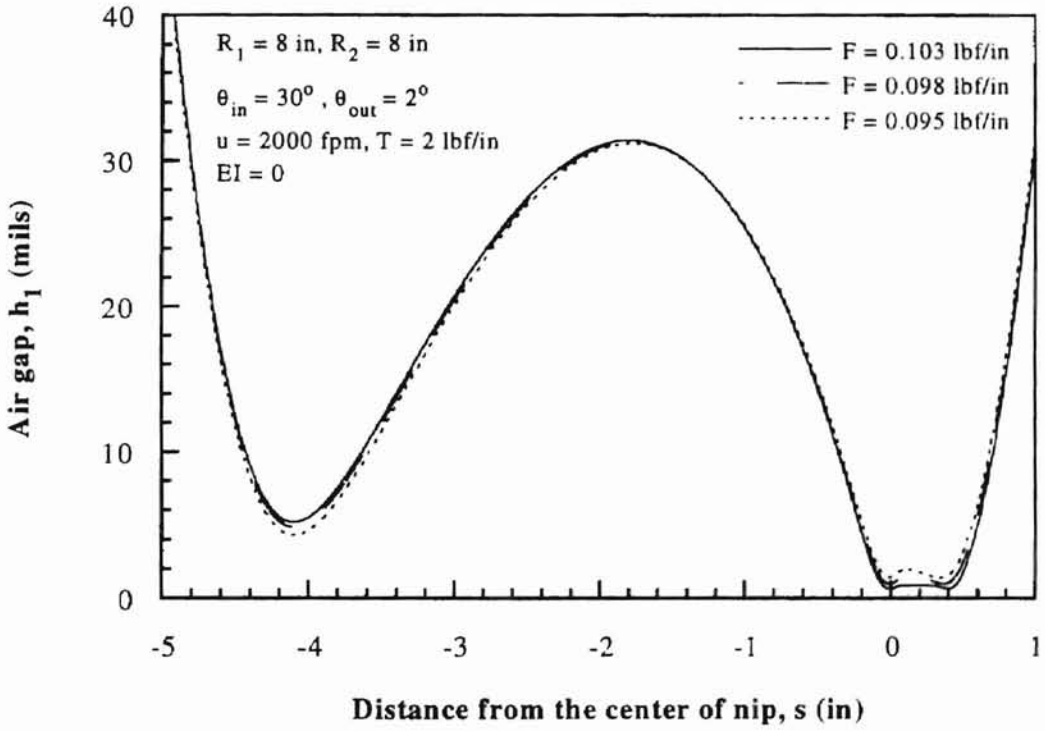

Figure 21. Gap profile h_1 for $\theta_{in} = 30^{\circ}$ and $EI = 0$

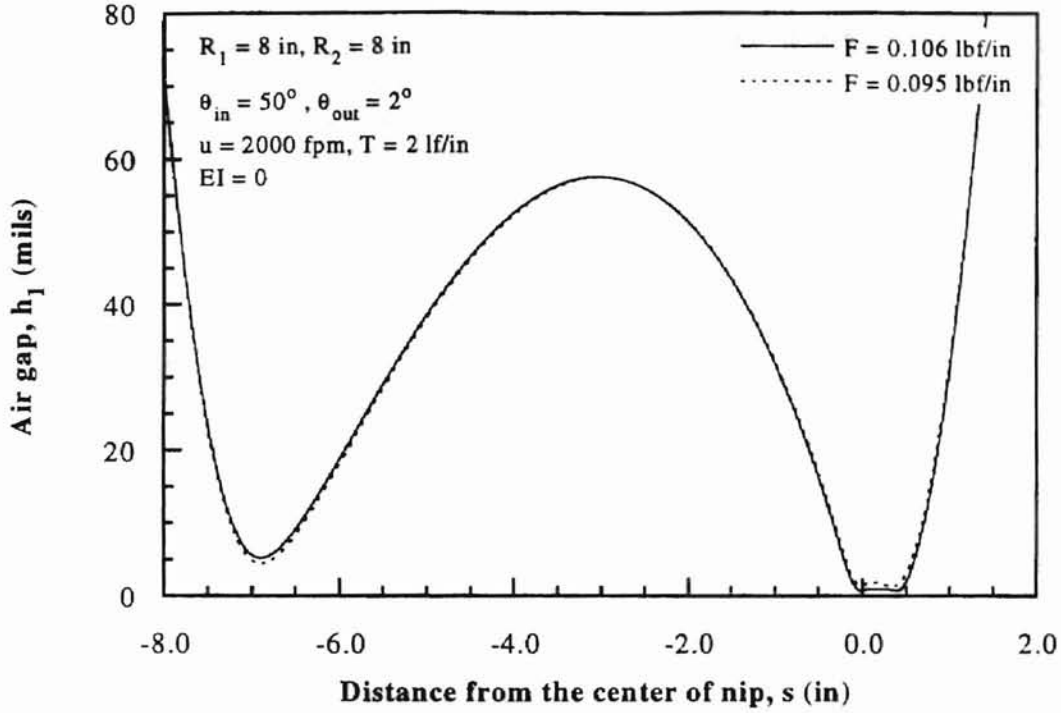

Figure 22. Gap profile h_1 for $\theta_{in} = 50^{\circ}$ and $EI = 0$

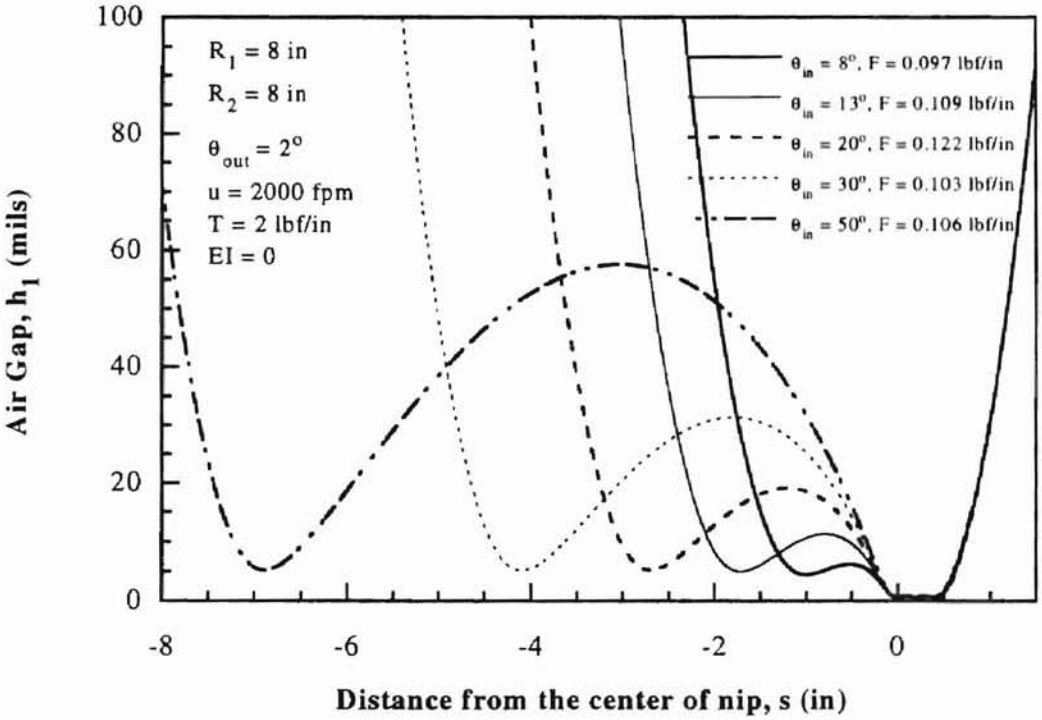

Figure 23. Gap profile h_1 for $\theta_{in} = 8$, 13, 20, 30, and 50° and $EI = 0$

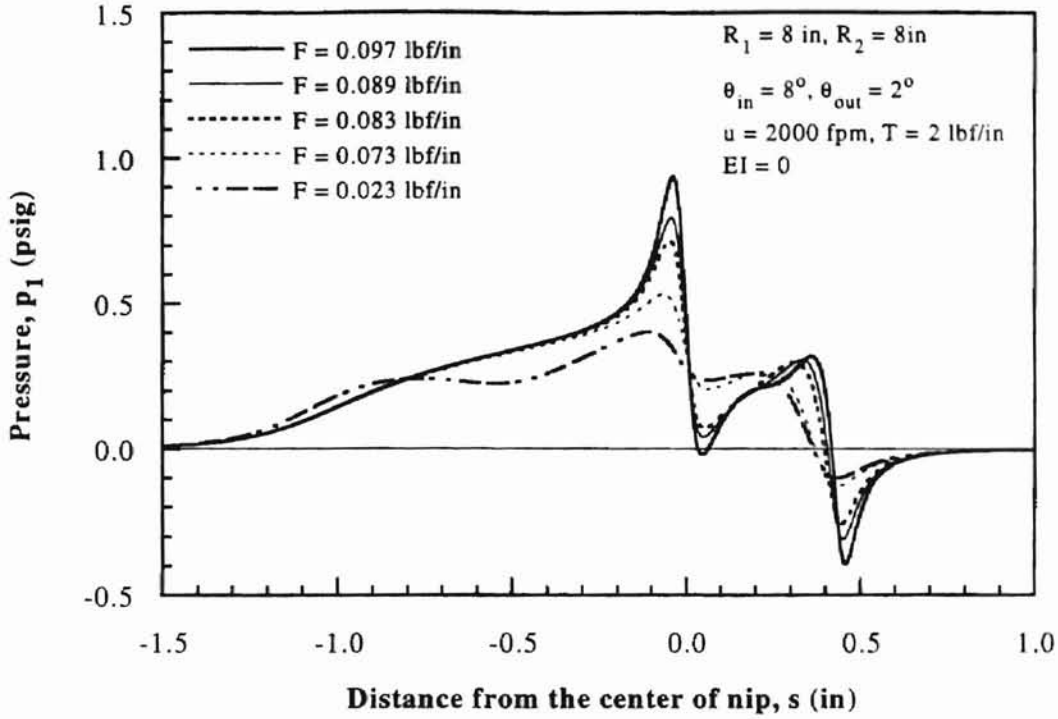

Figure 24. Pressure profile p_1 for $\theta_{in} = 8^\circ$ and $EI = 0$

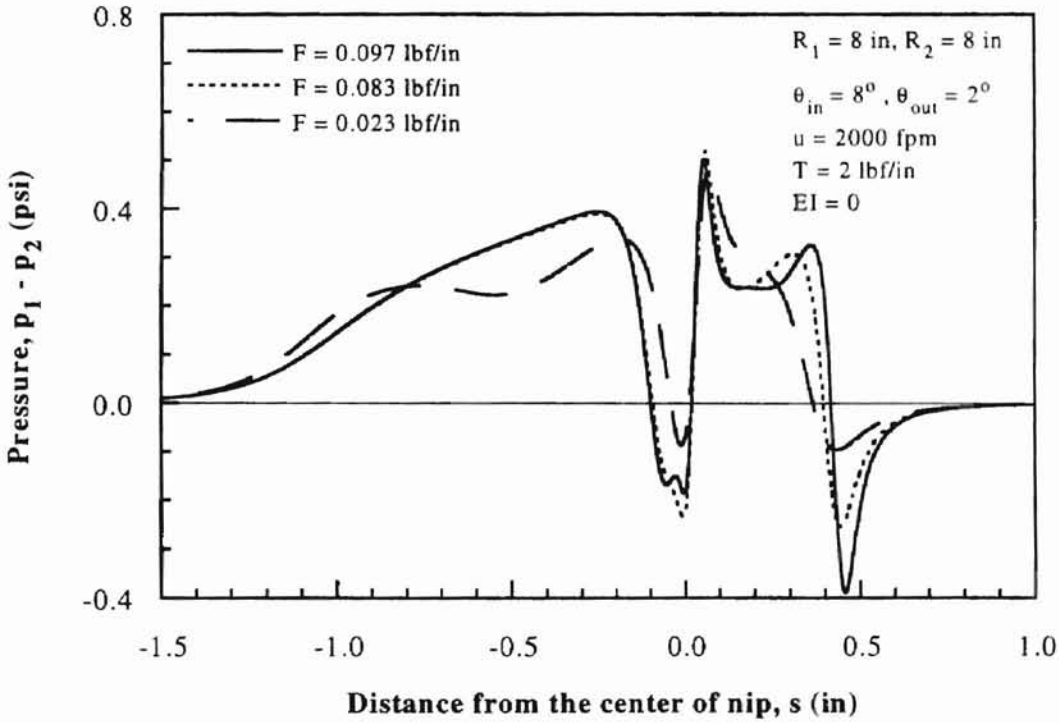

Figure 25. Pressure difference $p_1 - p_2$ for $\theta_{in} = 8^\circ$ and $EI = 0$

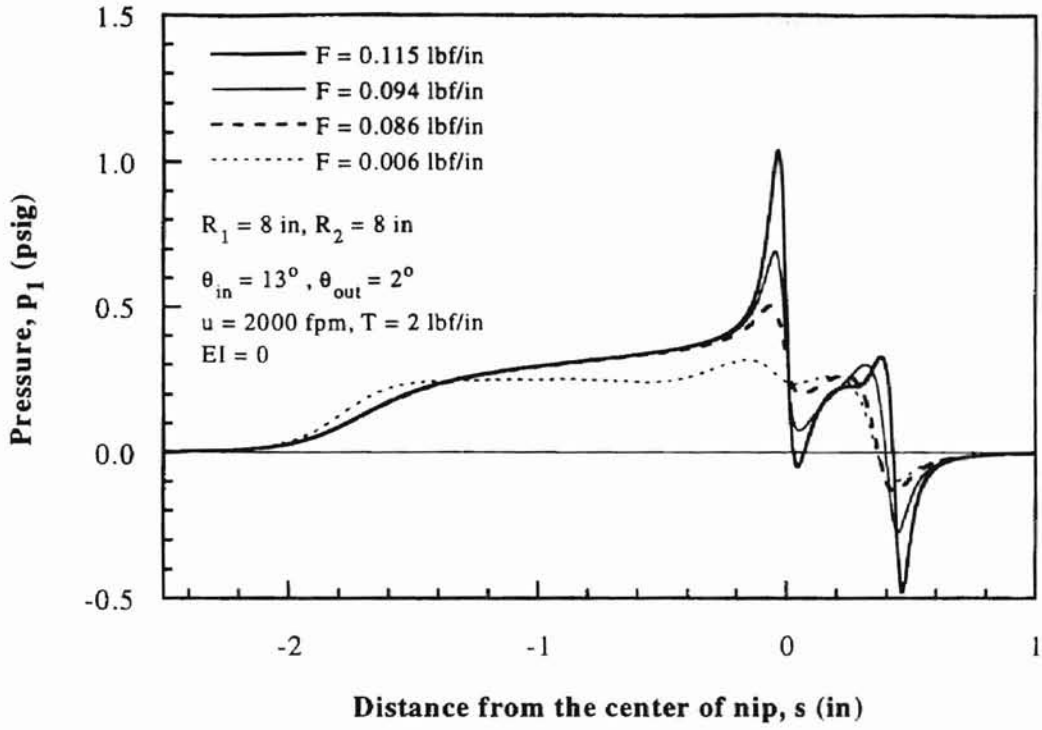

Figure 26. Pressure profile p_1 for $\theta_{in} = 13^{\circ}$ and $EI = 0$

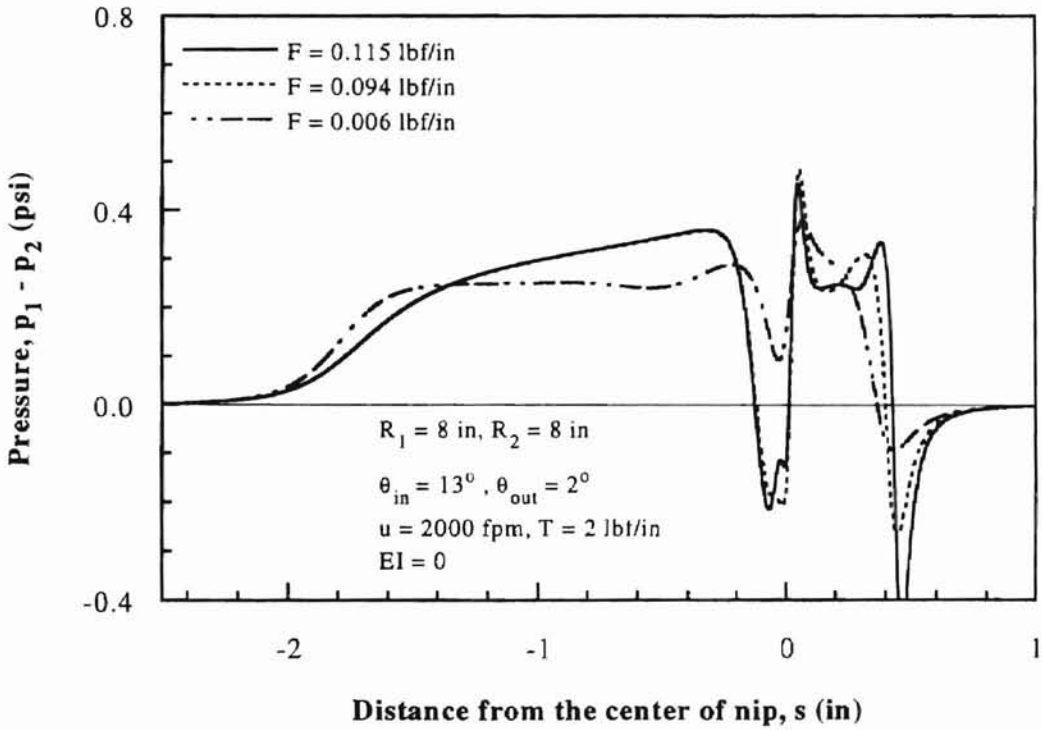

Figure 27. Pressure difference $p_1 - p_2$ for $\theta_{in} = 13^{\circ}$ and $EI = 0$

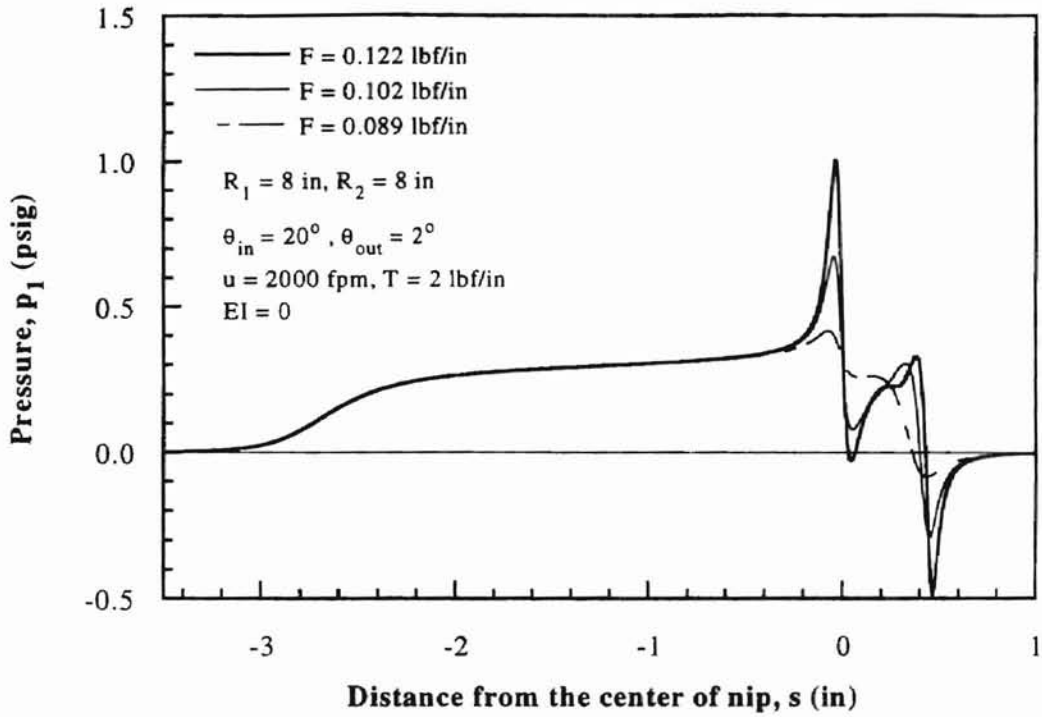

Figure 28. Pressure profile p_1 for $\theta_{in} = 20^{\circ}$ and $EI = 0$

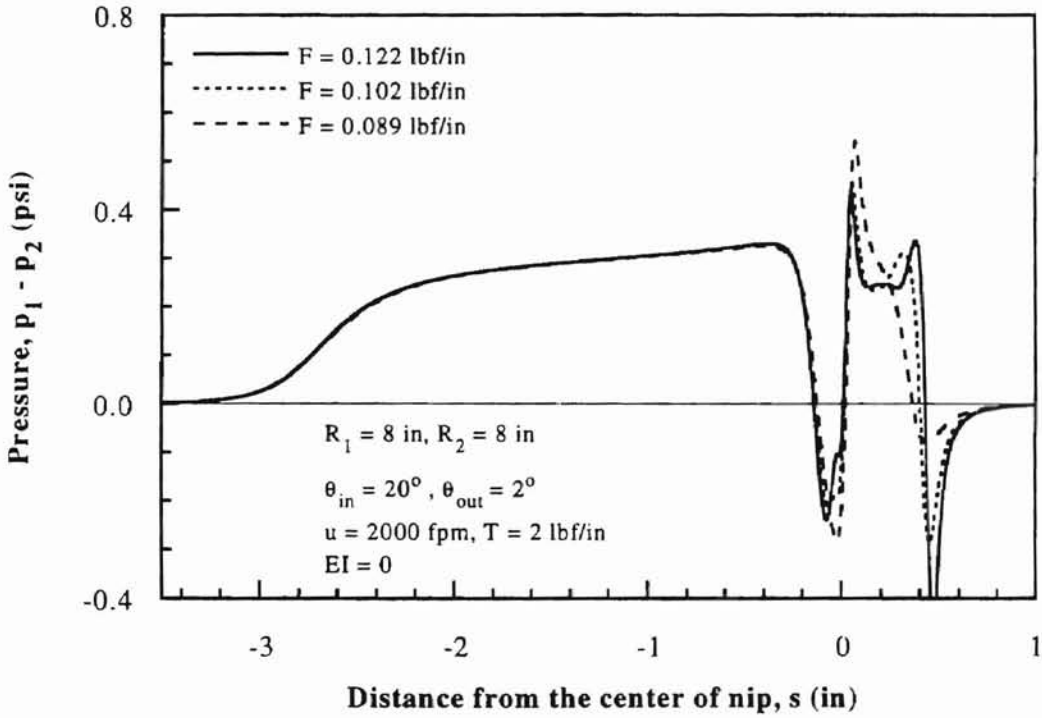

Figure 29. Pressure difference $p_1 - p_2$ for $\theta_{in} = 20^{\circ}$ and $EI = 0$

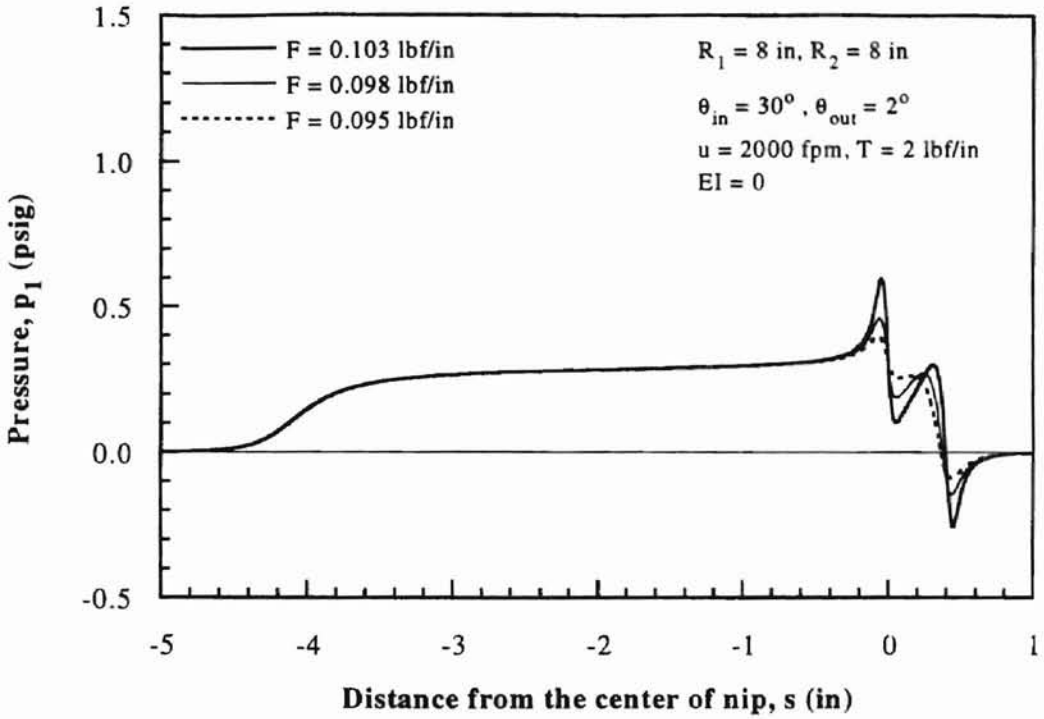

Figure 30. Pressure profile p_1 for $\theta_{in} = 30^{\circ}$ and $EI = 0$

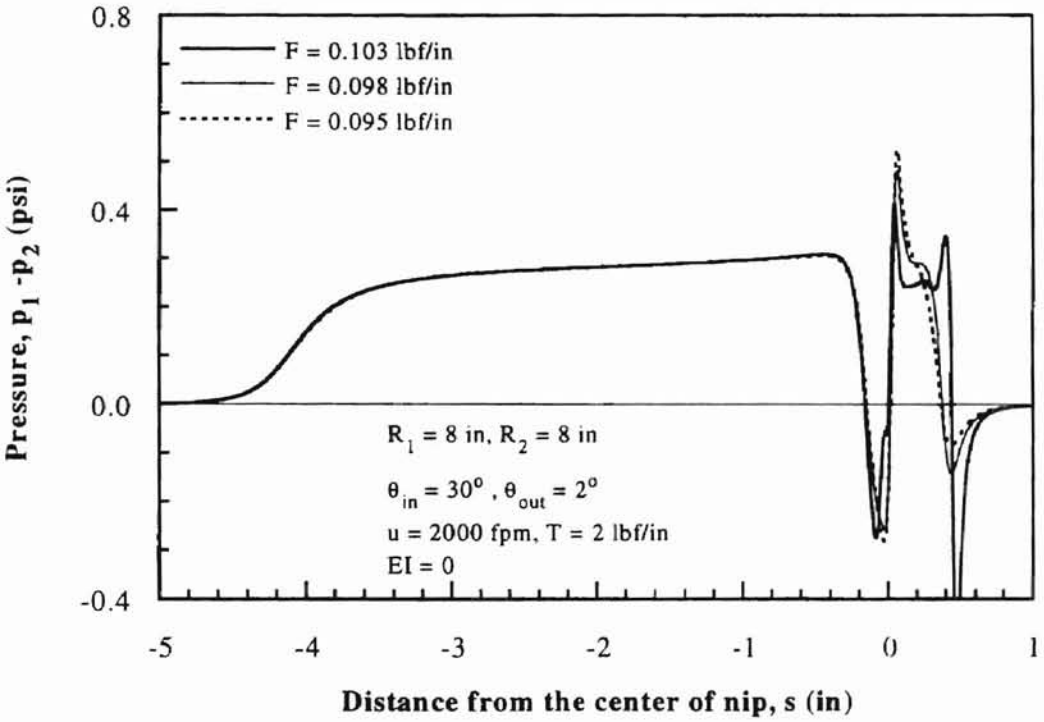

Figure 31. Pressure difference $p_1 - p_2$ for $\theta_{in} = 30^{\circ}$ and $EI = 0$

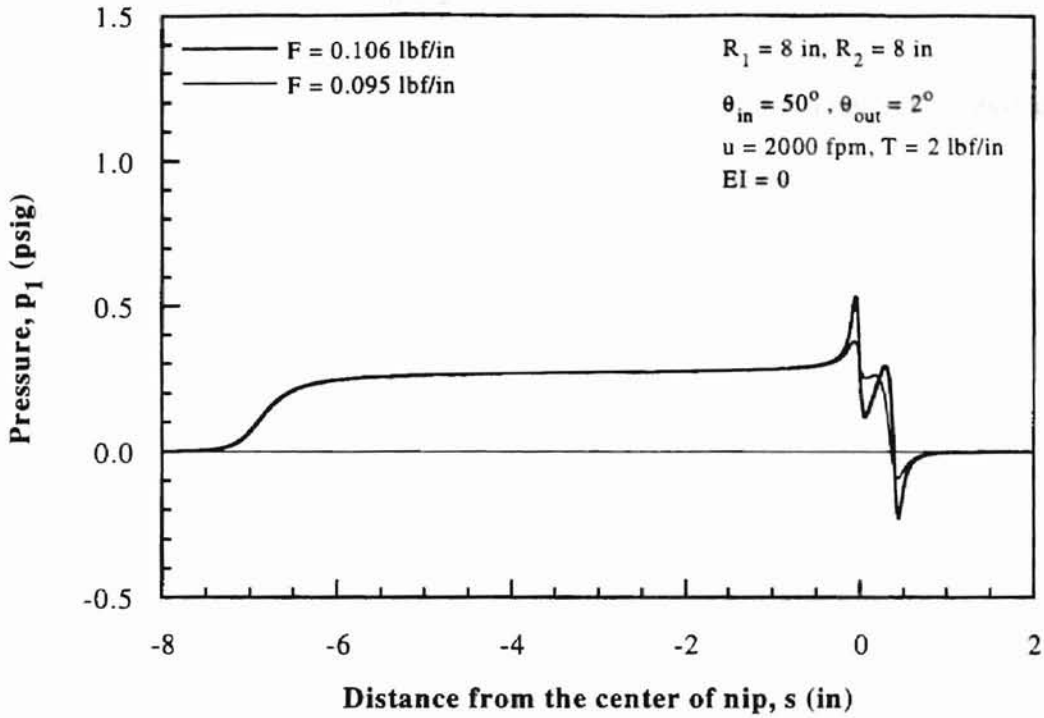

Figure 32. Pressure profile p_1 for $\theta_{in} = 50^{\circ}$ and $EI = 0$

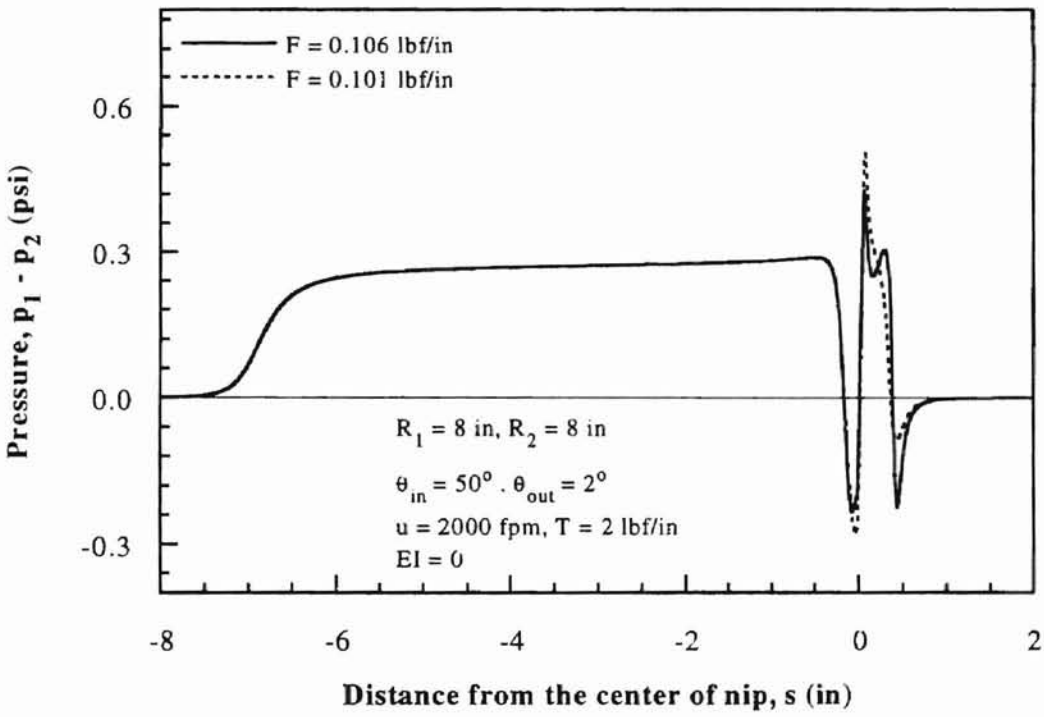

Figure 33. Pressure difference $p_1 - p_2$ for $\theta_{in} = 50^{\circ}$ and $EI = 0$

4.2.2 Effects of wrap angle on ballooning ($EI = 0$)

As shown in Figure 34, the maximum balloon height for a perfectly flexible web is nearly proportional to the incoming wrap angle. Example calculations were done for three different radii: 4 *in*, 8 *in*, 12 *in*. It is shown that

$$\frac{h_{\max}}{R_1} \propto \theta_{in}^{1.199} \tag{57}$$

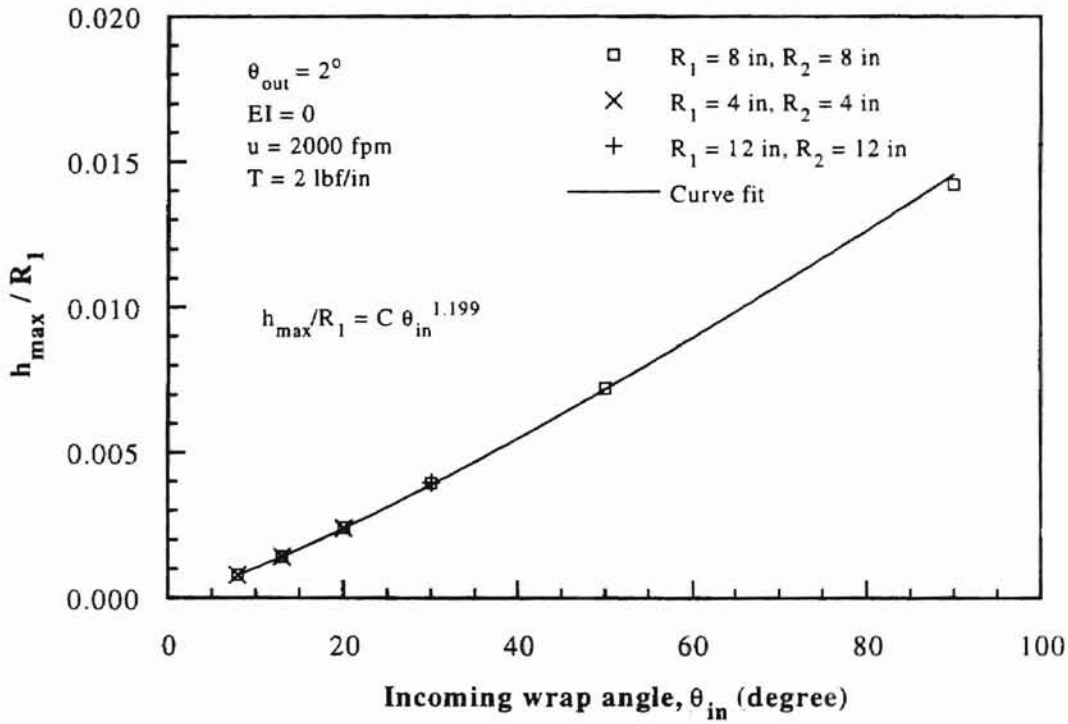

Figure 34. Maximum balloon height vs. incoming wrap angle ($EI = 0$)

4.3 Ballooning for a Web with Bending Stiffness ($EI > 0$)

4.3.1 Effects of bending stiffness on ballooning ($EI > 0$)

Within the entire range of example calculations, the effects of web thickness or bending stiffness on ballooning are negligible as shown in Figure 35. Also note that, as described in Section 4.2, the ballooning height is not sensitive to the nip force.

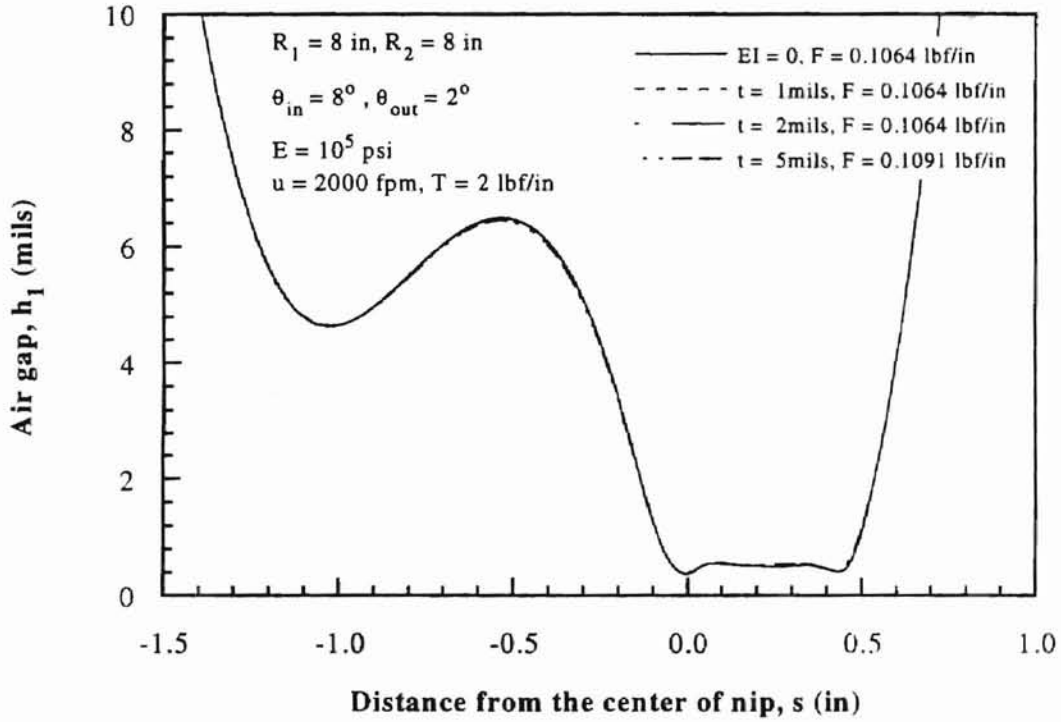

Figure 35. Effect of web thickness on ballooning ($EI > 0$)

4.3.2 Effects of web speed on ballooning ($EI > 0$)

The maximum balloon height increases with web speed as shown in Figure 36. The air gap after the nip also increases with web speed.

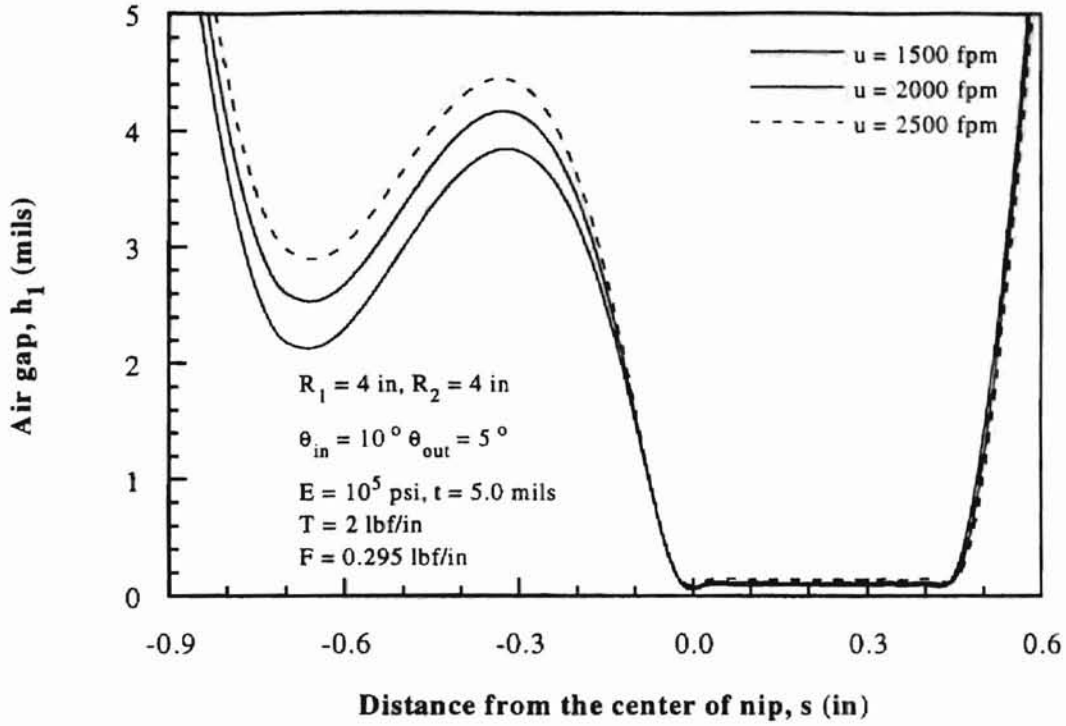

Figure 36. Effects of web speed on ballooning

4.3.3 Effects of web tension on ballooning ($EI > 0$)

The maximum balloon height decreases when tension increases as shown in Figure 37. On the contrary, the air gap after the nip increases with web tension (Figure 38). This trend is not verified for other values of nip forces and web stiffness parameters in this study.

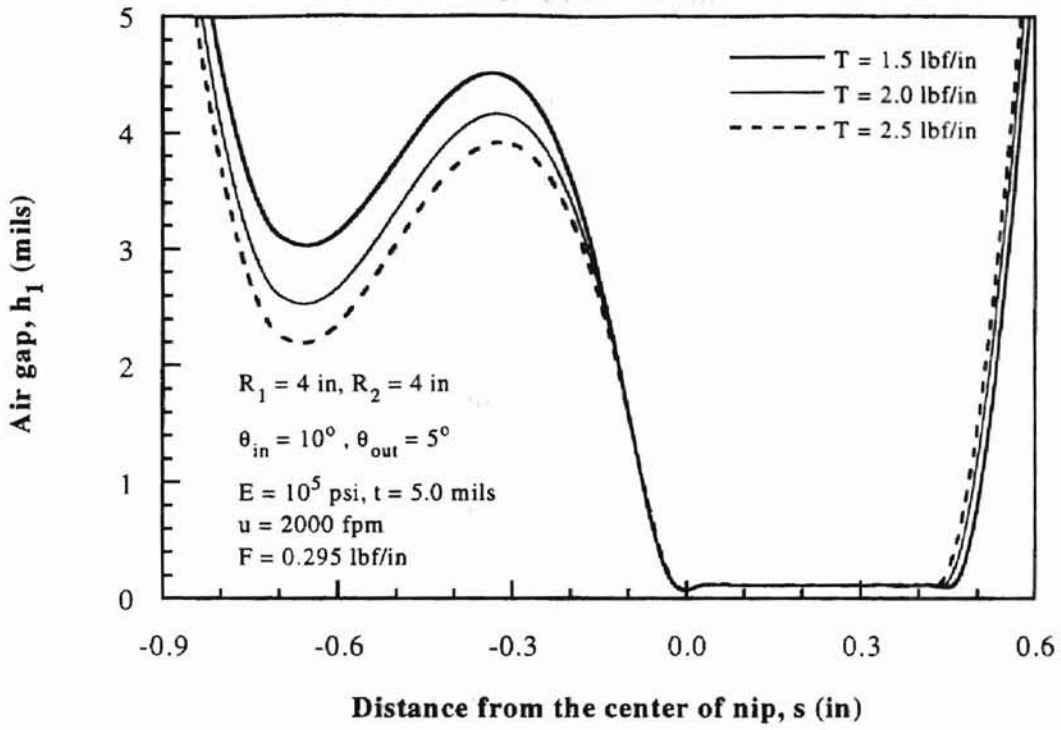

Figure 37. Effects of web tension on ballooning

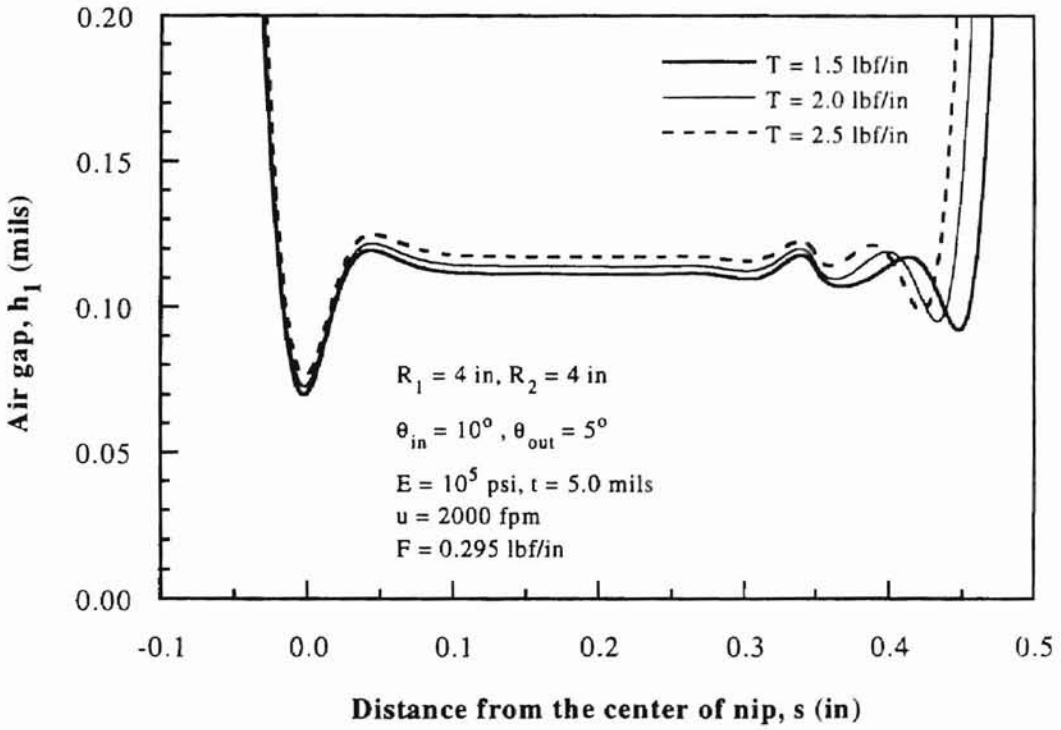

Figure 38. Detailed description of Figure 37

4.4 Air Entrainment

In Section 4.4.1, general trends of air entrainment versus nip force are shown for a perfectly flexible web, and the critical nip force for ballooning is explained. In addition, the convergence problem of numerical calculation is mentioned. In Section 4.4.2, the current computational model is compared with a simplified model. In Sections 4.4.3 and 4.4.4, the effects of web speed and web tension are examined, respectively.

4.4.1 Air entrainment for perfectly flexible web ($EI = 0$)

The relationship between the amount of entrained air and the nip force for a perfectly flexible web is shown in Figure 39 through Figure 45. When there is no nip roller or $F = 0$, the air entrainment in the winding roll, h_{1c}, can be calculated as

$$h_{1c} = h_1 \frac{p_1}{p_a} = 0.643 \cdot R_1 \left(\frac{12\mu u}{T} \right)^{2/3} \left(1 + \frac{T}{R_1 p_a} \right) \tag{58}$$

where the air gap (h_1) and the pressure (p_1) are from Eq. (48) and the force balance condition of the web:

$$h_1 = 0.643 \cdot R_1 \left(\frac{12\mu u}{T} \right)^{2/3}$$

$$p_1 = p_a + \frac{T}{R_1}$$

The nominal clearance constant, 0.643 in Eq. (58), may have a different value when the effects of the compressibility and web stiffness are included (Figure 4, Figure 11, Figure 12).

Once ballooning occurs, the amount of entrained air reduces dramatically as the nip force increases. When the web is not wide, the effects of side leakage should be considered. In this study, the effects of side leakage are not considered. The amounts of air entrainment, h_{1c} and h_{2c}, seem to converge to each other. However, this cannot be verified because of insufficient data for large values of the nip force.

Generally, the convergence problem becomes worse when the wrap angle, radius of roll, or nip forces increases. In addition, it depends on the boundary conditions, as described in Section 4.1.1. With the boundary conditions expressed by Eq. (56), the following convergence difficulties were experienced for perfectly flexible web and zero nip force cases ($EI = 0$ and $F = 0$). Solutions could not be obtained for $R_1 > 8''$ even when the wrap angle is small, and it also could not be obtained for over 20 degrees of wrap angle with $R_1 = 8''$. With $R_1 < 8''$, solutions were obtained for over 20 degrees of wrap angle. For perfectly flexible web and non-zero nip force cases, very similar convergence problems were experienced. In addition, the convergence becomes more difficult to be achieved as the nip force increases. Even when θ_{wrap} and R_1 are small, no solution could be obtained for large nip forces; Figure 39 through Figure 45 contain the data points for maximum possible nip forces for computation. Solutions could be obtained for some conditions with the wrap angle larger than 20 degrees as shown in Figure 41 through Figure 43. In those cases (Figure 41 through Figure 43), solutions could not be obtained for very small nip forces.

When the other boundary conditions (Eq. (55) instead of Eq. (56)) are chosen, the solution converged for larger nip forces. The solutions are shown in Figure 48 through Figure 52. However, calculations could not be done with very large nip forces. Each calculation took much more time, and the weighting factor needed to be very small, less than 0.00005. Web stiffness also improves the convergence of calculations slightly, but the detail is not examined in this study. Many factors seem to affect the convergence problem.

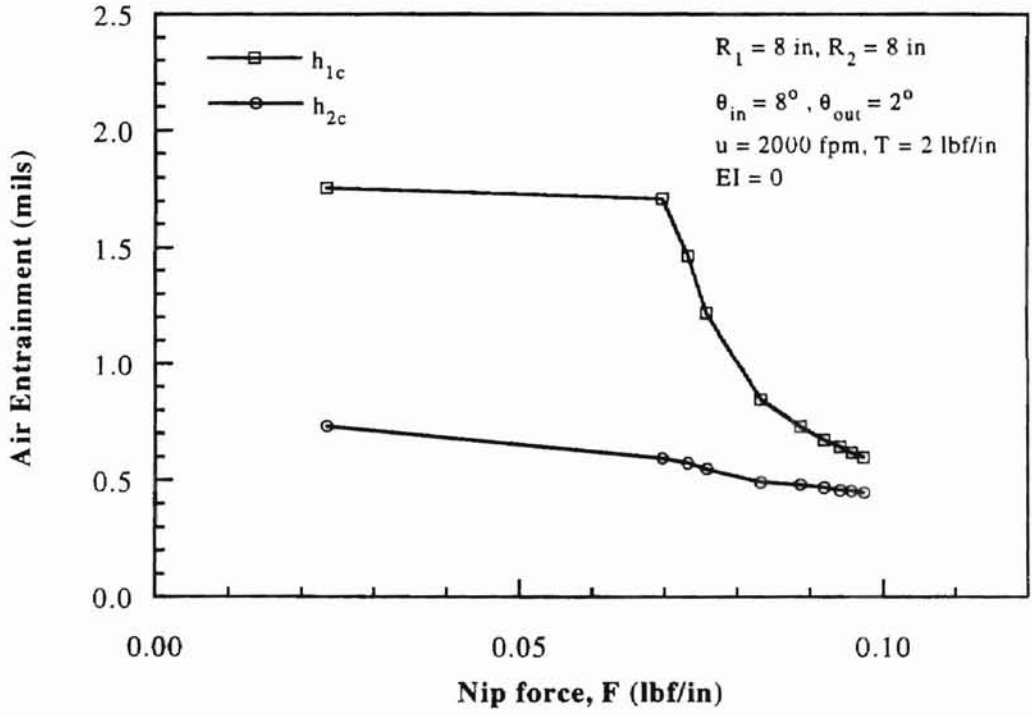

Figure 39. Air entrainment for $\theta_{in} = 8^{\circ}$ and $EI = 0$

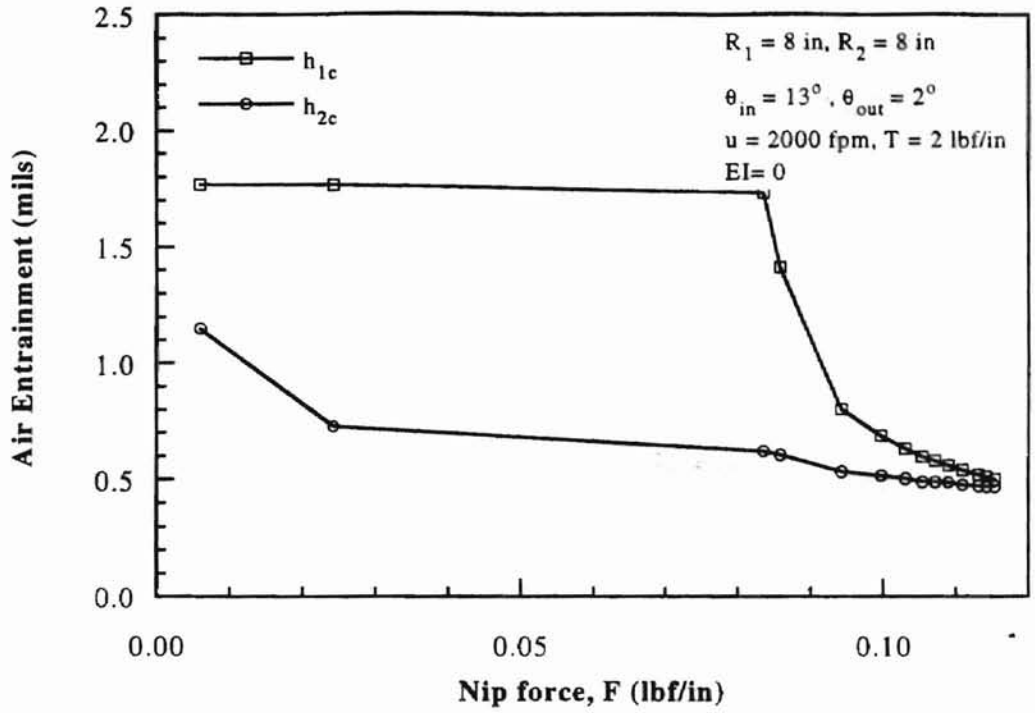

Figure 40. Air entrainment for $\theta_{in} = 13^{\circ}$ and $EI = 0$

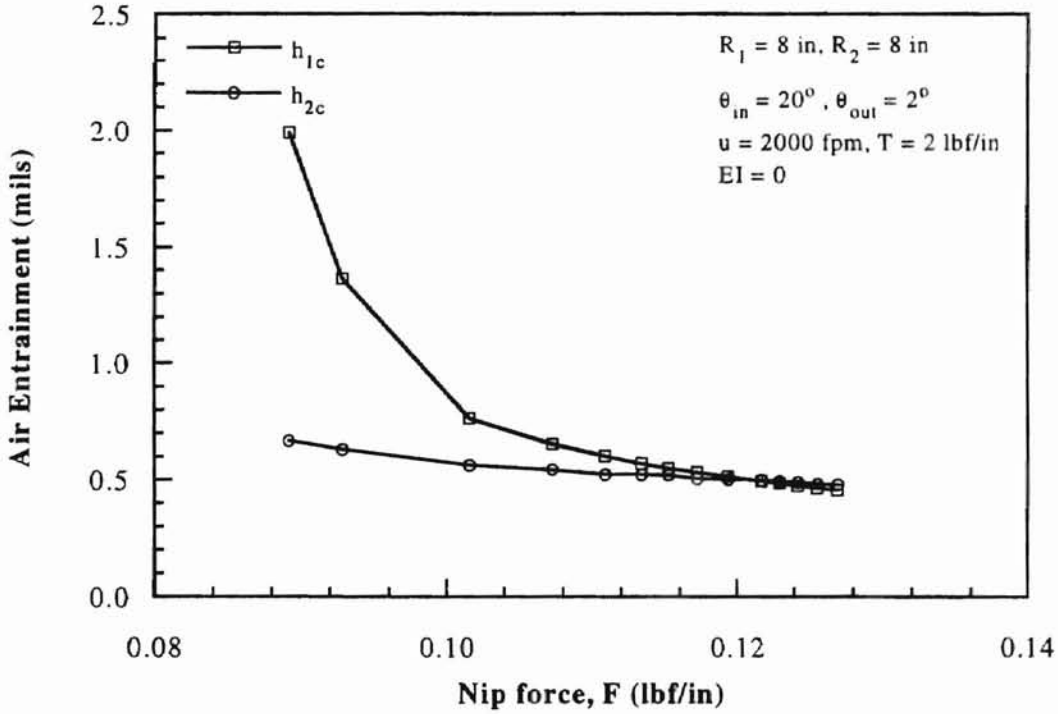

Figure 41. Air entrainment for $\theta_{in} = 20^{\circ}$ and $EI = 0$

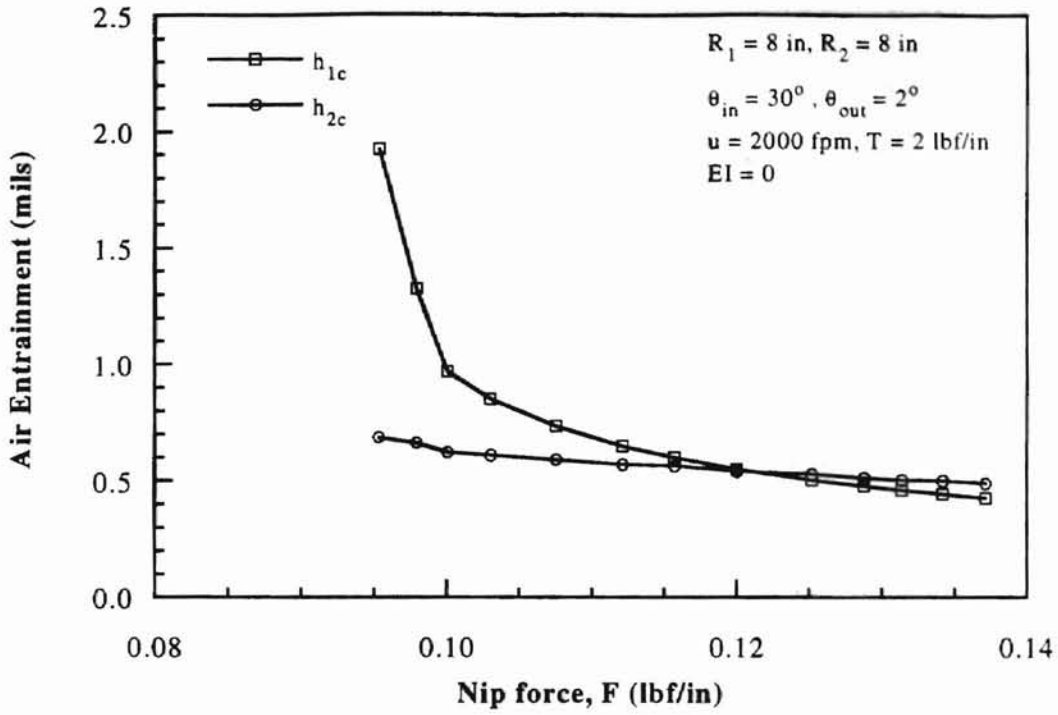

Figure 42. Air entrainment for $\theta_{in} = 30^{\circ}$ and $EI = 0$

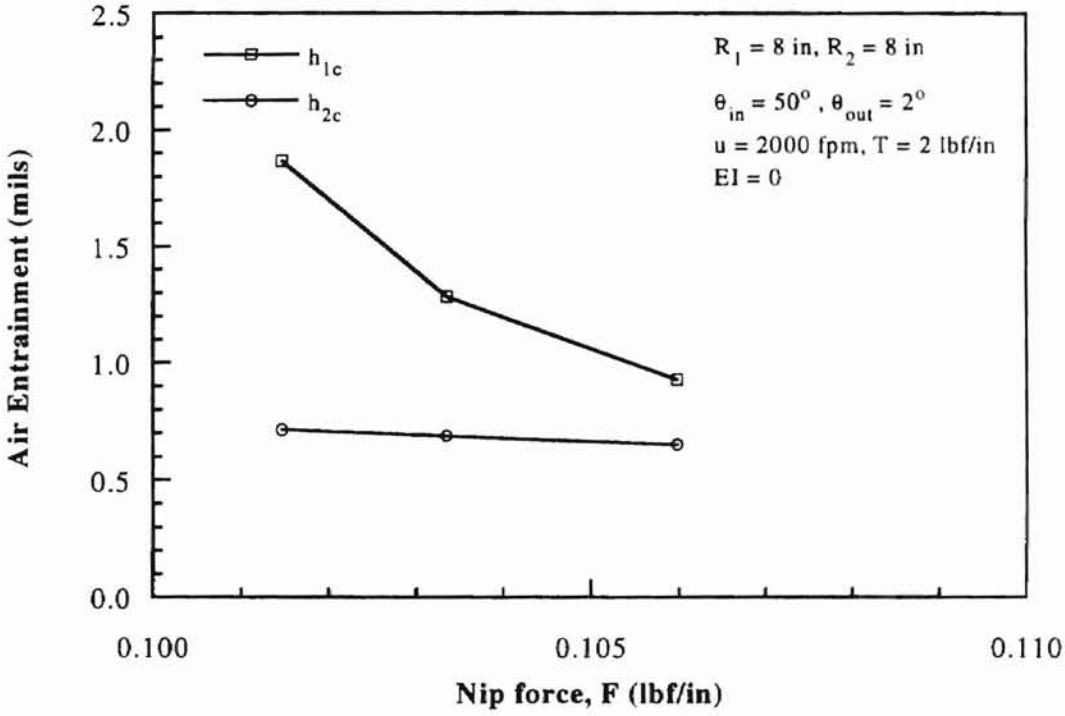

Figure 43. Air entrainment for $\theta_{in} = 50^{\circ}$ and $EI = 0$

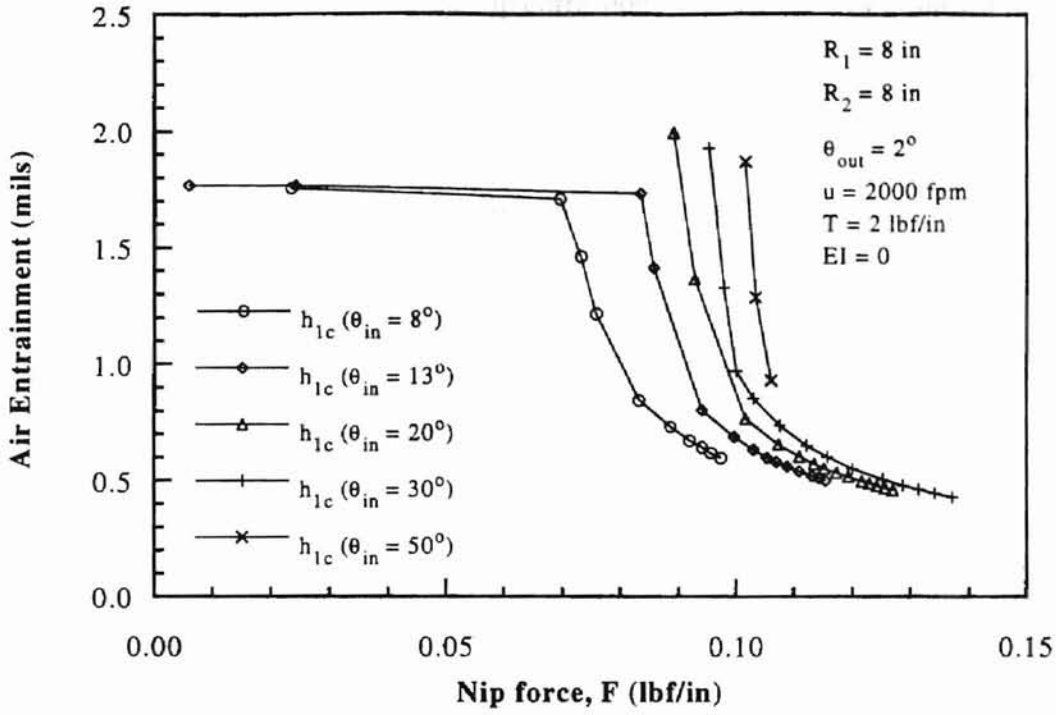

Figure 44. Air entrainment for $\theta_{in} = 8$, 13, 20, 30, and 50° and $EI = 0$

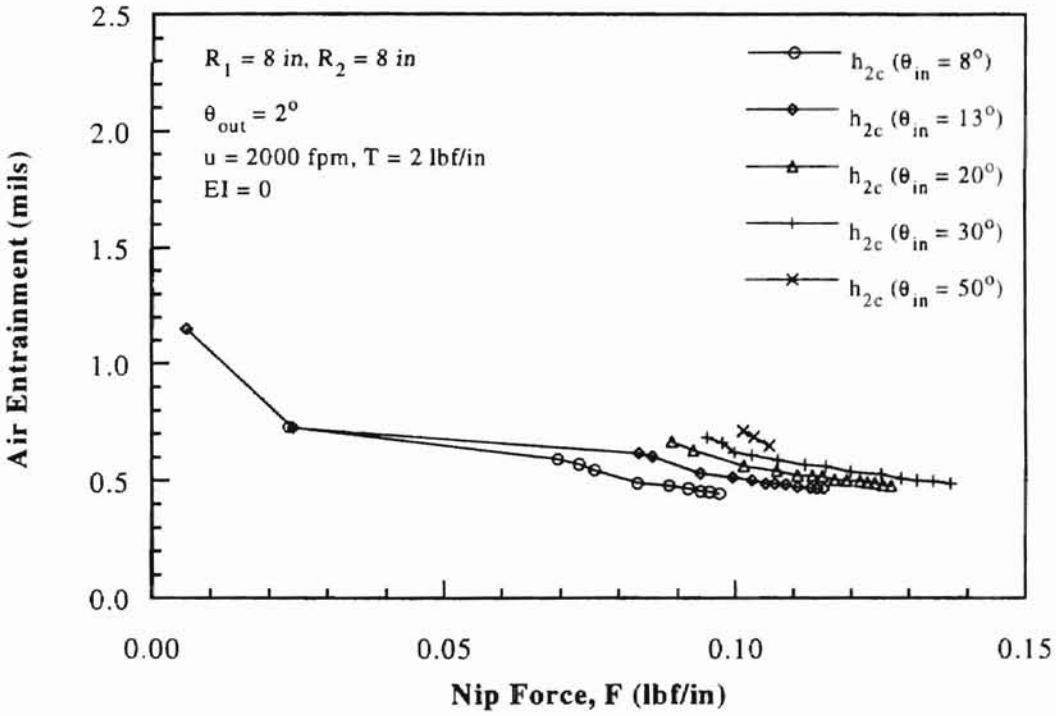

Figure 45. Air entrainment for $\theta_{in} = 8$, 13, 20, 30, and 50° and $EI = 0$

The web profile at and near the nip corresponding to Figure 19 is shown for various values of the nip force in Figure 46.

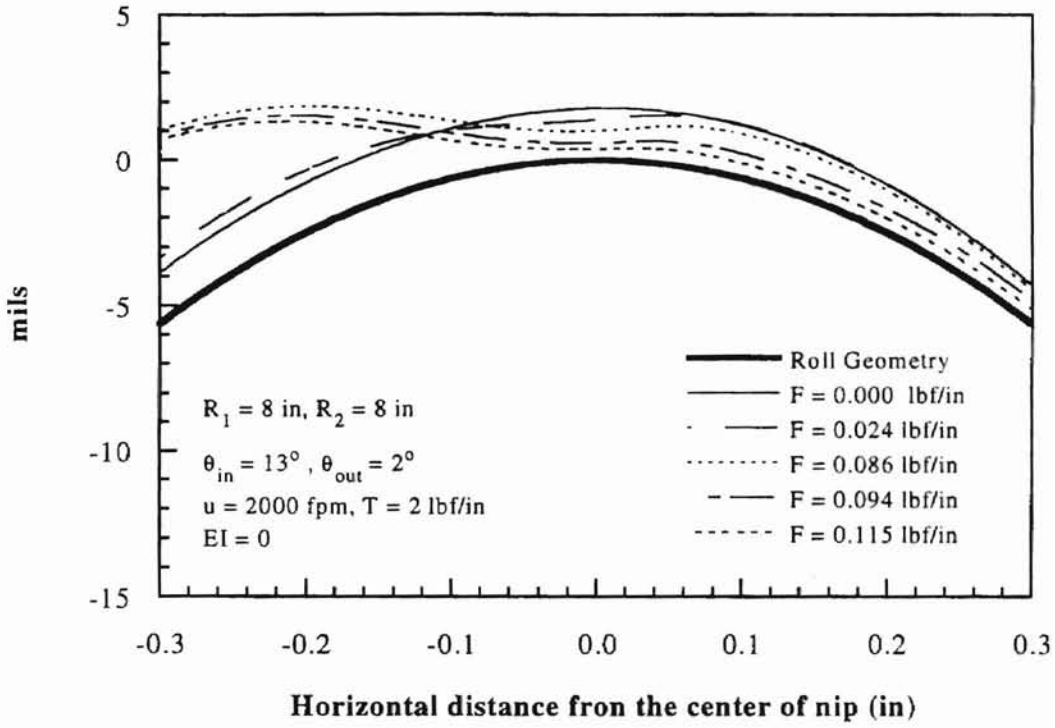

Figure 46. Web profiles

4.4.2 Effects of nip force on air entrainment

It appears very difficult to obtain a closed form correlation equation of the air entrainment because the air entrainment varies dramatically near the critical nip force for ballooning. Therefore, the current model is compared with a simplified model shown in Figure 47 in order to find a simple way to calculate the amount of air entraiment. The model 2 in Figure 47 describes a rigid roller rotating near a rigid flat plate, moving at the same speed of u. The notations of the air entrainment for model 1 are h_{1c} and h_{2c} and the air entrainment for model 2 is denoted by h_c. Example calculations were done for $R_1 = R_2 = 4''$ ($R_\epsilon = 2$, Model 1) and $R = 4''$ (Model 2) for different values of the incoming wrap

angle (2, 8, and 10 degrees) as shown in Figure 48 through Figure 52. Example calculations were also done for different sizes of rolls as shown in Figure 50 and Figure 51. Test conditions are tabulated in Table 3.

Table 3. Test conditions ($EI > 0$)

R_1 (inches)	R_2 (inches)	T (lb/in)	u (ft/min)	θ_{in} (degree)	θ_{out} (degree)	E (Psi)	t (mils)
4	2, 4, 8	2	2000	2, 8, 10	2, 5, 8	10^5	5

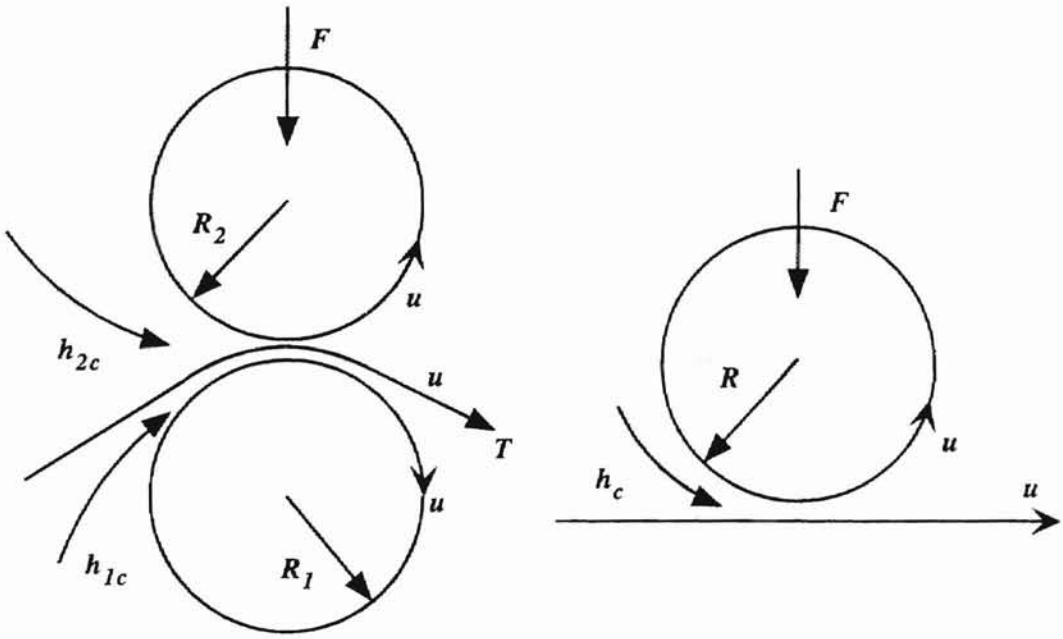

$R_e = R_1R_2 / (R_1+R_2)$ $R = 2R_1R_2 / (R_1+R_2)$

Model 1 **Model 2**

Figure 47. Comparison of two computational models

In Figure 48, Figure 49, and Figure 52, h_{1c} and h_{2c} for $R_1 = R_2 = 4''$ ($R_e = 2$, Model 1) and h_c for $R = 4''$ (Model 2) approach to each other as the nip force increases. Regardless of the wrap angle and web stiffness, all three values of air entrainment approach to each other. This observation holds even when $R_1 \neq R_2$. The example

calculations shown in Figure 50 are for $R_1 = 4''$, $R_2 = 8''$, $R_e = R_1 \cdot R_2/(R_1+R_2) = 8/3''$, $R = 2 \cdot R_e = 16/3''$. Figure 51 shows the calculation results for $R_1 = 4''$, $R_2 = 2''$, $R_e = 4/3''$, $R = 2 \cdot R_e = 8/3''$. Therefore, for any combination of R_1 and R_2, the air entrainment can be determined as $h_{1c} = h_{2c} = h_c$, where h_c is from Model 2 with $R = 2 \cdot R_e = 2 \cdot R_1 \cdot R_2/(R_1+R_2)$. This is the most important result of this study.

As a result, the prediction equation for Model 2 developed by Chang, Chambers, and Shelton (1994) is suggested to be used:

$$\frac{h_{1c}}{2R_e} = \frac{h_{2c}}{2R_e} = \frac{h_c}{R} = 2.4\frac{\mu u}{F} + 2.408\left(\frac{\mu u}{p_a R}\right)^{2/3} - 1.8\times10^{-6} \qquad (59)$$

which has good agreement with the air entrainment of model 2 when the nip force is high (when the second and third terms in Eq. (59) are dominant). In order to predict the air entrainment of model 1, Eq. (59) can be used with $R = 2 \cdot Re = 2 \cdot R_1 \cdot R_2/(R_1+R_2)$.

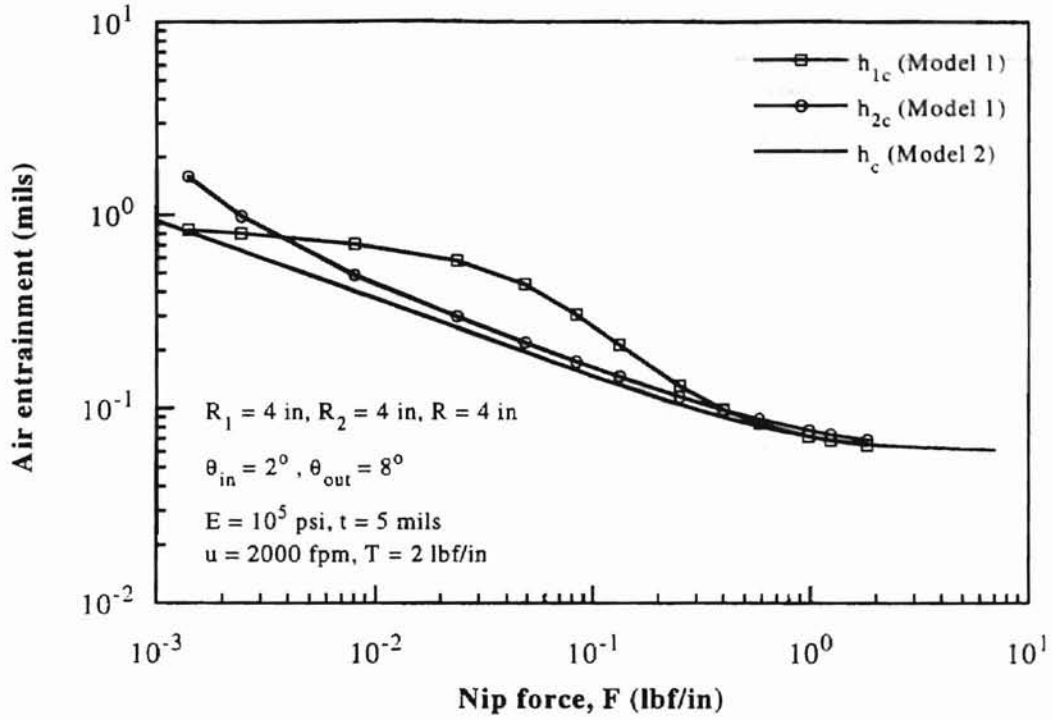

Figure 48. Effects of nip force on air entrainment

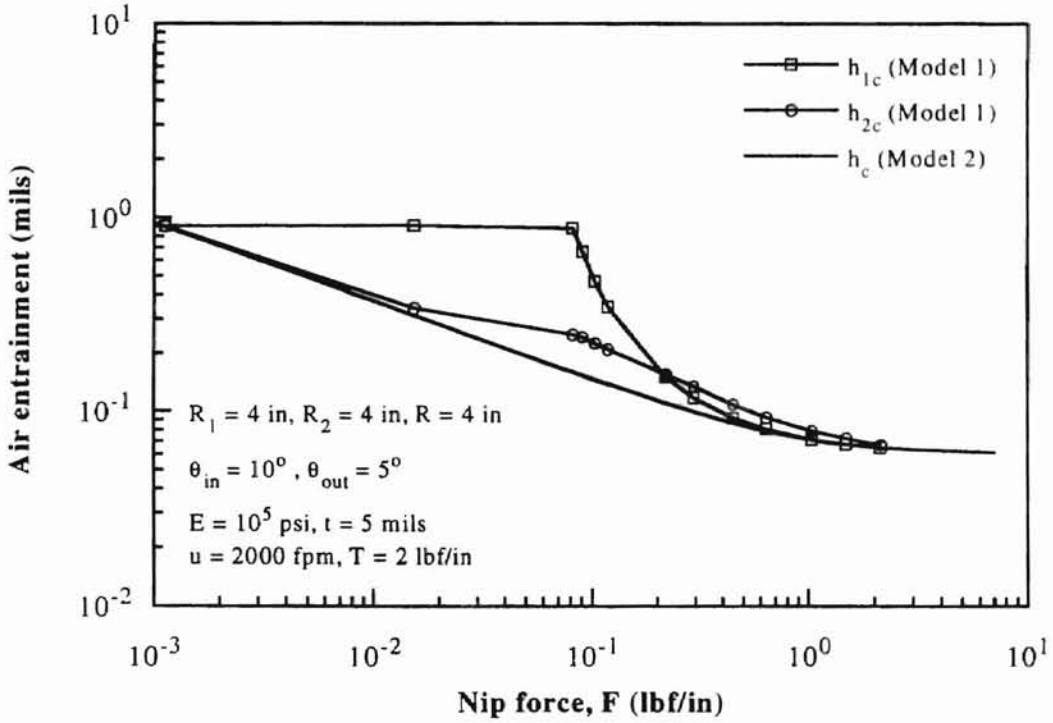

Figure 49. Effects of nip force on air entrainment

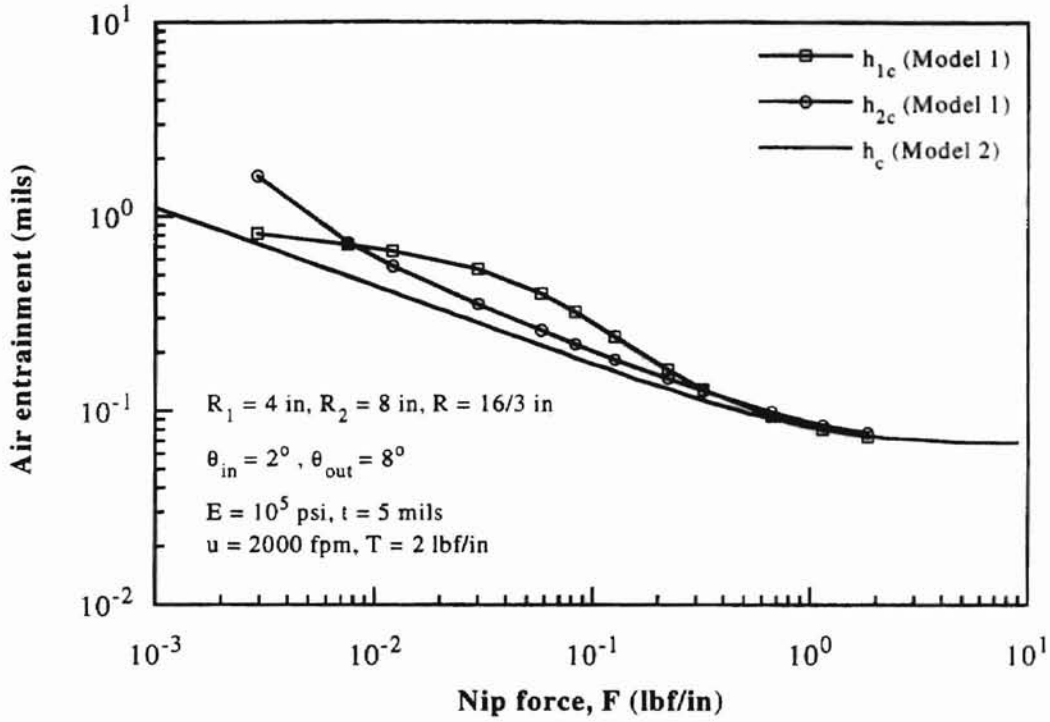

Figure 50. Effects of nip force on air entrainment

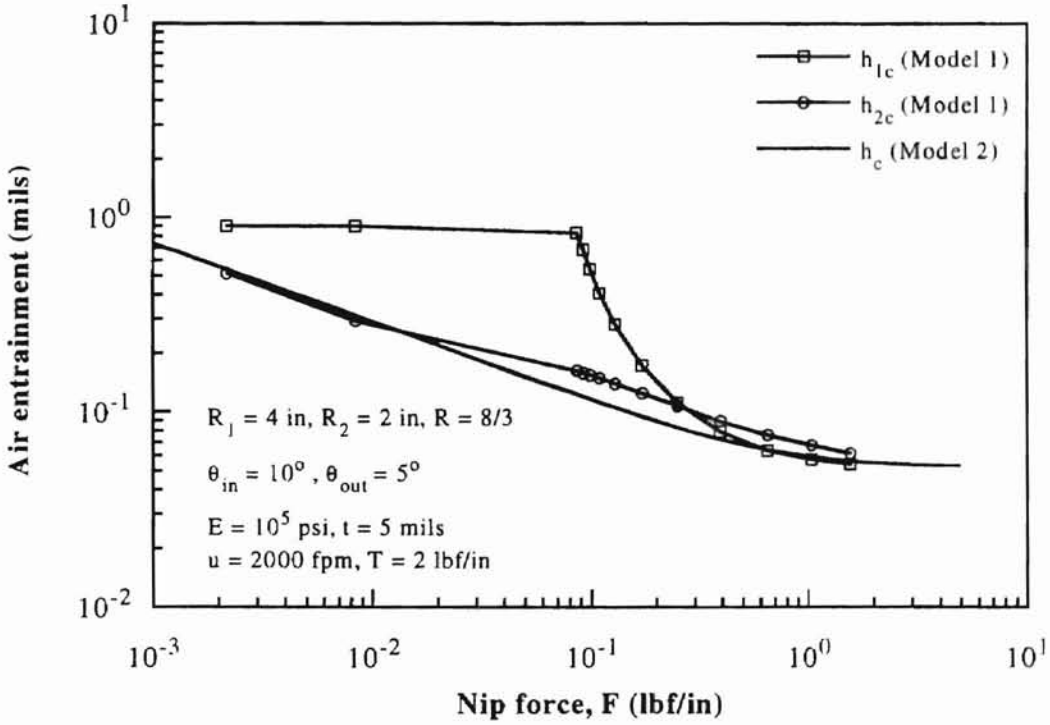

Figure 51. Effects of nip force on air entrainment

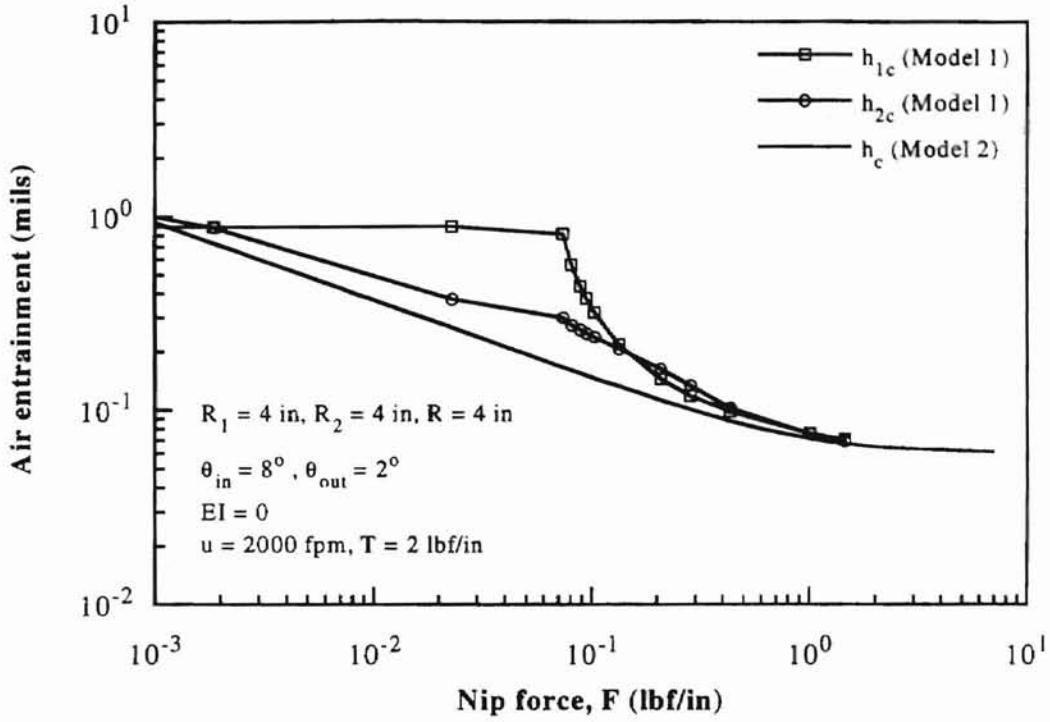

Figure 52. Effects of nip force on air entrainment

4.4.3 Effects of web speed on air entrainment

The amounts of air entrainment, h_{1c} and h_{2c}, increase with web speed as shown in Figure 53. The effects of web speed on the air entrainment examined only for the test conditions indicated in Figure 53. When the nip force is very large, however, the effect of web speed on the air entrainment can be predicted as shown in Section 4.4.2.

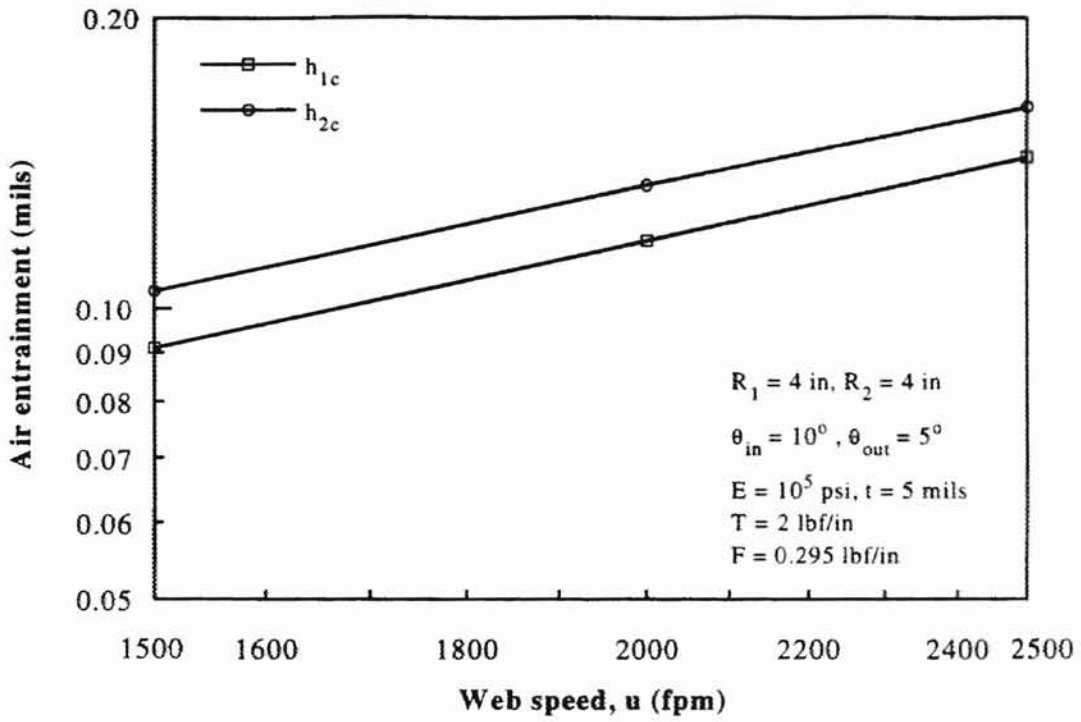

Figure 53. Effects of web speed on air entrainment

4.4.4 Effects of web tension on air entrainment

Figure 54 shows the effects of web tension on air entrainment. As mentioned in Section 4.3.3, higher web tension reduces the amount of air entrainment for simple foil bearing (zero nip force). However, the air entrainment with a nip roller ($F > 0$) seems to slightly increase with web tension at the conditions indicated in Figure 54. The effects of web tension on the air entrainment need to be examined for different values of nip force, bending stiffness, and other variables.

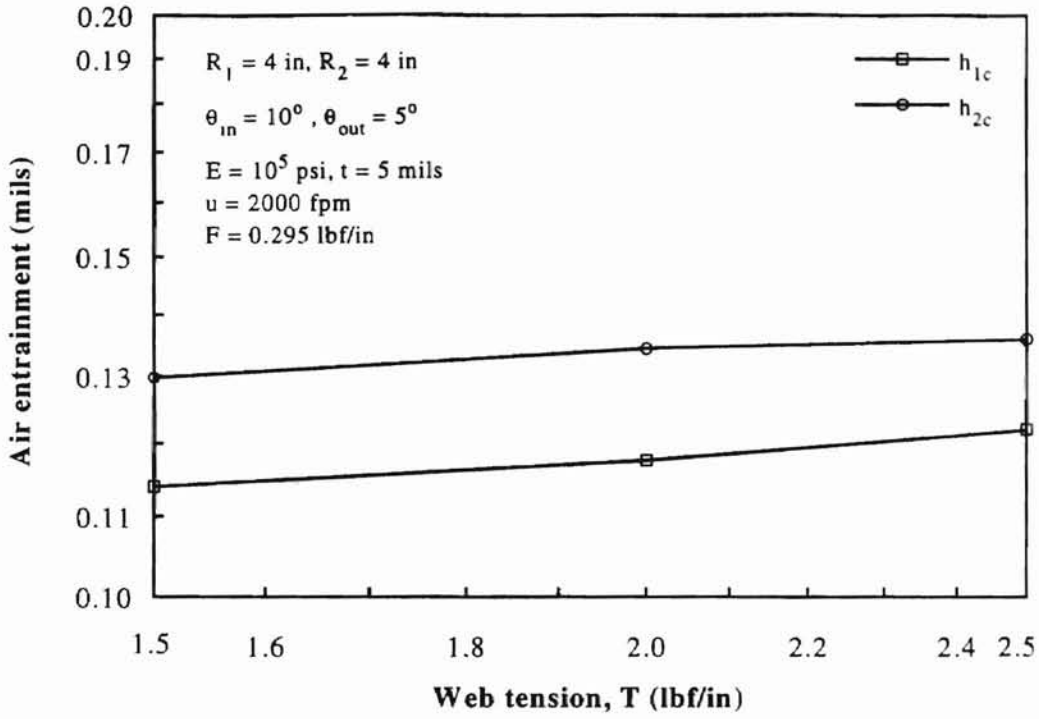

Figure 54. Effects of web tension on air entrainment

CHAPTER V

SUMMARY AND CONCLUSIONS

The effects of a nip roller on the ballooning phenomenon and the air entrainment in a winding roll have been analyzed numerically. The effects of a variety of design parameters and operating conditions have been examined. The following conclusions were obtained from this computational study:

1. There is a critical value of nip force above which ballooning occurs.
2. Once ballooning has occurred, its shape is not strongly affected by the nip force.
3. Ballooning does not occur when the incoming wrap angle is small.
4. The maximum balloon height is nearly proportional to the incoming wrap angle for a perfectly flexible web.
5. The balloon height is strongly affected by the incoming wrap angle, web tension, and web speed, but not by the bending stiffness of the web in typical applications.
6. When the nip force is smaller than the critical value for ballooning, the amount of air entrainment is nearly independent of the nip force.
7. The effect of the nip force on the air entrainment is dramatic near the critical nip force.
8. When the nip force is very large, the amounts of the air entrainment on the two sides of the web approach an asymptotic value. The asymptotic value can be predicted

using Eq. (59) with $R = 2 \cdot Re = 2 \cdot R_1 \cdot R_2/(R_1+R_2)$. This conclusion hols even when $R_1 \neq R_2$.

9. A nip roller with smaller radius is more effective than a larger one.

10. Air entrainment increases with web speed.

CHAPTER VI

RECOMMENDATIONS FOR FUTURE STUDY

It is recommended to extend this computational study by including the following effects:

1. Side leakage from the ballooned incoming web.
2. Elastic deformation of the rolls.
3. Asperity contact at the nip.

In order to improve the convergence of solutions, it is recommended to consider the following:

1. Reducing the number of nodes reduces the round-off error, but too small number of nodes increases the truncation error.
2. The finite-element method can be more efficient than the finite-difference method.
3. Non-uniform grid schemes can be applied so that the zone near the center of the nip has dense grids while the other zones have sparse grids. The grid size should be changed gradually.

REFERENCES

Barlow, E. J., 1967, "Derivation of Governing Equations for Self-Acting Foil Bearings," Journal of Lubrication Technology, Transaction of the ASME, pp. 334-340.

Baumann, G. W., 1975, "Controlling Hydrodynamic Foil Air-Bearing Clearance With an Opposing Pressure Pad," Journal of Lubrication Technology, Transaction of the ASME, pp. 73-80.

Burgdorfer, A., 1959, "The Influence of Molecular Mean Free Path on the Performance of Hydrodyanmic Gas Lubricated Bearings," Journal of Basic Engineering, Transaction of the ASME, pp. 94-100.

Cameron, A., 1966, Principles of Lubrication, John Wiley and Sons, pp. 49~50.

Chang, Y. B., Chambers, F. W., and Shelton, J. J., 1996, "Elastohydrodynamic Lubrication of Air-Lubricated Rollers," Journal of Tribology, Transaction of the ASME, Vol 118, pp. 623-628.

Chang, Y. B., Chambers, F. W., and Shelton, J. J., 1994, "Air Entrainment with a Force-Loaded Nip Roller," Project 9091-2, Web Handling Research Center, Oklahoma State University.

Eshel, A., 1967, "Stiffness Effects on the Infinitely Wide Foil Bearing," Journal of Lubrication Technology, Transaction of the ASME: Vol. 89, pp. 92-97.

Eshel, A. and J. H. G. Elrod, 1965, "The Theory of the Infinitely Wide, Perfectly Flexible, Self-Acting Foil Bearing," Journal of Basic Engineering, Transaction of the ASME, pp. 831-836.

Eshel, A., 1968, "Compressibility Effects on the Infinitely Wide, Perfectly Flexible Foil Bearing," Journal of Lubrication Technology, Transaction of the ASME, pp. 221-225.

Eshel, A., 1974, "Reduction of Air Film in Magnetic Recording by External Air Pressure," Journal of Lubrication Technology, Transaction of the ASME, pp. 247-249.

Eshel, A., 1984a, "Effects of Fluid Inertia on Hydrostatic Foil Bearings," ASLE Special Publication Tribology and Mechanics of Magnetic Storage Systems, pp. 59-62.

Eshel, A., 1984b, "Mechanical Aspects of Archival Storage of Magnetic Tape," Tribology and Mechanics of Magnetic Storage Systems, ASLE Special Publication SP-16, pp. 148-157.

Forrest, A. W., 1995, "Air Entrainment During FIlm Winding with Layon Rolls," Proceedings of the Third International Conference on Web Handling, Stillwater, Oklahoma, pp. 78-92.

Gross, W. A., 1980a, Fluid Film Lubrication, John Wiley & Sons, pp. 58.

Gross, W. A., 1980b, Fluid Film Lubrication, John Wiley & Sons, pp. 491-501.

Hashimoto, H., 1997, "Effects of Foil Bending Rigidity on Spacing Height Characteristics of Hydrostatic Porous Foil Bearings for Web Handling Processes," Journal of Tribology, Transaction of the ASME, Vol. 199, pp. 422-427.

Knox, K. L. and T. L. Sweeney, 1971, "Fluid effects Associated with Web Handling," Industrial & Engineering Chemistry, Process Design & Development. Vol. 10, No. 2, pp. 201-206.

Muftu, S. and R. C. Benson, 1995, "Modeling the Transport of Paper Webs Including the Paper Permeability Effects," Advances in Information Storage and Processing Systems, ASME ISPS-Vol. 1, pp. 247-258.

Muftu, S. and R. C. Benson, 1996, "A Study of Cross-Width Variations in the Two-Dimensional Foil Bearing Problem," Journal of Tribology, Transaction of the ASME, Vol. 118, pp. 407-414.

APPENDIX A

DERIVATION OF THE NON-DIMENSIONAL FORMS OF THE MODIFIED REYNOLDS EQATION AND WEB DEFLECTION EQUATION

Reynolds Equation

As mentioned in Section, 3.1, the foil bearing number, $\varepsilon = \frac{12\mu U}{T}$, is used for scaling. By using the following relations,

$$\varepsilon = \frac{12\mu U}{T}, \quad S = \frac{s}{R_1}\varepsilon^{-1/3}, \quad H = \frac{h}{R_1}\varepsilon^{-2/3}, \quad P = \frac{p}{P_a}$$
$$ds = R_1\varepsilon^{1/3}dS, \quad dh = R_1\varepsilon^{2/3}dH, \quad dp = P_a dP \tag{A.1}$$

the modified Reynolds equation, $\frac{d}{ds}\left(ph^3\frac{dp}{ds} + 6\lambda_a p_a h^2 \frac{dp}{ds} \right) = 12\mu U \frac{d}{ds}(ph)$, can be rewritten as

$$\frac{d}{R_1\varepsilon^{1/3}dS}\left(P_a P\left(R_1\varepsilon^{2/3}H\right)^3 \frac{P_a dP}{R_1\varepsilon^{1/3}dS} + 6\lambda_a P_a \left(R_1\varepsilon^{2/3}H\right)^2 \frac{P_a dP}{R_1\varepsilon^{1/3}dS} \right)$$
$$= \varepsilon T \frac{d}{R_1\varepsilon^{1/3}dS}\left(P_a P R_1\varepsilon^{2/3}H\right) \tag{A.2}$$

Now it is changed to non-dimensional form as follows:

$$\frac{1}{R_1\varepsilon^{1/3}}\frac{d}{dS}\left(\frac{P_a^2R_1^3\varepsilon^2}{R_1\varepsilon^{1/3}}PH^3\frac{dP}{dS}+\frac{6\lambda_aP_a^2R_1^2\varepsilon^{4/3}}{R_1\varepsilon^{1/3}}H^2\frac{dP}{dS}\right)=\frac{\varepsilon TP_aR_1\varepsilon^{2/3}}{R_1\varepsilon^{1/3}}\frac{d}{dS}(PH)$$

$$\frac{d}{dS}\left(P_a^2R_1^2\varepsilon^{5/3}PH^3\frac{dP}{dS}+6\lambda_aP_a^2R_1\varepsilon H^2\frac{dP}{dS}\right)=TP_aR_1\varepsilon^{5/3}\frac{d}{dS}(PH)$$

$$\frac{d}{dS}\left(PH^3\frac{dP}{dS}+\frac{6\lambda_a}{R_1\varepsilon^{2/3}}H^2\frac{dP}{dS}\right)=\frac{T}{P_aR_1}\frac{d}{dS}(PH)$$

$$\frac{d}{dS}\left(PH^3\frac{dP}{dS}+\Lambda_aH^2\frac{dP}{dS}\right)=\frac{1}{B}\frac{d}{dS}(PH) \qquad \text{(A.3)}$$

where $\Lambda_a=\frac{6\lambda_a}{R_1}\varepsilon^{-2/3}$ and $B=\frac{P_aR_0}{T}$.

Web Deflection Equation

For the web deflection equation, slightly different notation of air film thickness is used as follows, which is mentioned in Eq. (18):

$$\varepsilon=\frac{12\mu U}{T},\quad W=\frac{w}{R_1}\varepsilon^{-2/3},\quad S=\frac{s}{R_1}\varepsilon^{-1/3},\quad P_1=\frac{p_1}{P_a},\quad P_2=\frac{p_2}{P_a}$$

$$dw=R_1\varepsilon^{2/3}dW,\qquad ds=R_1\varepsilon^{1/3}dS \qquad \text{(A.4)}$$

Now the web deflection equation, $\bar{d}\frac{d^4w}{ds^4}-T\frac{d^2w}{ds^2}=p_1-p_2-\bar{p}_{bw}$, can be rewritten as

$$(P_1-P_2)P_a-\bar{p}_{bw}=\bar{d}\frac{d^4\left(R_1\varepsilon^{2/3}W\right)}{R_1^4\varepsilon^{4/3}dS^4}-T\frac{d^2\left(R_1\varepsilon^{2/3}W\right)}{R_1^2\varepsilon^{2/3}dS^2}$$

$$= \left(\frac{\bar{d}}{R_1^3 \varepsilon^{2/3}} \right) \frac{d^4 W}{dS^4} - \left(\frac{T}{R_1} \right) \frac{d^2 W}{dS^2} \tag{A.5}$$

Eq. (A.5) is divided by T/R_1,

$$\left(\frac{\bar{d}}{T R_1^2 \varepsilon^{2/3}} \right) \frac{d^4 W}{dS^4} - \frac{d^2 W}{dS^2} = \frac{R_1 P_a}{T} (P_1 - P_2) - \bar{P}_{bw} \frac{R_1}{T} \tag{A.6}$$

then the non-dimensional form of web deflection can be obtained as

$$D \frac{d^4 W}{dS^4} - \frac{d^2 W}{dS^2} = B(P_1 - P_2) - P_{bw} \tag{A.7}$$

where

$$D = \frac{E t^3}{12\left(1-\nu^2\right) T R_1^2} \varepsilon^{-2/3}$$

$$P_{bw} = \begin{cases} 0 & \text{inlet zone} \\ 1 & \text{wrapped zone} \\ 0 & \text{outlet zone} \end{cases}$$

APPENDIX B

DERIVATION OF THE FINITE-DIFFERENCE EQUATIONS OF EQ. (23) AND EQ. (26)

Reynolds Equation

As mentioned in Section 3.2, the non-linear term, $P\frac{dP}{dS}$, in Reynolds equation is linearized, then the linearized equation is

$$\frac{d}{dS}\left[H^3\left(P\frac{d\bar{P}}{dS}-\bar{P}\frac{d\bar{P}}{dS}+\bar{P}\frac{dP}{dS}\right)+\Lambda_a H^2\frac{dP}{dS}\right]=\frac{1}{B}\frac{d}{dS}(PH) \tag{B.1}$$

where

$$P\frac{dP}{dS}\simeq P\frac{d\bar{P}}{dS}-\bar{P}\frac{d\bar{P}}{dS}+\bar{P}\frac{dP}{dS} \tag{B.2}$$

Then the linearized dimensionless Reynolds equation, (B.1), can be changed to a finite-difference equation by taking a central difference approximation.

$$\begin{aligned}\frac{1}{2\Delta S}\Bigg\{&H_{i+1}^3\left[P\frac{d\bar{P}}{dS}-\bar{P}\frac{d\bar{P}}{dS}+\bar{P}\frac{dP}{dS}\right]_{i+1}-H_{i-1}^3\left[P\frac{d\bar{P}}{dS}-\bar{P}\frac{d\bar{P}}{dS}+\bar{P}\frac{dP}{dS}\right]_{i-1}\\&+\Lambda_a H_{i+1}^2\left[\frac{dP}{dS}\right]_{i+1}-\Lambda_a H_{i-1}^2\left[\frac{dP}{dS}\right]_{i-1}\Bigg\}=\frac{1}{B2\Delta S}\left(P_{i+1}H_{i+1}-P_{i-1}H_{i-1}\right)\end{aligned} \tag{B.3}$$

where

$$\left.\frac{dP}{dS}\right|_{i+1} = \frac{1}{2\Delta S}\left(3P_{i+1} - 4P_i + P_{i-1}\right) + O(\Delta S)^2 \tag{B.4}$$

by taking backward difference approximation, and

$$\left.\frac{dP}{dS}\right|_{i-1} = \frac{1}{2\Delta S}\left(-P_{i+1} + 4P_i - 3P_{i-1}\right) + O(\Delta S)^2 \tag{B.5}$$

by taking forward difference approximation.

Substituting Eq.(B.3) and Eq.(B.4) into Eq.(B.2) yields

$$H_{i+1}^3\left[\left(P_{i+1} - \overline{P}_{i+1}\right)\left(3\overline{P}_{i+1} - 4\overline{P}_i + \overline{P}_{i-1}\right) + \overline{P}_{i+1}\left(3P_{i+1} - 4P_i + P_{i-1}\right)\right]$$

$$-H_{i-1}^3\left[\left(P_{i-1} - \overline{P}_{i-1}\right)\left(-\overline{P}_{i+1} + 4\overline{P}_i - 3\overline{P}_{i-1}\right) + \overline{P}_{i-1}\left(-P_{i+1} + 4P_i - 3P_{i-1}\right)\right]$$

$$+\Lambda_a H_{i+1}^2\left(3P_{i+1} - 4P_i + P_{i-1}\right) - \Lambda_a H_{i-1}^2\left(-P_{i+1} + 4P_i - 3P_{i-1}\right)$$

$$= \frac{2\Delta S}{B}\left(P_{i+1}H_{i+1} - P_{i-1}H_{i-1}\right)$$

The above equation can be rewritten as a set of simple linear finite-difference equations. The coefficients of the following Eq. (B.5) consist of constants, pressure profile of previous step, and given gap profile.

$$A_i P_{i-1} + B_i P_i + C_i P_{i+1} = D_i \qquad i = 1, 2, \ldots \text{n} \tag{B.6}$$

where

$$A_i = H_{i+1}^3 \overline{P}_{i+1} + H_{i-1}^3 \left(\overline{P}_{i+1} - 4\overline{P}_i + 6\overline{P}_{i-1} \right) + \Lambda_a \left(H_{i+1}^2 + 3H_{i-1}^2 \right) + 2\Delta S H_{i-1} / B$$

$$B_i = -4\left(H_{i+1}^3 \overline{P}_{i+1} + H_{i-1}^3 \overline{P}_{i-1} \right) - 4\Lambda_a \left(H_{i+1}^2 + H_{i-1}^2 \right)$$

$$C_i = H_{i+1}^3 \left(6\overline{P}_{i+1} - 4\overline{P}_i + \overline{P}_{i-1} \right) + H_{i-1}^3 \overline{P}_{i-1} + \Lambda_a \left(3H_{i+1}^2 + H_{i-1}^2 \right) - 2\Delta S H_{i+1} / B$$

$$D_i = H_{i+1}^3 \overline{P}_{i+1} \left(3\overline{P}_{i+1} - 4\overline{P}_i + \overline{P}_{i-1} \right) + H_{i-1}^3 \overline{P}_{i-1} \left(\overline{P}_{i+1} - 4\overline{P}_i + 3\overline{P}_{i-1} \right)$$

The matrix form can be obtained as

$$\begin{bmatrix} B_1 & C_1 & 0 & & & \\ A_2 & B_2 & C_2 & 0 & & \\ 0 & . & . & . & 0 & \\ & 0 & . & . & . & 0 \\ & & 0 & A_{n-1} & B_{n-1} & C_{n-1} \\ & & & 0 & A_n & B_n \end{bmatrix} \begin{Bmatrix} P_1 \\ P_2 \\ . \\ . \\ P_{n-1} \\ P_n \end{Bmatrix} = \begin{Bmatrix} D_1 - A_1 P_0 \\ D_2 \\ . \\ . \\ D_{n-1} \\ D_n - C_n P_{n+1} \end{Bmatrix} \tag{B.7}$$

where the boundary conditions can be applied as $P_{n+1} = P_o = 1$.

Web Deflection Equation

The non-dimensional form of the web deflection equation is a fourth-order linear differential equation so that we can use the following central difference approximations.

$$\frac{d^2W}{dS^2} = \frac{-W_{i+2} + 16W_{i+1} - 30W_i + 16W_{i-1} - W_{i-2}}{12\Delta S^2} + O(\Delta S)^4 \tag{B.8}$$

$$\frac{d^4W}{dS^4} = \frac{W_{i+2} - 4W_{i+1} + 6W_i - 4W_{i-1} + W_{i-2}}{\Delta S^4} + O(\Delta S)^2 \tag{B.9}$$

The dimensionless web deflection equation, $D\frac{d^4W}{dS^4}-\frac{d^2W}{dS^2}=B(P_1-P_2)-P_{bw}$, can be written as follows with the Eq. (B.7) and (B.8).

$$B(P_{1i}-P_{2i})-P_{bw}=\frac{D}{\Delta S^4}(W_{i+2}-4W_{i+1}+6W_i-4W_{i-1}+W_{i-2})$$

$$-\frac{1}{12\Delta S^2}(-W_{i+2}+16W_{i+1}-30W_i+16W_{i-1}-W_{i-2})$$

$$=\left(\frac{D}{\Delta S^4}+\frac{1}{12\Delta S^2}\right)W_{i+2}-\left(\frac{4D}{\Delta S^4}+\frac{4}{3\Delta S^2}\right)W_{i+1}+\left(\frac{6D}{\Delta S^4}+\frac{5}{2\Delta S^2}\right)W_i$$

$$+\left(\frac{D}{\Delta S^4}+\frac{1}{12\Delta S^2}\right)W_{i-2}-\left(\frac{4D}{\Delta S^4}+\frac{4}{3\Delta S^2}\right)W_{i-1}$$

Now we can see the finite-difference form as

$$E_1W_{i-2}+E_2W_{i-1}+E_3W_i+E_4W_{i+1}+E_5W_{i+2}=F_i \qquad i=1,2,\ldots n \tag{B.10}$$

where

$$E_1=E_5=\frac{D}{\Delta S^4}+\frac{1}{12\Delta S^2}$$

$$E_2=E_4=-\left(\frac{4D}{\Delta S^4}+\frac{4}{3\Delta S^2}\right)$$

$$E_3=\frac{6D}{\Delta S^4}+\frac{5}{2\Delta S^2} \tag{B.11}$$

$$F_i=B(P_{1i}-P_{2i})-P_{bw}$$

After applying the boundary conditions, we can obtain the complete matrix form, Eq. (B.10). The boundary conditions can be written in finite-difference form:

$$W\big|_{S=0} = 0,\ \left.\frac{d^2W}{dS^2}\right|_{S=0} = 0,\ W\big|_{S=L} = 0, \text{and } \left.\frac{d^2W}{dS^2}\right|_{S=L} = 0 \qquad \text{(B.12)}$$

The boundary condition at start point for finite-difference equation can be written as

$$W_0 = 0$$

$$\left.\frac{d^2W}{dS^2}\right|_{i=1} = \frac{-W_3 + 16W_2 - 30W_1 + 16W_0 - W_{-1}}{12\Delta S^2} = 0$$

Rewrite the above two equations

$$W_0 = 0$$

$$W_{-1} = -30W_1 + 16W_2 - W_3$$

At node 1 and 2, the finite-difference equations can be written as

$$E_1 \times (-30W_1 + 16W_2 - W_3) + E_2 \times 0 + E_3W_1 + E_4W_2 + E_5W_3 = F_1 \quad \text{for node 1}$$

$$E_1 \times 0 + E_2W_1 + E_3W_2 + E_4W_3 + E_5W_4 = F_2 \quad \text{for node 2}$$

Rewrite the above equations

$$(E_3 - 30E_1)W_1 + (16E_1 + E_4)W_2 + (E_5 - E_1)W_3 = F_1 \quad \text{for node 1}$$

$$E_2W_1 + E_3W_2 + E_4W_3 + E_5W_4 = F_2 \quad \text{for node 2}$$

The boundary condition at the end point for finite-difference equation can be written as

$$W_{n+1} = 0$$

$$\left.\frac{d^2W}{dS^2}\right|_{i=n} = \frac{-W_{n+2} + 16W_{n+1} - 30W_n + 16W_{n-1} - W_{n-2}}{12\Delta S^2} = 0$$

Rewrite the above equations as

$$W_{n+1} = 0$$

$$W_{n+2} = -30W_n + 16W_{n-1} - W_{n-2}$$

At the node n and n-1, the finite-difference equations can be written as

$$E_1W_{n-3} + E_2W_{n-2} + E_3W_{n-1} + E_4W_n + E_5 \times 0 = F_{n-1} \qquad \text{for node n-1}$$

$$E_1W_{n-2} + E_2W_{n-1} + E_3W_n + E_4 \times 0 + E_5\left(-30W_n + 16W_{n-1} - W_{n-2}\right) = F_n \text{ for node n}$$

Rewrite the above equations as

$$E_1W_{n-3} + E_2W_{n-2} + E_3W_{n-1} + E_4W_n = F_{n-1} \qquad \text{for node } n-1$$

$$\left(E_1 - E_5\right)W_{n-2} + \left(E_2 + 16E_5\right)W_{n-1} + \left(E_3 - 30E_5\right)W_n = F_n \text{ for node } n$$

Now the matrix form can be written as

$$\begin{bmatrix} E_{1,1} & E_{1,2} & E_{1,3} & 0 & & & & & \\ E_2 & E_3 & E_4 & E_5 & 0 & & & & \\ E_1 & E_2 & E_3 & E_4 & E_5 & 0 & & & \\ 0 & . & . & . & . & . & 0 & & \\ & 0 & . & . & . & . & . & 0 & \\ & & 0 & E_1 & E_2 & E_3 & E_4 & E_5 & \\ & & & 0 & E_1 & E_2 & E_3 & E_4 & \\ & & & & 0 & E_{n,n-2} & E_{n,n-1} & E_{n,n} & \end{bmatrix} \begin{bmatrix} W_1 \\ W_2 \\ W_3 \\ . \\ . \\ W_{n-2} \\ W_{n-1} \\ W_n \end{bmatrix} = \begin{bmatrix} F_1 \\ F_2 \\ F_3 \\ . \\ . \\ F_{n-2} \\ F_{n-1} \\ F_n \end{bmatrix} \tag{B.13}$$

where the modified six elements can be written as follows:

$$E_{1,1} = E_3 - 30E_1 = \left(\frac{6D}{\Delta S^4} + \frac{5}{2\Delta S^2}\right) - 30\left(\frac{D}{\Delta S^4} + \frac{1}{12\Delta S^2}\right) = -24\frac{D}{\Delta S^4}$$

$$E_{1,2} = 16E_1 + E_4 = 16\left(\frac{D}{\Delta S^4} + \frac{1}{12\Delta S^2}\right) - \left(\frac{4D}{\Delta S^4} + \frac{4}{3\Delta S^2}\right) = 12\frac{D}{\Delta S^4}$$

$$E_{1,3} = E_5 - E_1 = 0$$

$$E_{n,n-2} = E_1 - E_5 = E_5 - E_1 = E_{1,3} = 0$$

$$E_{n,n-1} = E_2 + 16E_5 = E_4 + 16E_1 = E_{1,2} = 12\frac{D}{\Delta S^4}$$

$$E_{n,n} = E_3 - 30E_5 = E_3 - 30E_1 = E_{1,1} = -24\frac{D}{\Delta S^4}$$

APPENDIX C

DERIVATION OF THE FINITE-DIFFERENCE EQUATION OF EQ. (54) FOR THE TWO DIFFERENT SETS OF BOUNDARY CONDITIONS

The dimensionless web deflection equation, Eq. (17), can be rewritten by ignoring the web stiffness term as

$$-\frac{d^2W}{dS^2} = B(P_1 - P_2) - P_w \tag{C.1}$$

The finite-difference form of the Eq. (C.1) can be written using central difference approximation as

$$W_{i-1} - 2W_i + W_{i+1} = \Delta S^2 P_w - \Delta S^2 B(P_{1i} - P_{2i}) \tag{C.2}$$

where

$$\frac{d^2W}{dS^2} = \frac{W_{i-1} - 2W_i + W_{i+1}}{\Delta S^2} \tag{C.3}$$

The matrix form of Eq. (C.2) can be written with the boundary conditions #1, mentioned in Section 4.1.1 as

$$\begin{bmatrix} -2 & 1 & 0 & & & & \\ 1 & -2 & 1 & 0 & & & \\ 0 & . & . & . & 0 & & \\ & 0 & 1 & -2 & 1 & 0 & \\ & & 0 & . & . & . & 0 \\ & & & 0 & 1 & -2 & 1 \\ & & & & 0 & 1 & -2 \end{bmatrix} \begin{bmatrix} W_1 \\ W_2 \\ . \\ W_i \\ . \\ W_{n-1} \\ W_n \end{bmatrix} = \begin{bmatrix} F_1 - W_0 \\ F_2 \\ . \\ F_i \\ . \\ F_{n-1} \\ F_n - W_{n+1} \end{bmatrix} \tag{C.4}$$

where

$$F_i = \Delta S^2 P_w - \Delta S^2 B(P_{1i} - P_{2i}) \tag{C.5}$$

$$W_0 = W_{n+1} = 0$$

Another matrix form for the second set of the boundary conditions is

$$\begin{bmatrix} -2 & 2 & 0 & & & & \\ 1 & -2 & 1 & 0 & & & \\ 0 & . & . & . & 0 & & \\ & 0 & 1 & -2 & 1 & 0 & \\ & & 0 & . & . & . & 0 \\ & & & 0 & 1 & -2 & 1 \\ & & & & 0 & 1 & -2 \end{bmatrix} \begin{bmatrix} W_1 \\ W_2 \\ . \\ W_i \\ . \\ W_{n-1} \\ W_n \end{bmatrix} = \begin{bmatrix} F_1 \\ F_2 \\ . \\ F_i \\ . \\ F_{n-1} \\ F_n - W_{n+1} \end{bmatrix} \tag{C.6}$$

where

$$F_i = \Delta S^2 P_w - \Delta S^2 B(P_{1i} - P_{2i})$$

$$\left.\frac{dW}{dS}\right|_{i=1} = \frac{W_2 - W_0}{2\Delta S} = 0 \tag{C.7}$$

$$W_{n+1} = 0$$

APPENDIX D

COMPUTER PROGRAM

```
#include<stdio.h>
#include<math.h>
#include<iostream.h>
#include<nrutil.h>
#include<fbando.c>
// fbando.c: source code to solve banded matrix without pivoting

/* This program calculates the pressure and gap profiles for
nipped case with bending stiffness of web (See the reports for
detail schematic configuration).
// Therefore, the main variables are P1[], P2[], H1[], H2[]
// P1[] : Pressure profile between winding roller and web
// P2[] : Pressure profile between nip roller and web
// H1[] : Gap profile between winding roller and web
// H2[] : Gap profile between nip roller and web
*/

#define M_PI     3.1415926535897943

//************************  Configuration data ; geometry & node
#define R1         4.0
                 // inches     : radius of roller 1  Winding roller
#define R2         4.0
                    // inches     : redius of roller 2, Nip roller
#define RE       ( R1*R2/(R1+R2) )   // inches  : equivalent radius
#define THETA1   (10.0*M_PI/180*pow(EE,-1./3) )
                                  // (degree) incomming wrap angle
#define THETA2   ( 5.0*M_PI/180*pow(EE,-1./3) )
                                  // (degree)  outgoing wrap angle
#define S_IN     ( 1.0/R1*pow(EE,-1./3) )
                                       // inches : inlet length
#define S_OUT    ( 1.0/R1*pow(EE,-1./3) )
                                      // inches : outlet length
#define DS      ( (S_IN+THETA1+THETA2+S_OUT) / (N+1) )
                                    // length of one cell - one Dim
#define N        3999       // total No. of nodes of winding roller
#define NC   int( (S_IN+THETA1)/DS )                  // center node
#define N1   int(  S_IN/DS )                           // inlet node
#define N2   int( (S_IN+THETA1+THETA2)/DS )
```

```
                                                        // outlet node
#define T       (1.5)                                 // lbf/in : tension
#define U       (2000.0/5.0)                       // ft/min : speed of web
#define M1       2                              // band size of matrix a[][]
#define M2       2                              // band size of matrix a[][]

//***************************** Configuration data for Nip Roller
#define THETA_NIP1 ( 10*M_PI/180*pow(EE,-1./3) )
                   // (degree) Incomming wrap angle of Nip Roller
#define THETA_NIP2 ( 10*M_PI/180*pow(EE,-1./3) )
                    // (degree) Outgoing wrap angle of Nip Roller
#define N1_NIP   int( THETA_NIP1/DS )             // Number of node
#define N2_NIP   int( THETA_NIP2/DS )             // Number of node
#define NN          (N1_NIP + N2_NIP)
                              // total No. of nodes of Nip Roller

//******************   Air properites and Web material properties
#define PA      14.7                          // Psi : ambient pressure
#define MU      2.6396e-9           // Psi.s     : dynamic viscosity
            /* 2.6056E-9 Psi S   at 62 degree[F], 16.85 degree[C]
               2.6396E-9 Psi S   at 71 degree[F], 21.85 degree[C]
               2.6764E-9 Psi S   at 80 degree[F], 26.85 degree[C]
             */
#define R_A     2.65e-6
                  // mean-free-path of the air molecules (inches)
#define BS      1.0e+5
                                    // elastic modulus of web (Psi)
#define t       5.0e-3                      // Web thickness (inches)
#define NU      0.4                                 // Poison's ratio

//*********************************   Constants : RAMDA_A, B, D, K
#define EE       ( 12*MU*U/T )
#define RAM_A    ( 6*R_A*pow(EE,-2./3)/R1 )
                                          // constant in reynolds EQ
#define B        ( R1*PA/T )              // constant in Reynolds EQ
#define D
      ( BS*pow(t,3.0)*pow(EE,-2.0/3.0)/(12*(1.0-NU*NU)*T*R1*R1) )

//************************************      Boundary Conditions
#define P0     (14.7/PA)                  // Psi : Pressure Boundary 1
#define PN_1   (14.7/PA)                  // Psi : Pressure Boundary 2

//***************************** Control data for Iteration Process
#define IT_R_MAX        10
             // Maximum iteration number of the function reynolds
#define RES_H_LIMIT     2.0e-5
#define RES_P_LIMIT     2.0e-5
#define WEIGHT_P        1.0

// Declaration of several global variables
int NI,j;
                                    // maximum iteration number (NI)
```

```
                                        // iteration interval of printing (j)
double WEIGHT_H, HC;

FILE *fi;

//*****************************************************************
/* this is a function for solving tridiagonal matrix.
Note : LU decomposition method for tridiagonal systems.
*/
void solve1(double a[], double b[], double c[],  double r[],
double x[], unsigned long n)
{
      unsigned long j;
      double bet, gam[N+5];

      if (b[1] ==0.0) cout << "Error 1 in tridag";
//    if this happens then you should rewrite your equations
//    as a set of order N-1, with x2 trivially eliminated.
      x[1]=r[1]/(bet=b[1]);
      // Decomposition and forward substitution
      for (j=2 ; j<=n ; j++) {
            gam[j] = c[j-1]/bet;
            bet = b[j]-a[j]*gam[j];
            if (bet == 0.0)       cout << "Error 2 in tridag";
            // algoththm fails
            x[j]=(r[j]-a[j]*x[j-1])/bet;
      }
      for (j=(n-1) ; j>=1 ; j--) // Backsubstitution
            x[j] -= gam[j+1]*x[j+1];

      for (j=1 ; j<=N ; j++)
            gam[j] = 0.0;
}     // the end of the function, slove1();

//*****************************************************************
void input(void)
{
cout << "\n Input data file = initial.txt\n Output data file = ";
cout << " result.txt & next_initial.txt";
cout << "\n\n Enter the gap between Nip and Winding Roller at
center ";
cout << "\n Start with big gap, about 5 milli inches suggested ";
cout << "\n Hc [unit : milli inche] = ? ";
cin >> HC;
cout << "\n\n Enter Maximum Iteration No ? ";
cin >> NI;
cout << " Enter Weighting factor of H ? ";
cin >> WEIGHT_H;
cout << "\n Weighting Factor is " << WEIGHT_H;
cout << "\n Enter Interval of printing data ?";
cin >> j;
}     // the end of the input function
```

```
//*****************************************************************
void initial(double **a, double P1[], double H1[], double P2[],
double HS[])
{
int i;
double s;

// read initial gap and pressure profiles
fi = fopen("initial.txt","r");      // 10initial.txt is input file

for(i = 0; i<=N+1; i++)
    fscanf(fi, "%lf", &P1[i]);                    // read pressure
for(i = 0; i<=N+1; i++)
    fscanf(fi, "%lf", &H1[i]);                        // read gap
for(i = 0; i <= NN+1 ; i++)
    fscanf(fi, "%lf", &P2[i]);                   // read pressure 2
fclose(fi);

// Set HS profile : Constant Gap Profile
for(i=0 ; i<=NN+1 ; i++)      // total No. of node of Nip Roller
    {
    s = (i-N1_NIP)*DS*pow(EE,1.0/3.0);
    HS[i] = ((R1+R2)/(2*R2)) * pow(EE,-2.0/3.0) * pow(sin(s),2) +
HC ;
    }

// calculate compactly stored array a[][] for shell equation
// elements range : from 0 to N-1 (that is different from the
others for Reynolds EQ.)
a[0][0] =  0.0;                                  // useless element
a[0][1] =  0.0;                                  // useless element
a[0][2] = -24.0*D*pow(DS,-4.0);
a[0][3] =  12.0*D*pow(DS,-4.0);
a[0][4] =  0.0;

for( i=1 ; i<=N-2 ; i++) {
    a[i][0] =       D*pow(DS,-4.0) + (1.0/12.0)*pow(DS,-2.0);
    a[i][1] = - 4.0*D*pow(DS,-4.0) - (4.0/3.0 )*pow(DS,-2.0);
    a[i][2] =   6.0*D*pow(DS,-4.0) + (5.0/2.0 )*pow(DS,-2.0);
    a[i][3] = - 4.0*D*pow(DS,-4.0) - (4.0/3.0 )*pow(DS,-2.0);
    a[i][4] =       D*pow(DS,-4.0) + (1.0/12.0)*pow(DS,-2.0);

a[N-1][0] =  0.0;
a[N-1][1] =  12.0*D*pow(DS,-4.0);
a[N-1][2] = -24.0*D*pow(DS,-4.0);
a[N-1][3] =  0.0;                                // useless element
a[N-1][4] =  0.0;                                // useless element

// Factorization (LU Decomposition) before solving a linear
banded system
i = bando(1, N, M1, M2, a, P1);     // mode 1 : factorization only
```

```
                // P1 vector is not in use for only factorization
}     // the end of the function, initial();

//*****************************************************************
void thickness2(double H1[], double H2[], double HS[])
{
register int i;
for(i=0 ; i<=NN+1 ; i++)      // total No. of node of Nip Roller
    H2[i] = HS[i] - H1[NC-N1_NIP + i];
}     // The end of the function, thickness2();

//*****************************************************************
double reynolds(double H[], double P[], int n, int& iter_r)
{
register int i;
double aa, ba, ab, bb, ac, bc, ad, bd;
double resi=100,res_p=0;
double AR[N+5], BR[N+5], CR[N+5], DR[N+5], P_old1[N+5],
P_old2[N+5];

for (i=1 ; i<=n ; i++)
   P_old1[i] = P[i];

iter_r = 0;

while(resi > RES_P_LIMIT && iter_r < IT_R_MAX)
                                  // run the loop until it converges
{
   iter_r ++;
   resi =0.0;

   //***************  calculate coefficients
   for( i=1 ; i<= n ; i++)
   {
        aa = pow(H[i+1],3)*P[i+1]
                     + pow(H[i-1],3)*(P[i+1]-4.*P[i]+6.*P[i-1]);
        ba = RAM_A*(pow(H[i+1],2)+3.*pow(H[i-1],2))
                                                + 2.*DS*H[i-1]/B;
      AR[i] = (aa+ba);
        ab = -4. * ( pow(H[i+1],3)*P[i+1]
                                          + pow(H[i-1],3)*P[i-1] );
        bb = -4. * RAM_A * ( pow(H[i+1],2) + pow(H[i-1],2) );
      BR[i] = (ab+bb);
        ac = pow(H[i+1],3)*(6.*P[i+1]-4.*P[i]+P[i-1])
                                            + pow(H[i-1],3)*P[i-1];
        bc = RAM_A*(3.*pow(H[i+1],2)+pow(H[i-1],2))
                                                - 2.*DS*H[i+1]/B;
      CR[i] = (ac+bc);
        ad = pow(H[i+1],3) * P[i+1]
                                     * ( 3.*P[i+1]-4.*P[i]+P[i-1] );
        bd = pow(H[i-1],3) * P[i-1]
                                     * ( P[i+1]-4.*P[i]+3.*P[i-1] );
```

```
      DR[i] = (ad+bd);
   }

   // coefficient with boundary conditions P1[0] and P1[N+1]
   P[0] = P0;
   P[n+1] = PN_1;
   DR[1] = DR[1] - AR[1]*P[0];
   DR[n] = DR[n] - CR[n]*P[n+1];

   for(i=1 ; i<=n ; i++)
      P_old2[i]=P[i];
   solve1(AR, BR, CR, DR, P, n);
                    // AR,BR,CR,DR,P1 are inputs and also outputs
   for(i=1 ; i<=n ; i++)
      resi += fabs(P[i]-P_old2[i]);

}     // the end of while loop

// calculate residual of Pressure profile
for(i=1 ; i<=n ; i++)
    res_p += fabs(P[i]-P_old1[i]) ;

for(i=1 ; i<=n ; i++)
    P[i] = P_old1[i] + ( WEIGHT_P*(P[i]-P_old1[i]) );

return(res_p);
}     // the end of the function, Reynolds();

//*****************************************************************
double shell( double **a, double H[], double P1[], double P2[])
                                                    // [A]{H} = {E}
{
register int i;
double f[N+5], w[N+5], w_old[N+5], p2_temp[N+5];
// the range of f[i] and a [i][j] in the function shell()
// i: from 0 to N-1 , j: from 0 to M1+M2 (array starts at 0)
// the range in other functions : from 1 to N (array starts at 1)
double s, res_w=0;

// calculate P2 as a scale of P1;
// (P1 : 0 ~ N+1), ( P2 : 0 ~ N1_NIP + N2_NIP+1 )
for(i=0 ; i < NC-N1_NIP ; i++)
   p2_temp[i] = 1.0;
for(i=NC-N1_NIP ; i<=NC+N2_NIP ; i++)
   p2_temp[i] = P2[i-(NC-N1_NIP)];
for(i=NC+N2_NIP+1 ; i<=N+1 ; i++)
   p2_temp[i] = 1.0;

// w profile for shell EQ; w = h - in&out geometry
for(i=0 ; i<N1 ; i++){
   s = (N1-i)*DS;
   w[i] = H[i] - pow(s,2)/2.0; }
```

```
   for(i=N1; i<=N2 ; i++)
      w[i] = H[i];
   for(i=N2+1 ; i<=N+1 ; i++){
      s = (i-N2)*DS;
      w[i] = H[i] - pow(s,2)/2.0; }

// calculate the coefficient, f[] for simple foil bearing
// the range of f[] : from 0 to N-1
// the range of P1[] : from 1 to N
for( i=1 ; i<N1 ; i++)
   f[i-1] =   B*(P1[i]-p2_temp[i]);
for( i=N1 ; i<=N2 ; i++)
   f[i-1] =   B*(P1[i]-p2_temp[i]) - 1.0;
for( i=N2+1 ; i<=N ; i++)
   f[i-1] =   B*(P1[i]-p2_temp[i]);

// then solve shell equation
for(i=0 ; i<=N+1 ; i++)
   w_old[i]=w[i];

i = bando(2, N, M1, M2, a, f);        //mode 1: factorization only
                                              //mode 2: solver only
                                 //mode 0: factorize then solve matrix
                                                    //output f[]

// Transfer output f[] to w[] and confirm the boundarys for
Reynolds Equation
for(i=1 ; i<=N ; i++)
     w[i] = f[i-1];
w[0]  = 0.0;
w[N+1]= 0.0;

// calculate residual
for(i=1 ; i<=N ; i++)
   res_w += fabs(w[i]-w_old[i]);

// update thickness profile with weighting factor
for(i=1 ; i<=N ; i++)
   w[i] = w_old[i] +  WEIGHT_H*(w[i]-w_old[i]) ;

// h profile for reynols EQ; h = w + in&out geometry
for(i=0 ; i<N1 ;i++){                                  // inlet region
    s    = (N1-i)*DS;
    H[i] = w[i] + pow(s,2)/2.0; }
for(i=N1 ; i<=N2 ; i++)                               // wraped region
    H[i] = w[i];
for(i=N2+1 ; i<=N+1 ;i++){                            // outlet region
    s    = (i-N2)*DS;
    H[i] = w[i] + pow(s,2)/2.0; }

return(res_w);
}     // end of function, shell()
```

```
//*****************************************************************
void next_initial(double P1[], double H1[], double P2[])
{
int i;
fi = fopen("next_initial.txt","w");
for(i=0 ; i<=N+1 ;i++)
   fprintf(fi,"%20.13e\n",P1[i]);
for(i=0 ; i<=N+1 ;i++)
   fprintf(fi,"%20.13e\n",H1[i]);
for(i=0 ; i<=NN+1 ;i++)
   fprintf(fi,"%20.13e\n",P2[i]);
fclose(fi);
}

//*****************************************************************
void main()
{
register int i;
int iter1, iter2;
double **a;      // Dynamic allocation of two-dimensional matrices
double H1[N+5],H2[N+5],HS[N+5],P1[N+5],P2[N+5];
double res_h, res_p1, res_p2, HCC;

a = dmatrix(0,N+5,0,M1+M2+5);
                      // dynamic allocation of a[0~N+5][0~M1+M2+5]
input();

HCC = HC;
HC  = HC*0.001/R1*pow(EE,-2./3);  // convert mils to dimless scale

initial(a, P1, H1, P2, HS);
                 // 1. Read initial pressure and thickness profile
                      // 2. Set banded coefficient matrix, (a[][])
                        // 3. Set HS profile: Constant Gap Profile
fi = fopen("result.txt","w");

fprintf(fi,"\n      Entered Weighting Factor=  %e",WEIGHT_H);
fprintf(fi,"\n      Entered The Gap Wetween Winding & Nip roller=
%e (mils)",HCC);
fprintf(fi,"\n       iteration        res_h       P1[NC]
H1[NC]  \n");
    printf("\n       iteration        res_h       P1[NC]
H1[NC]  \n");

for(i=1 ; i<=NI ; i++)
{
   // calculate Thickness profile between web and nip roller
   thickness2(H1,H2,HS);                                  // make H2

   // solve P1
   res_p1 = reynolds(H1, P1, N, iter1);
```

```
   // solve P2
   res_p2 = reynolds(H2, P2, NN, iter2);

   // solve H1
   res_h = shell(a, H1, P1, P2);
   if(i%j == 0){          // "j" is the interval of printout data
   printf("%2d %2d %10d %14.5e %19.11e
%17.9e\n",iter1,iter2,i,res_h,(P1[NC]-1)*B,H1[NC]);
   // print on screen
   fprintf(fi,"%2d %2d %10d %14.5e %19.11e
%17.9e\n",iter1,iter2,i,res_h,(P1[NC]-1)*B,H1[NC]);
   // print on file
   }
} // the end of for loop

fclose(fi);
next_initial(P1, H1, P2);

}     // the end of the main function
```

APPENDIX E

COMPUTER PROGRAM TO CALCULATE NIP FORCE AND THE AMOUNT OF THE AIR ENTRAINMENT

```
// This program calculates the nip force and the amount of
// the air entrainment with converged solution, gap and pressure
// profiles (P1, P2, H1)

#include<stdio.h>
#include<math.h>
#include<iostream.h>

#define M_PI     3.1415926535897943

//************************** Configuration data ; geometry & node
#define R1         4.0
                  // inches     : radius of roller 1  Winding roller
#define R2         4.0
                     // inches     : redius of roller 2, Nip roller
#define RE       ( R1*R2/(R1+R2) )   // inches  : equivalent radius
#define THETA1   (10.0*M_PI/180*pow(EE,-1./3) )
                                  // (degree) incomming wrap angle
#define THETA2   ( 5.0*M_PI/180*pow(EE,-1./3) )
                                  // (degree)  outgoing wrap angle
#define S_IN     ( 1.0/R1*pow(EE,-1./3) )
                                          // inches : inlet length
#define S_OUT    ( 1.0/R1*pow(EE,-1./3) )
                                         // inches : outlet length
#define DS      ( (S_IN+THETA1+THETA2+S_OUT) / (N+1) )
                                    // length of one cell - one Dim
#define N        3999       // total No. of nodes of winding roller
#define NC   int( (S_IN+THETA1)/DS )                    // center node
#define N1   int(  S_IN/DS )                             // inlet node
#define N2   int( (S_IN+THETA1+THETA2)/DS )
                                                        // outlet node
#define T       (1.5)                                // lbf/in : tension
#define U       (2000.0/5.0)                 // ft/min : speed of web

//***************************** Configuration data for Nip Roller
#define THETA_NIP1 ( 10*M_PI/180*pow(EE,-1./3) )
                   // (degree) Incomming wrap angle of Nip Roller
```

```
#define THETA_NIP2 ( 10*M_PI/180*pow(EE,-1./3) )
                    // (degree) Outgoing wrap angle of Nip Roller
#define N1_NIP   int( THETA_NIP1/DS )            // Number of node
#define N2_NIP   int( THETA_NIP2/DS )            // Number of node
#define NN          (N1_NIP + N2_NIP)
                              // total No. of nodes of Nip Roller


//******************   Air properites and Web material properties
#define PA     14.7                        // Psi : ambient pressure
#define MU     2.6396e-9          // Psi.s     : dynamic viscosity
            /* 2.6056E-9 Psi S   at 62 degree[F], 16.85 degree[C]
               2.6396E-9 Psi S   at 71 degree[F], 21.85 degree[C]
               2.6764E-9 Psi S   at 80 degree[F], 26.85 degree[C]
             */
#define R_A    2.65e-6
                  // mean-free-path of the air molecules (inches)

//**************   Constants : RAMDA_A and B in Reynolds equation
#define EE      ( 12*MU*U/T )

//************************************* Declaration of functions
void hc_nip_force(double [], double [], double [], double []);
                                        // arguments: P1, P2, H1, H2
void initial(double [], double [], double[], double[]);
                                          // arguments: P1, H1, P2
void excel_print(double [], double [], double [], double []);
                                        // arguments: P1, P2, H1, H2

//****************************** Declaration of saveral variables
double HC;
FILE *fi;

void main()
{
double H1[N+5],H2[N+5],P1[N+5],P2[N+5];
double HCC;

cout << "\n\n Enter the gap between Nip and Winding Roller at
center ";
cout << "\n Hc [unit : milli inche] = ? ";
cin >> HC;
HCC = HC;
HC  = HC*0.001/R1*pow(EE,-2./3);

initial(P1, H1, P2, H2);
                // 1. Read initial pressure and thickness profile
      // 2. Set tirdiagonal coefficient matrix for shell equation
                      // 3. Set HS profile : Constant Gap Profile

fi = fopen("hc&nip_force.txt","w");
```

```
fprintf(fi,"\n      Entered The Gap Wetween Winding & Nip roller=
%e",HCC);

//  excel_print(P1,P2,H1,H2);
hc_nip_force(P1,P2,H1,H2);
fclose(fi);

}  // the end of the main function

//*****************************************************************
void initial(double P1[], double H1[], double P2[], double H2[])
{
int i;
double s,hs;

// read converged solution; thickness and pressure profiles
fi = fopen("initial.txt","r");

for(i = 0; i<=N+1; i++)
   fscanf(fi, "%lf", &P1[i]);                    // read pressure
for(i = 0; i<=N+1; i++)
   fscanf(fi, "%lf", &H1[i]);                   // read thickness
for(i = 0; i <= NN+1 ; i++)
   fscanf(fi, "%lf", &P2[i]);                    // read pressure
fclose(fi);

// Set HS profile : Constant Gap Profile
for(i=0 ; i<=NN+1 ; i++)       // total No. of node of Nip Roller
{
   s = (i-N1_NIP)*DS;
   hs = ((R1+R2)/R2) * pow(s,2)/2.0 + HC ;
   H2[i] = hs - H1[NC-N1_NIP + i];
}

}  // the end of the function, initial();

//*****************************************************************
void hc_nip_force(double P1[], double P2[], double H1[], double
H2[])
{
int i,j=0;
double g,gg,s,s_1,p,p_1,h,h_1,dp,dp_1,hc,hc_1,hcc[100]
       ,hc_avg=0.0,nip_force=0.0;

//*********************************************  calculating h1c
fprintf(fi, "\n\n  the amount of entrained air, h1c[mils] between
winding roller and web\n");
fprintf(fi, "\n ***********************************************");
fprintf(fi, "\n   s[inches]         dp1            h1c[mils]");
fprintf(fi, "\n ***********************************************");
// find dp1/ds =0, then calculate hc
g = P1[2] - P1[0];
```

```
for(i=2 ; i <N ; i++)
{  gg = P1[i+1] - P1[i-1];
   if(gg*g < 0)
   {  j+=2;
      s    = (i-NC)*DS*R1*pow(EE,1./3);
      s_1  = (i-NC-1)*DS*R1*pow(EE,1./3);      // at previous node
      p    = (P1[i]  -1)*14.7;
      p_1 = (P1[i-1]-1)*14.7;                  // at previous node
      h    = H1[i]  *R1*1000*pow(EE,2./3);
      h_1 = H1[i-1]*R1*1000*pow(EE,2./3);      // at previous node
      dp  = gg;
      dp_1= g;
      hc   = P1[i]  *14.7*h  /14.7;
      hc_1 = P1[i-1]*14.7*h_1/14.7;            // at previous node

      fprintf(fi, "\n %10.4f     %e    %e",s_1,dp_1,hc_1);
      fprintf(fi, "\n %10.4f     %e    %e",s,  dp,  hc);
      fprintf(fi, "\n ----------------------------------------
--");

      hcc[j-1]=hc;
      hcc[j]=hc_1;
   }
   g = gg;
}
for (i=4 ; i<=j-2 ; i+=2)
   hc_avg += (hcc[i-1]+hcc[i]);
hc_avg = hc_avg/(j-4);
fprintf(fi, "\n avergae of h1c between winding roller and web is
%e",hc_avg);

fprintf(fi,"\n\n
**********************************************");

//*********************************************  calculating h2c
fprintf(fi, "\n\n  the amount of entrained air, h2c[mils] between
nip roller and web\n");
fprintf(fi, "\n ==============================================");
fprintf(fi, "\n   s[inches]         dp1            h2c[mils]");
fprintf(fi, "\n ==============================================");
// find dp2/ds =0, then calculate hc
g = P2[2] - P2[0];
j=0;
hc_avg = 0;
for(i=2 ; i<NN ; i++)
{  gg = P2[i+1] - P2[i-1];
   if(gg*g < 0)
   {  j+=2;
      s    = (i-NN/2)*DS*R1*pow(EE,1./3);
      s_1  = (i-NN/2-1)*DS*R1*pow(EE,1./3);    // at previous node
      p    = (P2[i]  -1)*14.7;
      p_1 = (P2[i-1]-1)*14.7;                  // at previous node
```

```
      h   = H2[i]  *R1*1000*pow(EE,2./3);
      h_1 = H2[i-1]*R1*1000*pow(EE,2./3);      // at previous node
      dp  = gg;
      dp_1= g;
      hc   = P2[i]  *14.7*h  /14.7;
      hc_1 = P2[i-1]*14.7*h_1/14.7;            // at previous node

      fprintf(fi, "\n %10.4f    %e    %e",s_1,dp_1,hc_1);
      fprintf(fi, "\n %10.4f    %e    %e",s,  dp,  hc);
      fprintf(fi, "\n ----------------------------------------
--");

      hcc[j-1]=hc;
      hcc[j]=hc_1;
   }
   g = gg;
}
for (i=2 ; i<=j ; i+=2)
   hc_avg += (hcc[i-1]+hcc[i]);
   hc_avg = hc_avg/j;
   fprintf(fi, "\n avergae of h2c between nip roller and web is
%e",hc_avg);

//*************************************   calculating nip force
//****************   Simpson's 1/3 Rule for numerical integration
for(i=1 ; i<=NN ; i+=2)
   nip_force += (4.0*(P2[i]-1.0));
for(i=2 ; i<=NN ; i+=2)
   nip_force += (2.0*(P2[i]-1.0));
nip_force = nip_force * PA * R1 * (DS/3.0) * pow(EE,1.0/3.0);
                                          // converting in Psig
fprintf(fi,"\n\n ***********************************************");
fprintf(fi,  "\n the nip force is %15.7e (lbf/in)",nip_force);
fprintf(fi,  "\n ***********************************************");

} // the end of the function, hc_print();

//*************************************************************
void excel_print(double P1[], double P2[], double H1[],
                 double H2[])
{
int i;

fprintf(fi,"\n\n\n  node   P1(dimless)   H1(dimless)
P2(dimless)    H2(dimless)");
fprintf(fi,"        node     P1(Psig)      H1(mils)
P2(Psig)        H2(mils)\n");

for ( i=0; i<NC-N1_NIP; i+=2){
   fprintf(fi,"\n%5d %14.5e %14.5e %14.5e %14.5e",i,(P1[i]-
1)*B,H1[i],0.0,100.0);
   fprintf(fi," %10d %14.5e %14.5e %14.5e %14.5e",i,(P1[i]-1)*PA,
```

```
H1[i]*R1*pow(EE,2.0/3.0)*1000,0.0,250.0);
}
for ( i=NC-N1_NIP; i<=NC+N2_NIP; i+=2){
   fprintf(fi,"\n%5d %14.5e %14.5e %14.5e %14.5e",i,
(P1[i]-1)*B,H1[i],(P2[i-(NC-N1_NIP)]-1)*B,H2[i-(NC-N1_NIP)]);
   fprintf(fi," %10d %14.5e %14.5e %14.5e %14.5e",i,
(P1[i]-1)*PA,H1[i]*R1*pow(EE,2.0/3.0)*1000,
(P2[i-(NC-N1_NIP)]-1)*PA,
H2[i-(NC-N1_NIP)]*R1*pow(EE,2.0/3.0)*1000);
}
for ( i=NC+N2_NIP+1 ; i<=N+1 ; i+=2){
   fprintf(fi,"\n%5d %14.5e %14.5e %14.5e %14.5e",i,
(P1[i]-1)*B,H1[i],0.0,100.0);
   fprintf(fi," %10d %14.5e %14.5e %14.5e %14.5e",i,(P1[i]-1)*PA,
H1[i]*R1*pow(EE,2.0/3.0)*1000,0.0,250.0);
}
fprintf(fi,"\n\n");

} // the end of the function, excel_print();
```

VITA

Jae-Yong Lee

Candidate for the Degree of

Master of Science

Thesis: A COMPUTATIONAL ANALYSIS OF AIR ENTRAINMENT WITH A NIP ROLLER

Major Field: Mechanical Engineering

Biographical:

Education: Graduated from An-Bob High School, Kyung-Ki, Korea in February 1993; received Bachelor of Science degree in Mechanical Engineering from Kon-Kuk University, Seoul, Korea. Completed the requirements for the Master of Science degree with a major in Mechanical Engineering at Oklahoma State University in December 1999.

Experience: Research Assistant, Department of Mechanical Engineering, Oklahoma State University, Stillwater, Oklahoma, May 1998 to July 1999. Project Engineer, Woodbridge Foam Fabricating, Inc., Chattanooga, Tennessee, August 1999 to present.